Department of Energy Technology

EVALUATING LOCAL AND OVERALL THERMAL COMFORT IN BUILDINGS USING THERMAL MANIKINS

Ehab Foda

Aalto University

DOCTORAL DISSERTATIONS

Aalto University publication series
DOCTORAL DISSERTATIONS 129/2012

EVALUATING LOCAL AND OVERALL THERMAL COMFORT IN BUILDINGS USING THERMAL MANIKINS

Ehab Foda

Doctoral dissertation for the degree of Doctor of Science in Technology to be presented with due permission of the School of Engineering for public examination and debate in Auditorium k216 at the Aalto University School of Engineering (Espoo, Finland) on the 9th of November 2012 at 12 noon.

Aalto University
School of Engineering
Department of Energy Technology
HVAC Technology

Supervising professor
Prof. Kai Sirén

Preliminary examiners
Prof. Ingvar Holmér, University of Lund, Sweden
Prof. Duanmu Lin, Dalian University, China

Opponent
Prof. Bjarne Olesen, Technical University of Denmark, Denmark

Aalto University publication series
DOCTORAL DISSERTATIONS 129/2012

ISBN 978-952-60-4814-7 (printed)
ISBN 978-952-60-4815-4 (pdf)
ISSN-L 1799-4934
ISSN 1799-4934 (printed)
ISSN 1799-4942 (pdf)
http://urn.fi/URN:ISBN:978-952-60-4815-4

Unigrafia Oy
Helsinki 2012

Finland

441 697
Printed matter

Aalto University

Abstract

Aalto University, P.O. Box 11000, FI-00076 Aalto www.aalto.fi

Author
Ehab Foda

Name of the doctoral dissertation
Evaluating Local and Overall Thermal Comfort in Buildings Using Thermal Manikins

Publisher School of Engineering

Unit Depertment of Energy Technology

Series Aalto University publication series DOCTORAL DISSERTATIONS 129/2012

Field of research HVAC Technology

Manuscript submitted 13 March 2012 **Date of the defence** 9 November 2012

Permission to publish granted (date) 23 May 2012 **Language** English

☐ **Monograph** ☒ **Article dissertation (summary + original articles)**

Abstract

Evaluation methods of human thermal comfort that are based on whole-body heat balance with its surroundings may not be adequate for evaluations in non-uniform thermal conditions. Under these conditions, the human body's segments may experience a wide range of room physical parameters and the evaluation of the local (segmental) thermal comfort becomes necessary. In this work, subjective measurements of skin temperature were carried out to investigate the human body's local responses due to a step change in the room temperature; and the variability in the body's local temperatures under different indoor conditions and exposures as well as the physiological steady state local temperatures. Then, a multi-segmental model of human thermoregulation was developed based on these findings to predict the local skin temperatures of individuals' body segments with a good accuracy. The model predictability of skin temperature was verified for steady state and dynamic conditions using measured data at uniform neutral, cold and warm as well as different asymmetric thermal conditions. The model showed very good predictability with average absolute deviation ranged from 0.3-0.8 K. The model was then implemented onto the control system of the thermal manikin 'THERMINATOR' to adjust the segmental skin temperature set-points based on the indoor conditions. This new control for the manikin was experimentally validated for the prediction of local and overall thermal comfort using the equivalent temperature measure. THERMINATOR with the new control mode was then employed in the evaluation of localized floor-heating system variants towards maximum energy efficiency. This aimed at illustrating a design strategy using the thermal manikin to find the optimum geometry and surface area of a floor-heater for a single seated person. Furthermore, a psychological comfort model that is based on local skin temperature was adapted for the use with the model of human thermoregulation. The latter combination was used with a virtual thermal manikin on a CFD code for the evaluation of indoor thermal conditions and was experimentally validated using human subjects' tests.

The results showed that these two approaches with the physical and virtual thermal manikins, using the introduced control mode, can produce a very reasonable predictability of the local and overall thermal comfort for sedentary activities. The average absolute deviation from subjective data for these two approaches was in a range from 0.25-0.5 on the thermal comfort scale. The thermal manikin with the new control mode may be used to optimize the design of HVAC systems towards energy-efficiency along with thermal comfort.

Keywords Thermal comfort, Thermoregulation, Skin temperature, Thermal manikin, Equivalent temperature

ISBN (printed) 978-952-60-4814-7 **ISBN (pdf)** 978-952-60-4815-4

ISSN-L 1799-4934 **ISSN (printed)** 1799-4934 **ISSN (pdf)** 1799-4942

Location of publisher Espoo **Location of printing** Helsinki **Year** 2012

Pages 187 **urn** http://urn.fi/URN:ISBN:978-952-60-4815-4

A? Aalto-yliopisto

Tiivistelmä

Aalto-yliopisto, PL 11000, 00076 Aalto www.aalto.fi

Tekijä
Ehab Foda

Väitöskirjan nimi
Paikallisen ja Kokonaislämpöviihtyvyyden Arviointi Rakennuksissa Lämpönuken Avulla

Julkaisija Insinööritieteiden Korkeakoulu

Yksikkö Energiatekniikan laitos

Sarja Aalto University publication series DOCTORAL DISSERTATIONS 129/2012

Tutkimusala LVI-tekniika

Käsikirjoituksen pvm 13.03.2012 **Väitöspäivä** 09.11.2012

Julkaisuluvan myöntämispäivä 23.05.2012 **Kieli** Englanti

☐ **Monografia** ☒ **Yhdistelmäväitöskirja (yhteenveto-osa + erillisartikkelit)**

Tiivistelmä

Ihmiskehon lämpöviihtyvyyden arviointimenetelmät, jotka perustuvat koko kehon ja ympäristön väliseen lämpötaseeseen, eivät ehkä ole riittäviä epähomogeenisissa lämpöoloissa tapahtuvaan tutkimukseen. Näissä olosuhteissa ihmiskehon osat voivat altistua lukuisille huonetilan fysikaalisille parametreille ja paikallisen segmentteihin jaetun lämpöviihtyvyyden määritys tulee tarpeelliseksi. Tässä työssä subjektiiviset ihon pintalämpötilamittaukset toteutettiin tutkimalla ihmiskehon paikallisia reaktioita sen altistuessa ulkoisiin tekijöihin, joita olivat sisälämpötilan askelmuutos, kehon osien paikallislämpötilan muutokset erilaisissa sisälämpötilaoloissa sekä paikalliset fysiologiset jatkuvuustilan lämpötilat. Monisegmenttinen ihmiskehon lämpösäätelymalli kehitettiin näihin havaintoihin perustuen määrittämään ihmiskehon osien paikallista ihon lämpötilaa hyvällä tarkkuudella. Mallin ennustamien ihon lämpötilojen luotettavuutta tutkittiin sekä jatkuvuustilassa että muuttuvissa olosuhteissa käyttäen tasaisen neutraaleissa, kylmissä, lämpimässä sekä epäsymmetrisissä lämpöoloissa mitattua aineistoa. Mallin luotettavuus osoittautui erittäin hyväksi keskimääräisen absoluuttisen poikkeaman vaihdellessa välillä 0.3-0.8K. Malli otettiin käyttöön lämpönuken "THERMINATOR" säätöjärjestelmässä sisäilman olosuhteisiin perustuvan kehon osien pintalämpötilojen asetusarvojen valinnan tarkistamiseksi. Tämä uusi lämpönuken säätötapa validoitiin kokeellisesti paikallisen ja kokonaislämpöviihtyvyyden ennustamista varten käyttäen mittana ekvivalenttilämpötilaa. Uudella säätöjärjestelmällä varustettua THERMINATOR-nukkea käytettiin paikallisen lattialämmitysjärjestelmän eri vaihtoehtojen testaukseen energiatehokkuuden parantamiseksi. Lämpönuken avulla pyrittiin löytämään lämmitetyille lattiaelementeille optimaalinen geometria ja pinta-ala yhden istuvan henkilön lämmöntarpeen tuottamiseksi . Lisäksi psykologinen viihtyvyysmalli, joka perustuu paikalliseen ihon lämpötilaan, mukautettiin käytettäväksi ihmiskehon lämpösäätelymallin kanssa. Jälkimmäistä yhdistelmää käytettiin virtuaalisen CFD-lämpönukkemallin kanssa sisälämpöolojen määrittämiseksi ja malli validoitiin kokeellisesti ihmistestien avulla.

Tulokset osoittivat, että nämä kaksi lähestymistapaa fyysisen ja virtuaalisen lämpönuken avulla käyttäen esitettyä säätötapaa, voivat tuottaa erittäin järkeviä ennusteita paikallisesta ja kokonaislämpöviihtyvyydestä istuvalle henkilölle. Subjektiivisen aineiston keskimääräinen absoluuttinen poikkeama lämpöviihtyvyysasteikolla vaihteli välillä 0.25-0.5 näiden kahden lähestymistavan kesken. Uudella säätötavalla varustettua lämpönukkea voidaan käyttää optimoimaan LVI-teknisten järjestelmien suunnittelua energiatehokkuuden ja lämpöviihtyvyyden yhdistämiseksi.

Avainsanat Lämpöviihtyvyys, Lämmönsäätely, ihon lämpötilaa, Lämpönukke, Ekuivalenttilämpötila

ISBN (painettu) 978-952-60-4814-7 **ISBN (pdf)** 978-952-60-4815-4

ISSN-L 1799-4934 **ISSN (painettu)** 1799-4934 **ISSN (pdf)** 1799-4942

Julkaisupaikka Espoo **Painopaikka** Helsinki **Vuosi** 2012

Sivumäärä 187 **urn** http://urn.fi/URN:ISBN:978-952-60-4815-4

Preface

The work of this thesis was conducted at the Department of Energy Technology, School of Engineering at Aalto University. The experimental work in this thesis was carried out in the HVAC laboratory. This work was financially supported by Aalto University MIDE project and the author acknowledges the financial support kindly provided by the project. The author would also like to acknowledge the financial support for this year by the K.V Lindholm Foundation.

I express my sincere gratitude to my supervisor, Professor Kai Sirén, for his constructive advices, encouragement and valuable comments on my published papers.

I wish to thank Professor Hazim Awbi for his contribution and supervision. Many thanks are due to Issa Almesri for the fruitful collaboration in part of the publications.

I would like to thank the reviewers of the thesis Professor Ingvar Holmér and Professor Duanmu Lin for their positive feedback and constructive comments on the thesis.

Special thanks to the Lab. manager MSc. Markku Sivukari and Technician Petteri Kivivuori for their help during the experimental work. I am also so grateful for all the human subjects who participated in that experimental work.

I wish to thank our Senior Researcher, Dr. Ala Hasan, for his brotherly support during my studying years. I also wish to thank the colleagues who shared the same room with me during these years: Mohamed, Martin and Tommaso; firstly for their support and secondly for being patient with my loud thinking.

I would like to thank my colleagues in the HVAC laboratory, Senior Researcher Jari Palonen, Dr. Juha Jokisalo, MSc. Lari Eskola, MSc. Matias Keto for the discussions and pleasant working atmosphere. I wish to thank the department controller Mirka Seppälä for her professional help.

I also would like to thank my colleagues in the 4D-Space MIDE project Arhi Kivilahti, Jussi Kuuti, Jussi Teirikangas, James Culley, Teemu Ropponen, Petri Sarikko, Simo Syrman and others for the cooperation.

Finally, I would like to dedicate the work of this thesis to the memory of my father who raised me to value knowledge and learning, and encouraged me always to pursue postgraduate studies.

Contents

List of original publications

This thesis was completed on the basis of the following six original publications, which are referred to in the text by their Roman numbers I-VI.

I Foda E, Sirén K (2011) A new approach using Pierce two-node model for different body parts, International Journal of Biometeorology, 55(4):519-532, DOI 10.1007/s00484-010-0375-4

II Foda E, Almesri I, Awbi H, Sirén K (2011) Models of human thermoregulation and the prediction of local and overall thermal sensations, Building and Environment Journal, 46: 2023-2032, DOI:10.1016/j.buildenv.2011.04.010

III Foda E, Sirén K (2011) Dynamics of human skin temperatures in interaction with different indoor conditions, Proceedings of Roomvent 2011- 12th international conference on air distribution in rooms, Trondheim, Norway

IV Foda E, Sirén K (2012) A thermal manikin with a human thermoregulatory control: Implementation and validation, International Journal of Biometeorology, 56(5): 959-971, DOI: 10.1007/s00484-011-0506-6

V Foda E, Sirén K (2012) Design strategy for maximizing the energy-efficiency of a localized floor heating system using a thermal manikin with human thermoregulatory control, Energy and Buildings Journal 51: 111-121, DOI: 10.1016/j.enbuild.2012.04.019

VI Almesri I, Awbi H, Foda E, Sirén K (2012) A new air distribution index for evaluating non-uniform thermal environments, Indoor and Built Environment Journal, DOI: 10.1177/1420326X12451186.

Author's contribution

The thesis author is the principal author of the first five publications: I-V. Papers I, III, IV, V are independent research that was initiated, carried out and written by the author and was supervised and reviewed by the co-author, Prof. Kai Sirén. In paper II, the author initiated, carried out most of the calculations and the writing of the paper. The co-author Issa Almesri provided part of the references from the literature and carried out the calculations using the UCB and Fiala models of human thermoregulation. In paper VI, the author of this thesis contributed in the calculations using the thermoregulation model, development of the comfort model, partly to the integration with the CFD software and the paper writing. The work in paper VI was initiated and written by Issa Almesri. Prof. Hazim Awbi supervised and reviewed the work in papers II and VI. The co-author, Prof. Kai Sirén reviewed the work in papers II and VI.

Abbreviations

AAD	average absolute deviation
AC	Air conditioned
ACS	Adaptive comfort standard
ASHRAE	American Society of Heating, Refrigerating and Air-Conditioning Engineers
CAVVAT	Constant air volume variable air temperature
CE	Comfort equation
CEN	Comité Européen de Normalisation
CFD	Computational fluid dynamics
CHF	Constant heat flux
CST	Constant surface temperature
DAQ	Data acquisition
DOS	Disk operating system
DV	Displacement ventilation
EU	European Union
HVAC	Heating, Ventilating and Air-Conditioning
ISO	International Organization for Standardization
LTC	Local thermal comfort
LTS	Local thermal sensation
MSP	Multi segmental Pierce
MV	Mixing ventilation
NRTD	Nickel resistance temperature detector
NV	Naturally ventilated
OTC	Overall thermal comfort
OTS	Overall thermal sensation
PID	Proportional Integral Derivative
PRTD	Platinum resistance temperature detector
PWM	Pulse width modulation
UCB	University of California Berkeley
RTD	Resistance temperature detector
SCATs	Smart controls for thermal comfort
SD	Standard deviation
SIMPLE	Semi-implicit method for pressure-linked equations
TAC	Task ambient conditioning
TSBE	Technologies for Sustainable Built Environment centre
USB	Universal serial bus

Nomenclature

The international system of units (SI) is mainly used throughout the thesis. In some places, other alternative units were adopted for some quantities to follow their original way of presentation.

Normal symbols

A	Surface area (m²)
A_D	Dubois area (m²)
B_{sk}	heat from blood to skin (W/m²)
B_{fc}	heat from blood to core (W/m²)
BMI	body mass index (kg/m²)
Bs_w	positive body thermal signal for warmth (°C)
C	sensible heat loss from skin by convection (W/ m²)
C_1	regression coefficient for the body parts
C_2	thermal capacitance at skin node
C_3	thermal capacitance at core node
c	body heat capacity (J/kg K)
c_{bl}	blood thermal capacity (J/LK)
Con(t)	vasoconstriction drive at time *t*
Cs_c	negative core thermal signal for cold (°C)
Cs_w	positive core thermal signal for warmth (°C)
C_{res}	rate of convective heat loss from respiration (W/m²)
Dil(t)	vasodilatation drive at time *t*
DISC	Thermal discomfort index
DTS	dynamic thermal sensation index
dw	Sweat distribution factor
E_{max}	evaporative heat loss at saturated skin surface (W/m²)
E_{res}	rate of evaporative heat loss from respiration (W/m²)
E_{sk}	total evaporative heat loss from the skin (W/ m²)
EHT	equivalent homogeneous temperature (°C)
fcl	fractional increase in body surface area attributed to clothing
f_{sk}	function accounts for the deviation in skin temperature
h_c	convective heat transfer coefficient (W/m² K)
h_{cal}	calibrated heat transfer coefficient (W/m² K)
h_e	evaporative heat transfer coefficient (W/m² K)

h_r	linear radiant heat transfer coefficient (W/m² K)
H_{c-s}	total heat from core to skin (W/m²)
H_{fc}	heat component through tissues from core to skin (W/m²)
Ht	body height (m)
G	CO_2 production per person (l/s)
I_a	air layer thermal resistance (m² K/W)
I_{cl}	intrinsic thermal insulation resistance of clothing (m² K/W)
I_T	total thermal resistance (m² K/W)
K	average body tissue conductance (W/m² K)
K_1	regression coefficient for the whole body effect on body parts
L	latent heat of water (J)
M	metabolic rate (W/m²)
M_{shiv}	shivering power (W/m²)
MTV	mean thermal vote
m_{co}	body core mass (kg)
m_{sk}	skin compartment mass (kg)
n	number of subjects
P	power (W)
P_a	ambient vapor pressure (mmHg)
P_B	barometric pressure (mmHg)
P_{sk}	saturated water vapor pressure at skin surface (mmHg)
PMV	predicted mean vote
PPD	predicted percentage of dissatisfied
Q_S	total sensible heat loss from the manikin (W/m²)
R	sensible heat loss from skin by radiation (W/m²)
R_{sw}	sweat regulation signal (g/m²sec)
RH%	relative humidity
SET*	standard effective temperature
$Skbf$	skin blood flow (L/m² hr)
Sks_c	negative skin thermal signal for cold (°C)
Sks_w	positive skin thermal signal for warmth (°C)
TSENS	Thermal sensation index
T_a	air temperature (°C)
T_{amb}	ambient temperature (°C)
T_b	body temperature (°C)
T_{bl}	blood temperature (°C)

T_{cl}	clothed body surface temperature (°C)
T_{co}	core temperature (°C)
T_{mrt}	mean radiant temperature (°C)
To	operative temperature (°C)
T_r	radiant temperature (°C)
T_{7S}	seven site average skin temperature (°C)
T_s	surface temperature (°C)
T_{sk}	skin surface temperature (°C)
$T_{skin,local}$	local skin temperature (°C)
$T_{skin,local,set}$	local skin set-point (°C)
$T_{skin,mean}$	mean skin temperature (°C)
$T_{skin,mean,set}$	mean skin set-point (°C)
T_{eq}	equivalent temperature (°C)
t	time (s)
v	air velocity (m/s)
W	rate of mechanical work (W/ m²)
Wt	total body mass (kg)
w	total skin wettedness
w_{dif}	wettedness due to diffusion
w_{sw}	wettedness due to regulatory sweat
x	floor heater geometry

Greek symbols

α	fraction of total body mass
Δ	difference
η	mechanical efficiency of the human body
ε	skin emissivity
σ	Stefan-Boltzmann constant ($5.67\times10^{-8}\,\mathrm{W/m^2K^4}$)
Φ	function accounts for the effect of core temperature
Ψ	function accounts for the dynamic changes in the core and skin nodes

Subscripts and superscripts

a	air
amb	ambient
B	Barometric

b	body
bl	blood
C	convective
c	cold
cal	calibrated
cl	clothing
co	core
C-S	from core to skin
D	Dubois
dif	diffusion
e	evaporative
eq	equivalent
fc	from core
max	maximum
mrt	mean radiant temperature
n	time increment
o	operative
r	radiant
res	respiration
rest	at rest
S	sensible
s	surface
7S	seven sites
sc	cold signal
set	set-point
shiv	shivering
sk	skin
sw	sweat
sw	warm signal
T	total
w	warm

1. Introduction

1.1. Background

Indoor thermal comfort was the original motivation and has been the main objective for constructing HVAC systems. The design of HVAC systems is a multi-objective driven process. The objectives incorporated into that process are mainly to achieve: thermal comfort, energy-saving, indoor air quality, and cost-efficiency. There usually is a trade-off between these objectives. For example, the energy-saving is constrained by the achievement of the indoor thermal comfort and air quality thresholds. The EU 2020 target for reduction of carbon emissions and energy consumption (EU Directive 2010) diverts attention in the buildings' sector to the energy-saving measures. However, the energy-saving in buildings need not come at the expense of the other objectives in the design process. In fact, it can further be enhanced by closer investigation of the interconnected objectives such as the indoor thermal comfort. The following sub-sections discuss important elements in the background of this thesis.

1.1.1. Thermal comfort

The thermal comfort is defined as the state of mind at which it expresses satisfaction with the surrounding thermal environment. People may complain about the outdoor environment but they understand that the only possible control is a behavioral one by adjusting their clothing and the durations they spend outdoors. On the other hand, they expect in their indoor environment, at which they spend most of their time, to have conditions that promote the thermal comfort state. These indoor conditions are created by the effectiveness of the building envelope and the use of HVAC systems. Evaluation and predictive methods are used for existing and under-design buildings, in order to assess whether these created conditions would promote the thermal comfort state or not. The prediction of the indoor thermal comfort under different conditions is commonly carried out using the famous *PMV* model (Fanger 1970). The *PMV* model is used till the present time and adopted by the standards and guidelines (e.g. ISO 7730, ASHRAE Standard 55, and CEN CR 1752). Additionally, ASHRAE Standard 55 includes a new adaptive comfort standard (ACS) that is based on the analysis of 21,000 sets of raw data (started in 1995) compiled from field studies in 160 buildings located on four continents in varied climatic zones. The results from these field studies showed that the *PMV* model fails to predict the thermal comfort for naturally ventilated (NV) buildings while in fully air-conditioned (AC) buildings it was

remarkably successful in predicting the comfort temperatures (de Dear and Brager 2002). Therefore, the ASHRAE Standard 55 proposes the use of the ACS to serve as an alternative method to the *PMV* model only for predictions in NV buildings. On the European path, the EU project smart controls for thermal comfort (SCATs) was launched in 1997 to build a database that is only collected in Europe mainly for NV buildings that are in a free running mode (building without mechanical cooling in summertime). Then, the European standard EN15251 introduced new adaptive comfort equations for NV buildings in a free running mode that seems, at a glance, similar to the ASHRAE's ACS equation. However, according to Nicol and Humphreys (2009) the two approaches are not directly comparable due to differences in the calculation methods.

While the *PMV* model is criticized for biases and limitations in the predictions for NV as well as AC buildings (Humphreys and Nicol 2002), it is also criticized for ignoring factors such as climate; social economy; expectation; psychological and behavioral adaptive abilities (R. Yao et al. 2009). On the other hand, the adaptive comfort models are criticized for being mainly based on low quality field studies and for not including physical factors such as human clothing, activity or the indoor environmental conditions in its predictions (Fanger and Toftum 2002). Nevertheless, these two methods are the recognized ones in the international standards.

1.1.2. Local thermal comfort

The previous section presents the current state-of-the-art for the evaluation of thermal comfort from the international standards. However, the situation is different in the research field. Thermal comfort research over the last ten years has gone extensively under a new wave of development of methods and concepts. The concept of the local thermal comfort, corresponding to body segments, underlies the prediction for whole body and represents the current state-of-the-art for the prediction of the thermal comfort. In non-uniform thermal environments, the body segments may experience a wide range of room physical parameters (i.e. air temperature, radiant temperature and air velocity). Thus, the predictive methods of the thermal comfort that are based on the body mean physiological variables and whole-body heat balance with its surroundings (e.g. *PMV* model) may not be adequate. The evaluation of the local (segmental) thermal comfort under these conditions becomes necessary. Thereafter, the evaluation of the overall (whole body) thermal comfort can be based on weighting these local effects from all body segments. The local thermal comfort may be predicted using two known methods: the

equivalent (homogeneous) temperature by Wyon et al. (1989); and the University of California, Berkeley (UCB) comfort models by Zhang (2003). The prediction of the local thermal comfort is based on the local skin temperature as stipulated in these two methods.

The equivalent temperature approach was first introduced, for local body segments, by Wyon et al. (1989) for assessing vehicle climate using a thermal manikin. The equivalent temperature is defined as the temperature of an imaginary space with uniform and still air condition at which the body exchanges the same dry heat loss as in the actual environment. This is usually estimated using a thermal manikin that is calibrated under uniform conditions. Wyon and Sandberg (1990) used the same approach for evaluating the local thermal discomfort due to vertical temperature gradients in buildings. The approach was then used in several studies for evaluating thermal comfort in buildings (e.g. Tanabe et al. 1994). The equivalent temperature (T_{eq}) is presented on a diagram that shows the so called ideal profile (neutral) and acceptable ranges (mean vote=±0.8 corresponds to 20% dissatisfied) for different body segments. A new diagram, called the comfort zone diagram, with a wider acceptable ranges (mean vote=±1.5) was later obtained by Nilsson (2004) from subjective tests in more than 30 sets of climatic condition. The T_{eq} at these conditions was estimated using two thermal manikins and correlated with the subjective votes under the same conditions. The T_{eq} approach originally predicts whether the body segment is in comfort or discomfort thermal condition without referring to predictions of comfort votes.

The UCB comfort model (Zhang 2003) is based on a large-scale experimental work at the University of California, Berkeley. This is a rational model for the estimation of local thermal sensation. The model has a static term that is based on the deviation of the local skin temperature from its set-point and a dynamic term based on the time derivative of the skin and core temperatures. The UCB comfort model is not a stand-alone model and needs coupling with a model of human thermoregulation or to be fed with a measured data.

The available methods for the prediction of the local thermal comfort are few and not sufficiently validated. Figure 1 shows the only two approaches used for the evaluation of the local thermal comfort. As illustrated in the figure, the local thermal comfort is evaluated either by using human physiological-psychological models that predict the human skin temperature and consequently the thermal sensations or by using a thermal manikin for the estimation of the equivalent temperature.

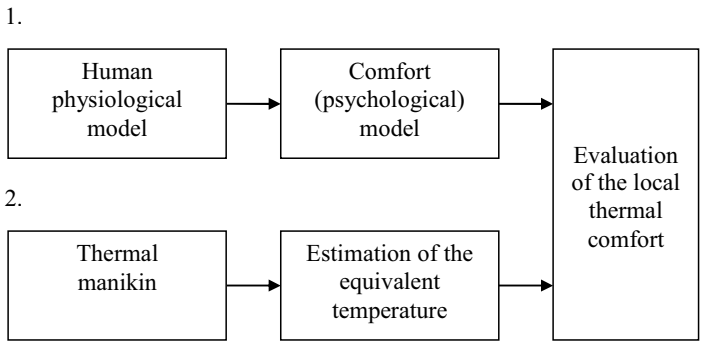

Figure 1 The available methodology for evaluating the local thermal comfort

1.1.3. Human physiological (thermoregulation) models

Human thermoregulatory system has been the focus of thermal comfort research since the early 1960's. Physiological models were developed to predict the responses of human body under different indoor environments. Most of the developed models are based on Stolwijk and Hardy research work (1966) at the J.B. Pierce foundation laboratory. The multi-segmental physiological models which predict local skin temperatures along with other physiological variables have gained more importance with the local thermal comfort concept. Recent multi-segmental models are based on statistical approach to simulate the human body's active controls (e.g. Fiala et al. 1999, 2001) or based on the approach that is given in Stolwijk's model (1966).

Stolwijk's model (Stolwijk and Hardy 1966) of a standard man divides the body parts into three main compartments: head, trunk and extremities as well as a central blood compartment. The heat balance equations at skin and core (also at muscle in case of trunk) nodes for the three compartments and central blood are set to calculate the physiological variables as functions in time.

Huizenga et al. (2001) developed a modified model on the basis of Stolwijk's model and the research work by Tanabe (Tanabe et al. 2002). In its original form, the model consists of 16 body segments but can be extended to have unlimited segmentation of body parts. The main modifications to the original Stolwijk's model (in addition to the segmentation) were: the improvement to the blood flow models including counter flow heat exchange at the limbs segments and perfusion from blood vessels to tissues; the addition of a clothing node to model the heat and moisture capacitances; the addition of heat transfer by conduction to surfaces in contact with the body; the improvement to the estimation of the convection and radiation heat transfer coefficients; the explicit radiation

heat transfer calculation using angle factors; and the addition of a radiation heat flux model. As stated by the developers, the model is able to predict the core and extremity skin temperatures with reasonable accuracy under a range of environmental conditions.

The 65MN model, also based on Stolwijk's model, by Tanabe et al. (2002) divides the human body into 16 segments and calculates the heat balance at skin, fat, muscle and core nodes plus a central blood compartment. Weighting and distribution factors were introduced for each body segment in the thermoregulation control system. Additionally, they introduced nodal thermal capacitances, basal metabolic and blood flow rates as well as thermal conductance values between nodes based on assumptions and earlier studies.

The Fiala model comprises the so called passive and active models (Fiala et al. 1999, 2001). The passive model consists of 15 spherical or cylindrical body elements and uses up to 7 different tissue materials. Most of the body parts were divided into anterior, posterior and inferior to account for asymmetries and hidden parts of the body. The passive model simulates the physical interaction between the human body parts and tissue layers as well as the interaction with the surrounding environment. The active model was based on statistical approach to simulate the human body's active controls such as the peripheral vasomotor, sweating and shivering heat production. The Fiala model contains lots of fine details, accounts for many different factors and is considered as a unique mathematical model of human thermoregulation.

The application of these models has not yet been adopted by standards and guidelines. However, it started few years ago to be investigated for possible adoption in European standards, when the European Union has funded the COST project (Action 730) in the development of the Universal Thermal Climate Index (UTCI) that involved the Fiala model. The disseminations of results from that project were just published in April 2012 in a special issue of the International Journal of Biometeorology (McGregor 2012).

1.1.4. Multi-segmental Pierce model

The Pierce two-node model was developed, as a simple model from Stolwijk's general model, by Gagge et al. (1971) to assess thermal comfort in buildings. The latest version of the original Pierce two-node model is presented in a study by Gagge et al. (1986). The model was primarily designed to predict whole body mean skin temperature, core temperature, sweating rate and shivering heat production as functions of time subject to indoor conditions, activity and clothing levels. This model was commonly

used with its comfort indices TSENS and DISC to evaluate the overall thermal comfort. Doherty and Arens (1988), in evaluating the Pierce model, mentioned that the accuracy of skin temperature prediction is influenced by exercise intensity. The error is close to zero for resting people and approximately 0.4K at low exercise level. Thus, the Pierce two-node model may be seen as a good tool to predict whole-body mean skin temperature for sedentary activities in buildings.

Pierce two-node model was used earlier to predict the local skin temperature of different body segments in a few recent studies. Kohri et al. (2002) developed a model which applies the two-node model to 11 body segments to calculate the standard effective temperatures (SET*) for these body segments in the vehicle environment. A common core temperature was used in the Pierce algorithm for all body parts. Additionally, distribution factors for metabolic heat production, shivering and blood flow as well as local tissue conductance values were introduced. A thermal manikin was used to estimate the segmental heat transfer coefficients. The target precision (i.e. ±1K) was not achieved for all body segments.

Kaynakli et al. (2005), in studying thermal comfort in vehicles, used the Pierce two-node model for 16 body segments that are uniformly clothed. A constant value for the radiant heat transfer coefficient and segmental values from a study by de Dear et al. (1997) for the convective heat transfer coefficients were used in the Pierce algorithm. They employed the heat balance calculation to estimate the thermal load and thereafter the thermal sensation index. Atmaca et al. (2007) used the same model of 16 body segments by Kaynakli et al. (2005) to study the effects of radiant temperature on the thermal comfort. The skin and core set-points were from a study by Tanabe et al. (2002). The model validation was showed in transient condition for only mean skin temperature and thigh segment. The authors stated that the model has a satisfactory predictability.

The accuracy of Pierce two-node model in estimating whole-body mean skin temperature along with its simplicity were the main motivations in all trials for the multi-segmental use. While the good accuracy is always a desirable target the simplicity is needed to enhance the calculation time and may be seen as an advantageous feature for practitioners. However, the accuracy of the Pierce model in the multi-segmental trials has not yet reached a balance with its simplicity.

The development of a multi-segmental Pierce model, that can predict local skin temperature with good accuracy, was one goal of the work of this thesis.

1.1.5. Thermal manikins

Thermal manikins have been used to simulate the physical and thermal presence of the human body in interaction with thermal environments. The major applications of thermal manikins include the evaluation of clothing insulation and the influence of thermal environments on human body. Traditionally, thermal manikins are used with three different control modes: constant skin surface temperature (*CST*) mode; constant heat flux (*CHF*) mode; and the comfort equation (*CE*) mode which is derived from Fanger (1970). Although a thermal manikin that has the shape of a human body provides the realism of the human physical presence, the three known control modes do not precisely suffice the simulation of the human's thermal presence. While the *CST* mode relies on pre-assumed values (not addressed to certain conditions) for the skin surface temperatures, the *CHF* mode usually results in unrealistic skin surface temperatures and the *CE* mode always represents a neutral condition. The disadvantages of these control modes have been overcome in different ways in earlier studies. For example, Cheong et al. (2006) in experimenting non-uniform environments served by displacement ventilation used a thermal manikin with the *CE* mode. Human subjects participated to correlate their responses, under the same conditions of the thermal manikin experiments, and were allowed to adjust their clothing to achieve thermal neutrality. Sakoi et al. (2007), in estimating the local sensible heat losses of the human body, employed a thermal manikin with a segmental *CST* mode using measured skin temperatures from human subjects' tests to set accordingly the skin temperature of the manikin segments. The use of subjective measurements with the manikin settings improves the realism for the simulation of the human thermal presence; however, using human subjects at each measurement case with thermal manikins is not an efficient procedure. The three control modes have been used in the evaluation of clothing (McCullough 2005, Oliveira et al. 2008), calculations of local heat transfer coefficients at different body segments (de Dear et al. 1997, Quintela et al. 2004) and in the estimation of the equivalent temperature (Melikov and Zhou 1999, Holmér et al. 1999, Nilsson 2004).

Thermal manikins nowadays are either physical or virtual ones that can be used in real-life measurements or in simulation environments respectively. Certainly, these manikins need better control modes that can simulate adequately the human thermal presence in space.

1.1.6. Localized HVAC systems based on local comfort

Localized HVAC systems with the task-ambient conditioning (TAC) concept represent a promising option towards energy-saving in buildings.

Conventional TAC systems from 1990's were mainly all air systems, for open-plan office spaces. These systems use under floor plenums and floor-based air diffusers; or air-outlets that is integrated with the room furniture. They provide the conditioned air thrown towards the occupant and use individual's control for thermal comfort and preference. The evaluation of the local thermal comfort can further assist the design of these localized systems towards energy-saving. This can be realized by focusing the energy use on occupant's body and even on certain body segments based on local comfort criteria. Azer and Nevins (1974) showed that the thermal comfort in hot environment could be improved, using an overhead cool air jet, respectively from hot to warm and from very uncomfortable to uncomfortable. Bauman et al. (1995) used a thermal manikin to evaluate the local thermal comfort and optimize the performance of the floor-based system. Finally they introduced general recommendations to improve the performance of that TAC system. Amai et al. (2007) used human subjects to evaluate the local thermal comfort; and hence, the performance of different TAC systems. The subjects' preferable directions of the supply air were different with each system; however, the individuals' control of the TAC systems contributed well to make the preferred environment. Arens et al. (2006), in a two-part paper, stated that hands and feet feel cooler than other body parts in cool environments while the head (excluding the breathing zone) is more sensitive to warm conditions than the rest of the body segments. This was based on large-scale human subjects' tests performed at the University of California, Berkeley (UCB) that is described in details in Zhang's thesis (Zhang 2003). The UCB research team made use of these results to develop an un-conventional TAC system integrated with a workstation and focused on the body's thermally sensitive segments (Zhang et al. 2010). The TAC system consisted of: palm warmer and hand ventilation device integrated with the computer's keyboard; under-desk feet warmer; and a head-ventilation device. The thermal comfort was evaluated for the use of that TAC system at ambient temperatures from 18 to 30 °C using 18 human subjects. The results showed that the thermal comfort level of subjects was improved by the system especially when enabling the subjects to control the heating level. Watanabe et al. (2009) introduced another un-conventional TAC system uses a chair equipped with fans that is individually controlled. Human subjects were used to evaluate the thermal comfort performance of that system. The ambient temperature was set at 26°C, 28°C, 30°C and 32°C. The subjects reported an acceptable thermal comfort level up to 30°C ambient temperature. While the use of radiant-heating panel is an optional heating source in some TAC systems, Sørlie et al. (1993) used that alone mounted under the occupant's desk and stated

acceptable overall thermal comfort limits with 60W heater output under ambient temperature around 17-18 °C. A thermal manikin was used to verify the overall thermal comfort based on the whole-body heat loss.

Generally, the introduced TAC systems are mostly all air systems and/or focused on the office building's application. The concept of TAC systems can be utilized further in many different applications. In the work of this thesis, a methodology using a thermal manikin in the design of a localized floor-heating system is introduced.

1.2. Objective and scope of the thesis

The work of this thesis generally aimed at contributing in the development and enhancement of the methods for the prediction of the local and overall thermal comfort. Figure 2 shows a chart that illustrates the used approach in this work.

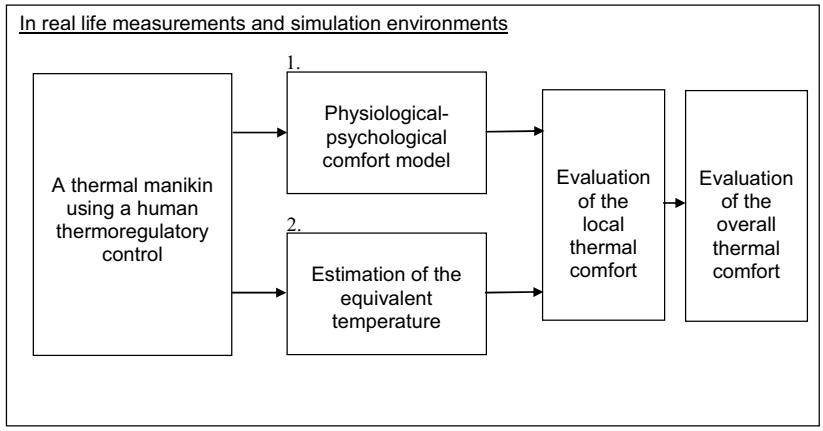

Figure 2 The approach of the work in the thesis

The work was focused on the following research gaps:

- The thermal comfort prediction needs to involve the local effects at the different body segments rather than using mean physiological or physical values in that prediction.
- The application of human physiological (thermoregulation) models has not yet been adopted by the standards and guidelines as a possible predictive method for the local and overall thermal comfort.
- Thermal manikin experiments provide the realism for the human physical presence but do not suffice the simulation of the human's thermal presence based on the used thermoregulatory controls.
- The research of the local thermal comfort needs further investigations, developments and validations.

1.3. Findings

The main findings of the work of this thesis were:

- The development of a multi-segmental physiological (thermoregulation) model that is simple and accurate.
- Implementation and validation of a new control mode for thermal manikins based on the multi-segmental physiological model.
- Employing the thermal manikin with the new control mode in the design of localized HVAC systems towards energy efficiency in buildings.
- The development of a local comfort model that is adapted for the use with the multi-segmental physiological model.
- Integration of the multi-segmental physiological model and its adapted comfort model with a virtual manikin on a CFD code.

The work of this thesis revealed valuable data from the subjective skin measurements over the local responses and the skin temperature distribution under the different indoor conditions. The work of this thesis also introduced useful comparisons and discussion of the available techniques and methods for the evaluation of local and overall thermal comfort. Furthermore, the work of this thesis introduced valuable analysis on the use of localized floor-heating systems under the task ambient conditioning concept.

2. Skin temperature measurements

2.1. Objectives

The measurements aimed at investigating the human body's local responses due to a step change in the room temperature; and the variability in the body local temperatures under different indoor conditions and exposures as well as the physiological steady state local temperatures.

2.2. Experimental setup

The experiments were conducted in a test room at the HVAC laboratory at Aalto University. The test room is part of a two-storey single family house that has large climate chamber equipped with all controls to simulate outdoor conditions and to control the air temperature and humidity over wide ranges. The rooms' layout and setup are shown in Figure 3. The main room (Room 1) was conditioned by the climate chamber system while the

pre-conditioning room (Room 2) was connected on the general ventilation system of the laboratory.

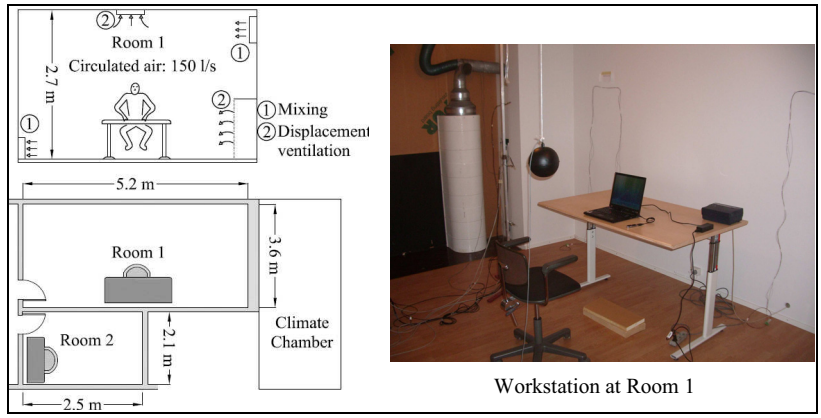

Figure 3 Rooms layout and the experimental setup

Room 2 was used in the step change measurements under the warm and cold conditions and was equipped with an infrared heater as an additional heating source with a rapid response. The skin temperature measurements were carried out under 3 different indoor conditions, in 5 weeks period, during February and March 2010. A total of 46 tests included 33 tests in 1-h duration, 12 tests in 2-h duration and 1 test in 4-h duration. The measurements in 1 and 2-h duration were planned to study the response due to a step change, check the variability and physiological steady state temperatures. The 4-h test was carried out to clarify the physiological steady state temperatures for some of the body segments under the cold condition.

2.3. Human subjects

Eleven male human subjects (University workers) voluntarily participated in the measurements. There were no female volunteers when called for participation in that experimental work. The mean age of the subjects was 32 years old (SD 4), mean body mass index (BMI=Weight/Height²) was 27 kg/m² (SD 3) and mean fat percentage, calculated using Hodgdon and Beckett (1984), was 23%. (SD 5). The subjects' clothes sizes varied from medium to extra large.

All subjects participated in the three different conditions at least in the 1-h tests. After their experience in the 1-h tests, they were asked to participate in the 2-h tests and got the acceptance from 6 of them. Allowing the human subjects to decide based on experience considered ethical guidelines for experiments that involve human subjects. Well known studies from the literature that are used widely in this research field such as: Hardy and Stolwijk (1966); Raven and Horvath (1970); and Werner and Reents (1980)

were carried out using only 3, 11 and 6 male subjects respectively. Therefore, the author was not discouraged to proceed by that number of subjects in these measurements especially with such a diverse sample of subjects (age from 27 to 40 years old and weight from 62 to 105 kg).

2.4. Indoor conditions

The indoor conditions were planned based on the clothing thermal insulation value and office work activity. Three cases were initially determined to nearly create uniform neutral, warm and cold conditions by calculating the operative temperatures (*To*) for predicted mean vote (*PMV*) values equal 0, +2 and -3 respectively. Air mixing system was used in the neutral (Case 1, *To*=25°C) and cold (Case 3, *To*=15°C) conditions while displacement ventilation was the supply air strategy in the warm condition (Case 2, *To*=30°C). The use of displacement ventilation in Case 2 was due to the failure in pilot tests to create uniform conditions using the mixing system. The relative humidity (RH%) was controlled and kept in a range from 40-60% over the 3 cases.

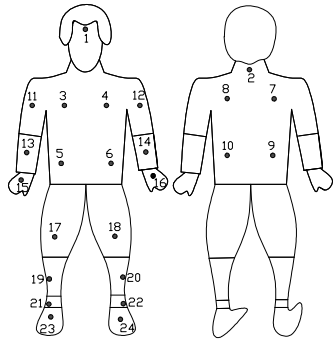

Figure 4 Measurements' body sites of the skin temperature

2.5. Measurements

Local skin temperatures at 24 body sites (see Figure 4) were measured using flexible thermocouples 0.13 mm thick that were soldered to copper plates (Φ8 mm, 0.2 mm thickness). All were calibrated (accuracy ± 0.3K), using a liquid bath temperature calibrator, and connected to a data acquisition unit in groups. The temperatures were recorded at 2-s time interval. The human subjects heart beat rate was monitored using a heart rate watch with a chest strap transmitter. The air velocity was measured, at four different levels in the occupied zone, using air velocity transducers. The air temperature, at same levels, was measured using type-U thermistors. The room measurements were recorded at 10-s time interval. The temperatures of the surfaces (walls, floor and ceiling) were measured using infrared thermometer and were used to calculate the radiant

temperatures according to ISO 7726 (1985). The operative temperature for each case was measured by a globe thermometer at the trunk level of the sitting subjects at the centre of the room. The clothing intrinsic thermal insulation value were measured (0.6clo, clo=0.155m²˚C/W) beforehand at the same test room using the thermal manikin 'THERMINATOR', in a sitting posture and according to ISO 9920 (2007) regulations.

The human subjects were asked to refrain from eating 2-3 h and to remain indoors at least for 1-h before the pre-conditioning period of the measurements. Upon their arrival to the test place, the measurements of their body weight, height using a regular balance beam scale and oral temperatures using ear thermometer were carried out. The subjects did normal office work with their own portable computers during the test period and were asked to record their own heart beat rate every 10-min. At the end of each test, they gave their thermal votes on the cases using ASHRAE 7-point scale (-3 cold, -2 cool, -1 slightly cool, 0 neutral, +1 slightly warm, +2 warm, +3 hot).

Figure 5 The used thermocouple sensor and part of the subjects after attaching the sensors at Room 2

2.6. Measurements' results and observations

The measurements results for the 3 cases in the different exposures are shown in Figures 6-16. Figures 6, 8, 10, 12 and 14 show the steady-state average, minimum and maximum measured values as well as the standard deviation. Figures 7, 9, 11, 13, 15 and 16 show the development of the skin temperatures in time during the different tests. The values in these figures are average values of the right and left body segments (4 segments average for the back). The 7-site weighted average for overall body temperature (T_{7S}) are shown on the figures with the steady-state temperatures and were calculated as (Hardy and DuBois 1938):

$$T_{7S} = 0.07T_1 + 0.14T_2 + 0.05T_3 + 0.07T_4 + 0.13T_5 + 0.19T_6 + 0.35T_7, (°C) \quad (1)$$

where the temperatures from T_1 to T_7 in °C are the temperatures of head, left lower arm, left hand, left foot, left lower leg, left thigh and left abdomen, respectively.

In Case 1 (neutral condition), the subjects reached a physiological steady state in less than 1 h. The variability in temperatures was high especially for the limbs segments (e.g. SD=1.34 for the feet). The averaged temperatures (n=11) were nearly in agreement with earlier measured data from the literature (e.g. Zhang 2003, Olesen and Fanger 1973) except for the thigh and abdomen segments which had in our measurements lower values (≈2K).

In Case 2 (warm condition), a clear physiological steady state was not reached during the 1-h tests (n=11) for all body parts. The 2-h tests (n=6) showed a clear steady state for all body segments. The subjects at the pre-conditioning stage in Room 2 (To=23°C, vertical temperature gradient 0.6K/m) reached the steady state with nearly similar level of the local temperatures for the two exposures (i.e. 1-h and 2-h tests).

In Case 3 (cold condition), the physiological steady state was not attained for most body segments in the 1-h tests (n=11). Moreover, it was not (clearly) attained for some of the body segments, especially feet and hands, in the 2-h tests (n=6). The 4-h test (n=1) aimed at clarifying the physiological steady state for those body parts in Case 3.

The results from the cold tests show that the body thermoregulation system has a priority in preserving the temperatures of the head and trunk segments and maintains a quasi steady state condition in time that was observed clearly in the 4-h test and coincides with Raven and Horvath (1970). The pre-conditioning stage at Room 2 (To=22°C, vertical temperature gradient 1.4K/m) showed slight variations in the averaged body temperatures between the different exposure durations. This was mainly due to the difference in the number of subjects in the different exposure tests and the higher variability observed in the cold condition.

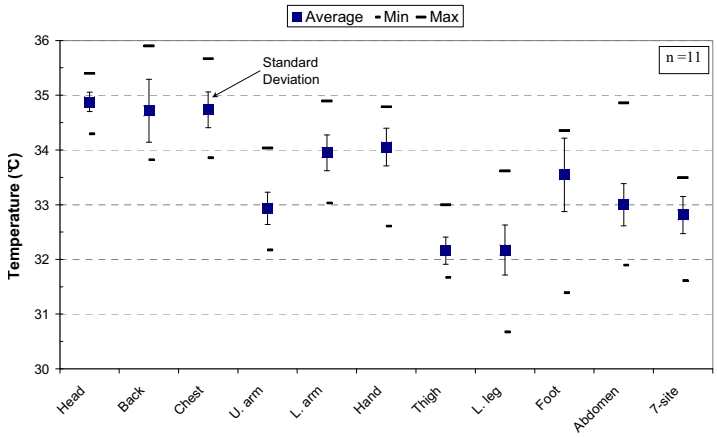

Figure 6 Measured steady-state skin temperatures, Case 1 (neutral)

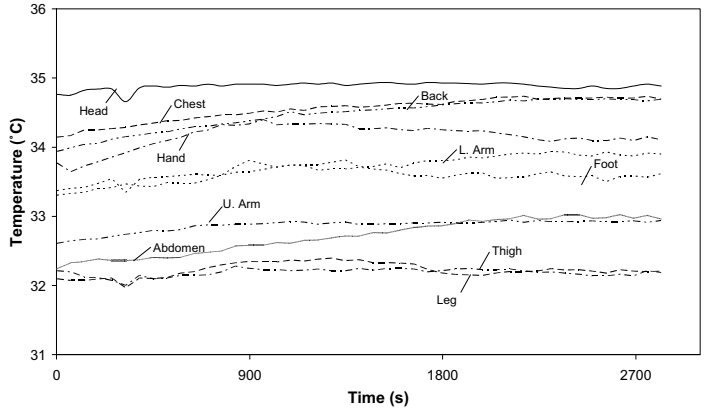

Figure 7 The development of the local skin temperatures in time, Case 1 (neutral)

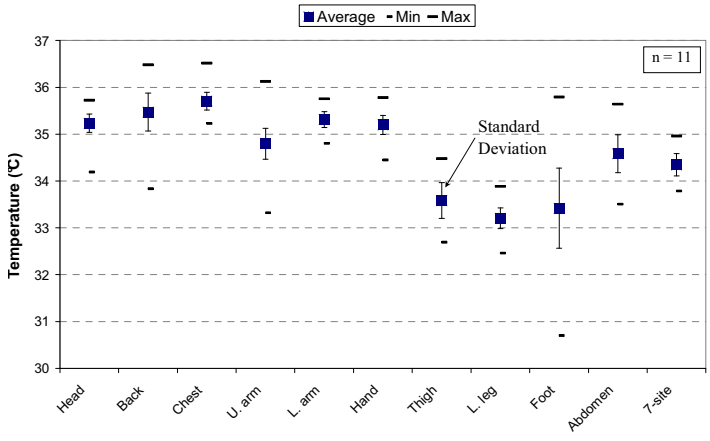

Figure 8 Measured steady-state skin temperatures, Case 2 (warm) 1-h test

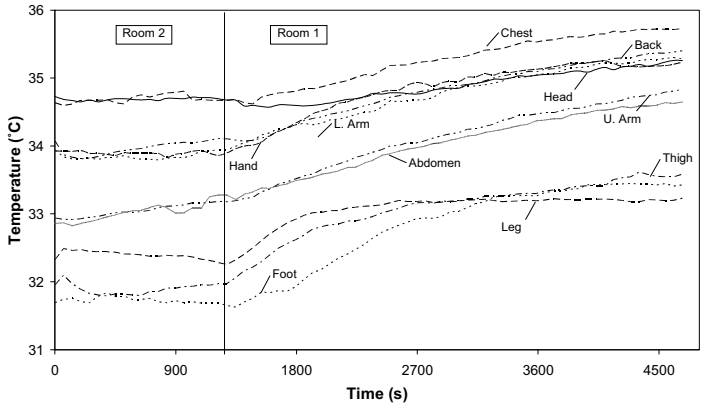

Figure 9 The development of the local skin temperatures in time, Case 2 (warm) 1-h test

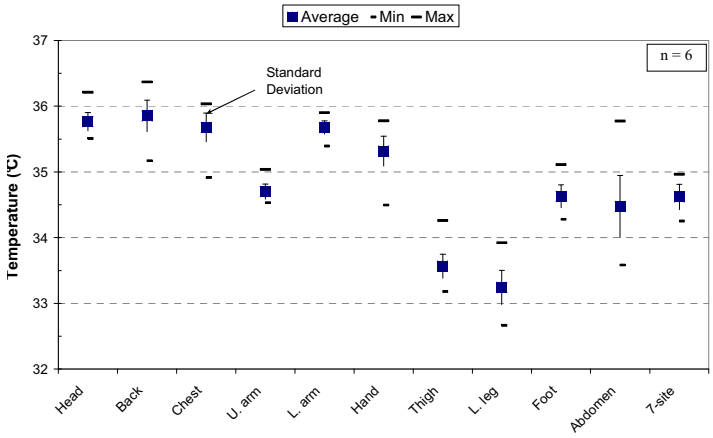

Figure 10 Measured steady-state skin temperatures, Case 2 (warm) 2-h test

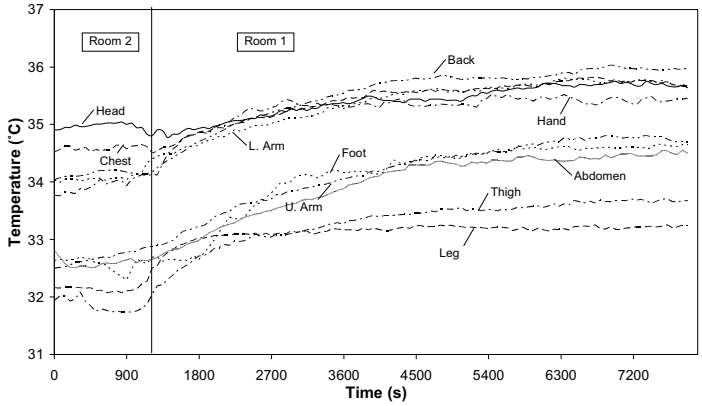

Figure 11 The development of the local skin temperatures in time, Case 2 (warm) 2-h test

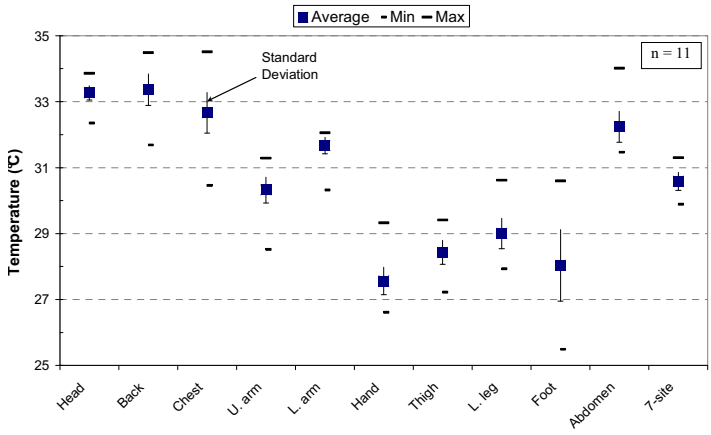

Figure 12 Measured steady-state skin temperatures, Case 3 (cold) 1-h test

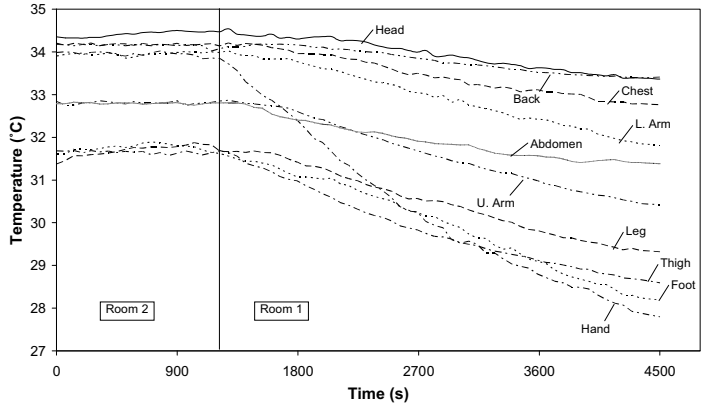

Figure 13 The development of the local skin temperatures in time, Case3 (cold) 1-h test

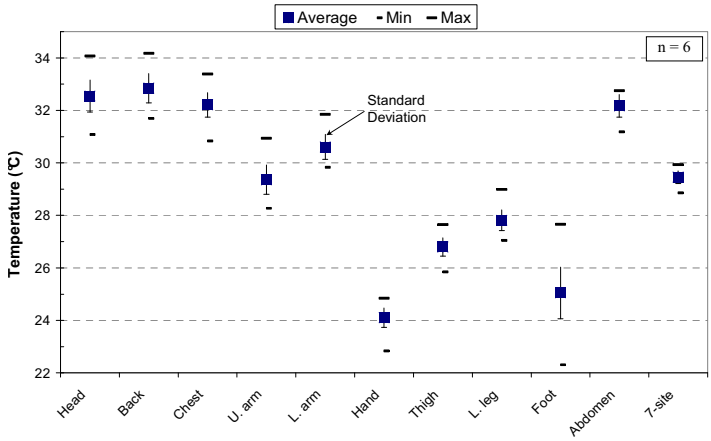

Figure 14 Measured steady-state skin temperatures, Case 3 (cold) 2-h test

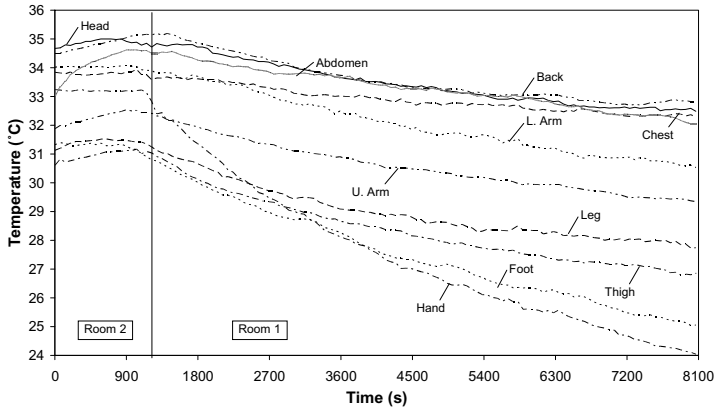

Figure 15 The development of the local skin temperatures in time, Case 3 (cold) 2-h test

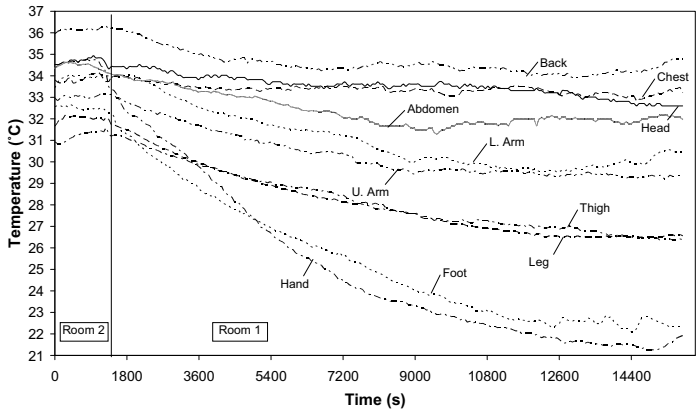

Figure 16 The development of the local skin temperatures in time, Case 3 (cold) 4-h test

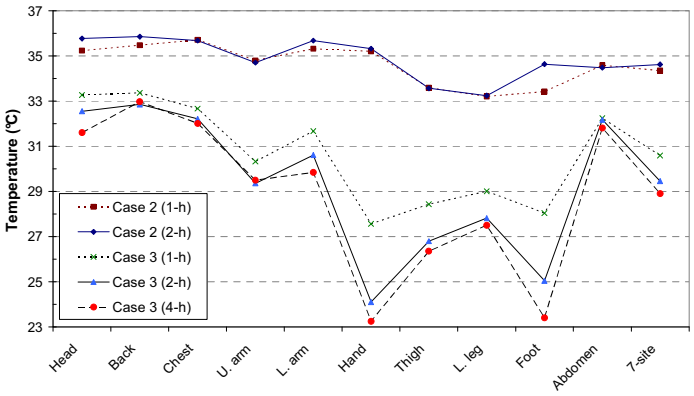

Figure 17 Comparison between the skin temperatures at the different exposure times for Case 2 and 3

Figure 17 shows the variation in the measured temperatures between 1 and 2-h tests for Case 2 and 3 as well as the physiological steady state temperatures under Case 3 conditions (based on the 4-h test). As can be seen, the variations between the two durations were not significant under

Case 2 conditions compared to the variations under Case 3. The variability in temperatures between 1 and 2-h tests based on the same test subjects decreased for most of the body segments in both cases. Table 1 shows the steady state temperatures of different body segments and standard deviation to indicate the variability.

The average heart beat rates per minute were 76 (SD 9), 81(SD 7) and 70 (SD 7) for the 3 cases respectively. This falls in the very light activity category defined by ASHRAE (Fundamentals, 1993). The heart beat rate measurements may have been partly influenced by psychological effects from the measurements atmosphere. Although the measurements setup was carefully planned to avoid other sources of discomforts, the fact of being measured should still have an influence on human subjects.

Table 1 The physiological steady state skin temperatures under the three cases (in °C) and the standard deviation [(a)]

	Head	Back	Chest	U. arm	L. arm	Hand	Thigh	Leg	Foot	Abdomen
Case 1 (neutral)	34.88 (0.35)	34.72 (1.15)	34.74 (0.65)	32.93 (0.59)	33.95 (0.66)	34.05 (0.69)	32.16 (0.49)	32.17 (0.91)	33.54 (1.34)	33.00 (0.77)
Case 2 (warm)	35.76 (0.28)	35.85 (0.47)	35.68 (0.44)	34.70 (0.23)	35.68 (0.2)	35.32 (0.45)	33.57 (0.36)	33.24 (0.52)	34.63 (0.35)	34.48 (0.94)
Case 3 (cold)	31.60 (1.21)	32.97 (1.12)	32.01 (0.93)	29.50 (1.12)	29.84 (0.95)	23.25 (0.74)	26.35 (0.69)	27.50 (0.78)	23.40 (1.9)	31.81 (0.86)

[(a)] Values in brackets refer to the standard deviation

2.7. Summary

In these experiments, measurements of local skin temperature were carried out under 3 different indoor conditions using a diverse sample of human subjects. The subjects wore normal office clothes and the measurements were focused on the office work activity. The measurements aimed at investigating the human body response due to a step change and checking the variability in the skin temperature under different duration tests with the same subjects as well as maintaining a physiological steady state at the different conditions. The measurements revealed valuable data over these aims.

In general, the variability in the body's local temperatures was high for the extremities under the neutral condition and it increased for all body segments under the cold condition while under the warm condition it decreased for all body segments. The differences in the variability at the different exposures, in the warm and cold conditions, was minor for the trunk and head segments while for the extremities in the longer exposure the variability decreased. The steady state temperatures under the neutral condition are comparable and nearly in agreement with measured data from the literature. The distribution of the body temperatures was in a narrow range (<2.5K) under the warm condition. The body thermoregulation mainly preserves the temperatures of the body's vital organs in the head and trunk under cold conditions; hence, these segments

have lower cooling rate and that was observed from the cold condition tests. In these tests, the difference between the local temperatures increased and was up to 10-14K. The body extremities needed longer exposure (>2 h) to reach the physiological steady state.

3. Development of the multi-segmental Pierce model

3.1. Objectives

The work described in this chapter aimed at developing a human physiological (thermoregulation) model—based on the Pierce two-node model— that is balanced for its accuracy and simplicity in predicting the body's local skin temperatures.

3.2. Pierce model construction

Pierce two-node model uses a finite difference procedure to estimate the mean physiological parameters for any given thermal environment, subject metabolic rate and clothing insulation level. Geometrically, the body is modeled as two concentric cylinders, the inner cylinder represents the body core and the thin, outer cylinder represents the skin shell (Doherty and Arens 1988). The skin and core temperatures are calculated in time by solving the heat balance at the core and skin nodes. The heat balance at the core and skin nodes may be written in finite difference form as (Gagge et al. 1986):

$$\frac{(T_{co}^{n+1} - T_{co}^{n})}{\Delta t} = \frac{A_D}{m_{co} c}\left(M - W - (C_{res} + E_{res}) - H_{c-s}\right), \quad (2)$$

$$\frac{(T_{sk}^{n+1} - T_{sk}^{n})}{\Delta t} = \frac{A_D}{m_{sk} c}\left(H_{c-s} - (C + R + E_{sk})\right), \quad (3)$$

where

m_{co} ; is the body core mass (kg)

m_{sk} ; is the skin compartment mass (kg)

c ; is the body heat capacity (J/kgK)

A_D ; is body surface area (DuBois area) (m²)

T_{co} ; is the core temperature (°C)

T_{sk} ; is the skin temperature (°C)

Δt ; is the chosen time step (s)

n ; is the time increment

M ; is the metabolic rate (W/m²)

W ; is the rate of mechanical work (W/m²)

C_{res} ; is the convective heat loss by respiration (W/m²)

E_{res} ; is the evaporative heat loss by respiration (W/m²)

C ; is the sensible heat loss by convection (W/m²)

E_{sk} ; is the total evaporative heat loss from the skin (W/m²)

R ; is the sensible heat loss from skin by radiation (W/m²)

H_{c-s} ; is the heat transfer from core to skin (W/m²).

The mass at core and skin nodes are calculated using the fraction of total body mass, also called the effective shell thickness, (α) as (Gagge et al. 1986):

$$m_{co} = (1-\alpha) Wt \text{ , (kg)} \tag{4}$$

$$m_{sk} = \alpha Wt \text{ , (kg)} \tag{5}$$

where

Wt ; is the body mass (kg), and the body surface area is calculated from (DuBois 1916):

$$A_D = 0.203 Ht^{0.725} Wt^{0.425} \text{ , (m²)} \tag{6}$$

where

Ht ; is the body height (m).

The model estimates the physiological variables at each time step using body thermoregulatory controls such as skin blood flow regulation (that accounts the vasoconstriction and vasodilatation), shivering and sweating.

In this work, a new approach is introduced to form a multi-segmental Pierce model, for short MS-Pierce model, that is based on:

- Adjusting the local skin set-points based on neutral condition measurements (presented in Chapter 2).
- Using additional correlations from literature, in a modified calculation procedure, for the convective heat transfer coefficients at the different body segments.
- Adjusting the heat transfer term from core to skin using common blood temperature along with local core temperatures.
- Calculating the local core set-points (using a line search method) as the values that allow the model to predict the skin temperatures of the measured neutral condition (Chapter 2) with ±0.1K maximum deviation.

In addition, a distribution factor for the regulatory sweat and a limitation rule for the shivering heat production are introduced for further improvement.

A flow chart (calculation procedure) of the MS-Pierce model is shown in Figure 18. Details of the algorithm calculations and modifications are discussed below.

3.3. Thermal signals

The thermoregulation processes are controlled through feedback thermal signals by deviations in the skin, core and body temperatures. The thermal signals for the skin (Sks), core (Cs) and body (Bs) are calculated as (Gagge et al. 1986):

$$Sks = T_{sk} - T_{sk(set)}, (°C) \quad (7)$$

$$Cs = T_{co} - T_{co(set)}, (°C) \quad (8)$$

$$Bs = T_B \ (\alpha T_{sk(set)} + (1-\alpha) T_{co(set)}), (°C) \quad (9)$$

where

$T_{sk(set)}$; is the skin set-point (°C)

$T_{sk(set)}$; is the core set-point (°C)

T_B ; is the mean body temperature weighted by α (°C)

The thermal signals from the skin and core are either cold ($_c$) or warm ($_w$) signals to control vasodilatation, vasoconstriction, blood flow and shivering while the body thermal signal is used only when indicates warmth to regulate sweating along with the skin thermal signal for warmth.

The segmental values of the skin and core set-point are listed in Table 2. The core set-point has an important role in the Pierce model; that is manifested when manipulating different parameters. Therefore, it was calculated to fit the model output for the neutral condition. The local core set-points for the segments may be seen only as a control parameter rather than a physiological quantity.

3.4. Peripheral blood flow

Pierce skin blood flow ($Skbf$) algorithm, adapted from Stolwijk and Hardy (1966), assumes that vasodilatation arises from activity of warm thermo-receptors in the core and that vasoconstriction arises from activity of cold thermo-receptors in the skin. The skin blood flow is calculated in the Pierce model from the following equation (ASHRAE Fundamentals 1993):

$$Skbf(t) = \frac{[6.3 + 200(Cs_w(t))]}{[1 + 0.5(Sks_c(t))]}, (L/m^2hr) \quad (10)$$

The min and max values of $Skbf$ are 0.5 and 90 L/m²hr respectively as specified by Gagge et al. (1986). The fraction of total body mass (α) is a factor that increases with vasoconstriction and decreases with vasodilatation. The factor is calculated in Pierce model as (Gagge et al. 1986):

$$\alpha(t) = 0.0418 + \frac{0.7425}{[Skbf(t) + 0.5854]}. \quad (11)$$

The MS-Pierce model uses the same approach in calculating the skin blood flow for the body segments.

3.5. Sensible heat losses at skin node

The heat losses by radiation and convection from the clothed body are calculated from the following equations (Gagge et al. 1986):

$$R = h_r \, f_{cl} \, (T_{cl} - T_r), \text{ (W/m²)} \quad (12)$$

$$C = h_c \, f_{cl} \, (T_{cl} - T_a), \text{ (W/m²)} \quad (13)$$

where

h_r ; is the linear radiant heat transfer coefficient (W/m²K)

T_{cl} ; is the clothed body surface temperature (°C)

T_r ; is the mean radiant temperature (°C)

h_c ; is the convective heat transfer coefficient (W/m²K)

T_a ; is the air temperature (°C)

The fractional increase in body surface area (f_{cl}) is calculated in the multi-segmental model from (ASHRAE Fundamentals 1993):

$$f_{cl} = \begin{cases} 1.00 + 1.290 I_{cl} \leftrightarrow I_{cl} < 0.078 \\ 1.05 + 0.645 I_{cl} \leftrightarrow I_{cl} > 0.078 \end{cases}, \quad (14)$$

where I_{cl} is the intrinsic thermal insulation resistances (m²K/W).

The linear radiant heat transfer coefficient for the different body segments is calculated from (Gagge et al. 1986):

$$h_r = 0.72 \, \sigma \, \varepsilon \, (4) \left(\frac{(T_{cl} + T_r)}{2} + 273.15 \right)^3, \text{ (W/m²K)} \quad (15)$$

where

0.72; is the ratio of the body's effective radiation area to the Dubois area

σ ; is Stefan-Boltzmann constant= $5.67 * 10^{-8}$ W/m^{2}K^4

ε ; is the skin emissivity (ε =0.97).

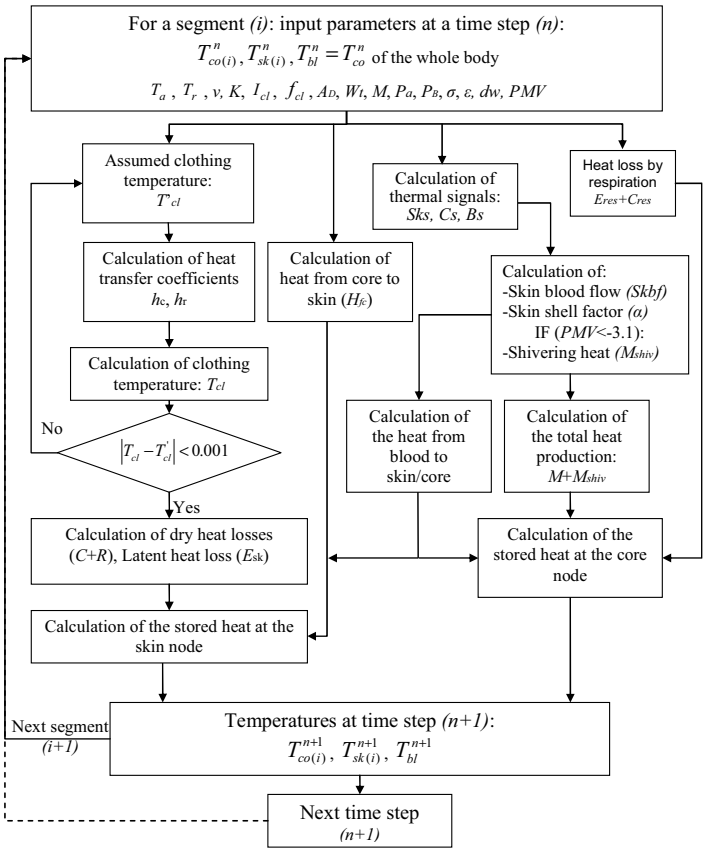

Figure 18 Flow chart of the MS-Pierce model

The convective heat transfer coefficient in the MS-Pierce model is calculated from the following correlations:

$$h_C = 3(P_B/760)^{0.53}, \text{(W/m}^2\text{ K)} \quad (16)$$

$$h_C = B(v)^n, \text{(W/m}^2\text{K)} \quad (17)$$

$$h_C = 5.66(M/58.2 - 0.85)^{0.39}, \text{(W/m}^2\text{ K)} \quad (18)$$

$$h_C = 2.38(T_{cl} - T_a)^{0.25}, \text{(W/m}^2\text{K)} \quad (19)$$

where

P_B ; is the barometric pressure (mmHg)

v ; is the relative air velocity (m/s)

B and n are the correlation constant and exponent (de Dear et al. 1997) given for each body segment (Values are shown in Table 2).

Correlations (16), (17) and (18) are adopted from the original Pierce model (Gagge et al. 1986) while correlation (19) is adopted from Fanger (1970).

In the model algorithm, the above correlations are used along with the measured values by de Dear et al. (1997) in still air (v <0.1m/s). Then, the convective heat transfer coefficient (h_c) is taken as the maximum value of: (16), (17), (18) and (19) for all body segments in case of high air velocities (v >0.1m/s) or high activities (M >80W/m²) and for limbs segments in all cases. In still air (v <0.1m/s), it is calculated, for the head and trunk segments, as the minimum value of: de Dear et al. (1997) measured values, correlations (16), (18) (excluded if M <55W/m²), and (19). This is implemented, as per the original Pierce model, to account for the dominance of air velocity and activity level plus the variations between the trunk and limbs segments in the rate of heat loss.

3.6. Latent heat losses at skin node

The heat loss by evaporation at skin surface is mainly by the sweat secretion process and controlled by the feedback thermal signal for warmth from the skin and body nodes. The evaporation heat loss is estimated by the following equation (Gagge et al. 1971):

$$E_{sk} = w\, h_e\, (P_{sk} - P_a), \text{(W/m}^2\text{)} \tag{20}$$

where

w; is the total skin wettedness that consists of wettedness due to regulatory sweating (w_{sw}) and diffusion through the skin (w_{dif}):

$$w = w_{sw} + w_{dif}, \tag{21}$$

The wettedness due to diffusion (w_{dif}) is assumed to be 6% of the dry skin area (Gagge et al. 1971):

$$w_{dif} = 0.06\,(1 - w_{sw}) \tag{22}$$

h_e; is the evaporative heat transfer coefficient (W/m²K) and it is calculated in Pierce model from (Gagge et al. 1971):

$$h_e = 2.2\, h_c / (1 + 0.92\, I_{cl}\, h_c), \text{(W/m}^2\text{K)} \tag{23}$$

P_a ; is the ambient vapor pressure which is estimated in the MS-Pierce model using a linear correlation (assuming 50% RH):

$$P_a = 0.6105\, T_a - 2.2934, \text{(mmHg)} \tag{24}$$

P_{sk} ; is the saturated water vapor pressure at skin surface and it is estimated in Pierce model using the following equation (Doherty and Arens 1988):

Table 2 Model input parameters

Segment	Surface area [(a)], (m^2) A_D	Body mass [(b)], (kg) W_i	Skin setpoint, (°C) $T_{sk(set)}$	Core setpoint, (°C) $T_{co(set)}$	Sweat distribution factor [(c)] (dw)	Convective heat transfer coefficient (h_c) by de Dear et al. (1997)		
						Correlation (21)		h_c if v <0.1 (W /m^2°C)
						constant (B)	exponent (n)	
Head	0.16	5.22	34.88	36.75	0.8	4.9	0.73	3.7
U. back	0.07	3.74	35.40	36.65	0.5	8.9	0.63	2.6
Chest	0.11	7.01	34.75	36.77	1	9.1	0.59	3
U. arm	0.08	2.44	32.93	37.20	0.7	11.4	0.64	3.4
L. arm	0.07	1.55	33.95	36.90	0.7	11.75	0.625	3.8
Hand	0.05	0.38	34.05	35.85	2.15	13.35	0.6	4.5
Thigh	0.20	7.93	32.16	37.35	0.45	8.9	0.6	3.7
L. leg	0.13	3.78	32.18	37.35	0.75	13.15	0.57	4
Foot	0.07	0.54	33.54	36.75	1.5	12.9	0.545	4.2
L. back	0.05	2.49	33.90	37.00	0.53	8.9	0.63	2.6
Abdomen	0.11	9.93	33.00	37.30	0.6	8.2	0.65	2.8
Whole body	2.04	84.77	33.70	36.80	1	8.6	0.53	3.3

(a) The segmental surface area ratios correspond to the manikin 'THERMINATOR'.
(b) The segmental body mass ratios were taken from Tanabe et al. (2002)
(c) The sweat distribution factor is estimated based on Werner and reents (1980).

$$P_{sk} = Exp(18.67 - 4030.18/(T_{sk} + 235)), \text{(mmHg)} \quad (25)$$

The regulatory sweat signal (R_{sw}) is estimated through body and skin signals for warmth in the Pierce model by the following equation (Gagge et al. 1986):

$$R_{sw} = 0.047.Bs_w.e^{(Sks_w/10.7)}, \text{(g/ m²sec)} \quad (26)$$

where the body and skin thermal signals are set to zero if negative.

The regulatory signal is then used to calculate the wettedness due to regulatory sweat (w_{sw}) from (Gagge et al. 1971):

$$w_{sw} = Minimum(L\,R_{sw}/E_{\max}, 1) \quad (27)$$

where:

L ; is the latent heat of water=2260 J/g

$E_{\max}$; is the evaporation heat loss when w =1 (W/m²)

In the MS-Pierce model, the same procedure is followed in the calculations for different body segments. A distribution factor (dw) (listed in Table 2) is multiplied by the regulatory sweat signal for each body segment. The factors are estimated based on the measured evaporation rate at different body segments from a study by Werner and Reents study (1980).

3.7. Heat transfer from core to skin

The heat transfer from core to skin node is calculated, in the original Pierce model, by the following equation (Gagge et al. 1971):

$$H_{c-s} = (K + c_b Skbf)(T_{co} - T_{sk}), \text{(W/m²)} \quad (28)$$

where

K ; is the conductance of body tissues (K =5.28 W/m² K)

c_{bl} ; is the blood thermal capacity (J/LK).

In the MS-Pierce model, the heat from core to skin is split into two components:

- Heat by peripheral blood flow:

$$B_{sk} = c_{bl} Skbf(T_{bl} - T_{sk}), \text{ (W/m²)} \quad (29)$$

- Heat through tissues:

$$H_{fc} = K(T_{co} - T_{sk}), \text{ (W/m²)} \quad (30)$$

where

T_{bl} ; is the central blood temperature (°C).

The blood temperature is calculated as the core temperature of the whole body, by running the Pierce model algorithm for whole body. The value of the blood temperature is used for all body segments in estimating the heat transfer from blood to skin and core nodes.

The use of a common blood temperature, in the MS-Pierce model, introduces a new term at the local cores heat balance that is the heat transfer between the central blood and local cores. This term is calculated by the following equation:

$$B_{fc} = c_{bl}.Skbf(T_{bl} - T_{co}), \text{ (W/m²)} \quad (31)$$

The exchanged heat between the central blood and local cores may be in both directions depending on the local cores temperatures.

3.8. Heat losses by respiration

The dry and latent heat loss by respiration are calculated from (Gagge et al. 1986):

$$E_{res} = 0.0023\ M\ (44 - P_a), \text{ (W/m²)} \quad (32)$$

$$C_{res} = 0.0014\ M\ (34 - T_a), \text{ (W/m²)} \quad (33)$$

The heat loss by respiration is taken only from the core nodes at the chest segments in the MS-Pierce model.

3.9. Metabolic rate and shivering heat

The heart beat rate records during the skin measurements (presented in Chapter 2) aimed at defining an average value of the metabolic rate (*M*) for the office work activity under the different conditions using a model developed by Zhang et al. (2002). The estimated values by the model were much higher than any specified values for that activity level. Therefore, the *M* value is estimated for a certain activity from the tables given in ISO 8996 (2004). The *M* value of 70W/m² is stated there for the office work activity.

The shivering heat production (M_{shiv}) is estimated in the MS-Pierce model using the following equation (Gagge et al. 1986):

$$M_{shiv} = 19.4\ d_m(-Sks_c)\ (-Cs_c)\ , (W/m^2) \qquad (34)$$

where d_m is the lean body mass ratio to Stolwijk's standard man as used by Havenith (1997).

Based on results from a study by van Ooijen (2004) and observations from the measurements under cold conditions (Chapter 2), a simple limitation rule for the shivering heat is assumed and implemented in the model. The rule corresponds to a limit of *PMV* value of -3.1 for whole body in applying Eq.34 otherwise the shivering heat is set to zero. The use of the *PMV* index for whole body in the shivering limitation may be justified by observation from Tikuisis et al. (1991) that shivering starts at the muscles of the trunk region sooner and at higher intensity than those of the limbs.

3.10. Model predictability

The MS-Pierce model was used initially to predict the local skin temperatures under the cold and warm test conditions (details are given in Chapter 2). The model calculations were based on 20 body segments plus the whole body calculation loop for the central blood temperature. The shown data are the average of the right and left body parts (also upper and lower in case of the back segments). Figure 19 shows the steady state measured and predicted skin temperatures. The average absolute deviation for the warm and cold conditions was 0.6K (SD 0.3) and 0.4K (SD 0.4) respectively. The maximum deviation was 1.28K at the foot segment under the cold condition. These results were based on the modifications of the set-points along with the modifications to the calculation of the convective heat transfer coefficient and the heat transfer term from core to skin.

Figure 20 shows the measured and predicted skin temperatures when using the sweat distribution factor and the limitation on the shivering heat plus the previously mentioned modifications. The absolute average deviation decreased to 0.3K (SD 0.2) for both cases (i.e. warm and cold conditions). The maximum deviation was 0.65K at the thigh segment under the cold condition. Figure 20 also shows the predicted skin temperatures for the warm and cold conditions (denoted with 'Z') when using the neutral condition measurements from Zhang (2003) in adjusting the local skin and core set-points. As can be seen, the predictability of the model in general was slightly lower and was lower specifically for the abdomen and thigh segments. This may be explained by the higher skin set-points (≈2K) given in Zhang (2003) than those measured ones for these particular group of subjects. The absolute average deviation, in general, was 0.6K (SD 0.3). The

set-points effect in the model predictability is clearly manifested in this particular comparison. The MS-Pierce model was adjusted and fitted using measurements under neutral condition based on a group of subjects; therefore, it may be stated that the model was individualized for the skin temperature prediction of such a group of subjects.

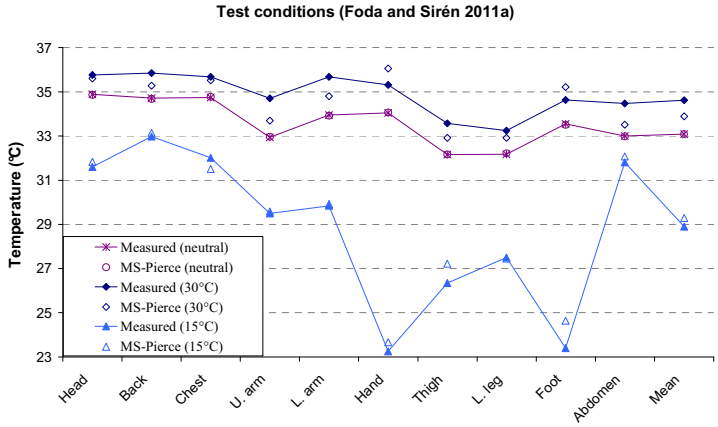

Figure 19 Measured and predicted skin temperatures

The model predictability was further tested against steady state measured data from the literature for different clothing values and activity levels. Figure 21 shows the steady-state measured (Werner and Reents 1980) and predicted skin temperatures by the MS-Pierce model. The subjects in those experiments wore only shorts and were laying in rest on a hammock in temperatures from 10 to 50°C. As can be seen, at 20°C (*PMV*<-6), the model predictability was low for the hand and foot segments. The model predictability was better under the 30 and 35°C as well as at higher temperatures given in that study. As stated by the authors in that study, the physiological steady state was not attained in that measurements at 10°C (*PMV*<-10) and was therefore excluded from the comparison. The absolute average deviation for this comparison was 0.6K (SD 0.4).

Furthermore, the model predictability was compared with two recognized physiological models. These two models were the Fiala model (Fiala et al. 1999, 2001) and the UCB physiological model (Huizenga et al. 2001). A brief description of these two models is given in Chapter 1 (section 1.1.3). The three models were tested with respect to the predictability of skin temperature against recently measured data from the literature.

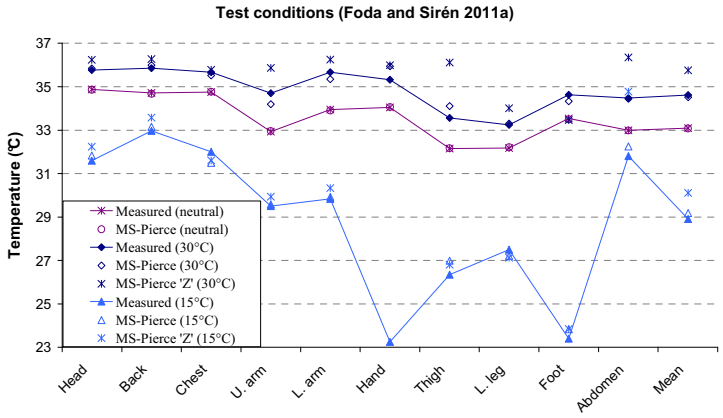

Figure 20 Calculated and measured skin temperatures modified with sweat distribution factor and shivering limitation

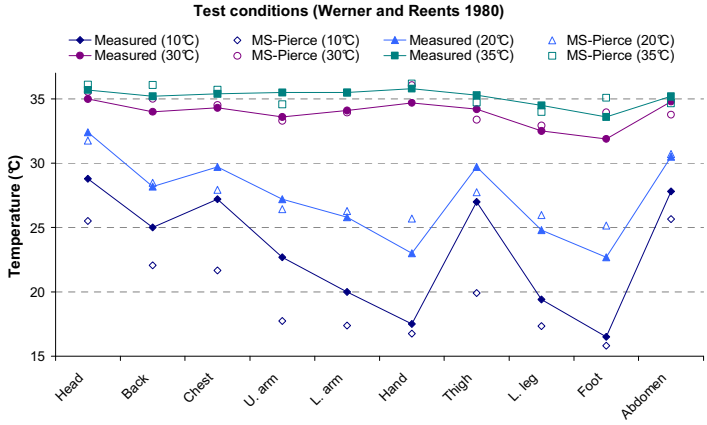

Figure 21 Calculated and measured (Werner and Reents 1980) skin temperatures

The detail description of the simulated conditions is represented in 4 recent studies; under steady-state conditions: Foda and Sirén (2011a), Sakoi et al. (2007), Almesri and Awbi (2011); and under dynamic conditions: Munir et al. (2009). The prediction of the skin temperature under the dynamic condition was carried out using only the Fiala and the MS-Pierce models.

Table 3 Models' average absolute deviation (K) from the measured data and the standard deviation [(a)]

Model	Foda and Sirén (2011a), warm	Foda and Sirén (2011a), cold	Almesri and Awbi (2011), neutral	Sakoi et al. (2007), test #9	Sakoi et al. (2007), test #28
MS-Pierce	0.3 (0.2)	0.3 (0.2)	0.8 (0.6)	0.5 (0.4)	0.5 (0.5)
Fiala	0.7 (0.6)	1.3 (1.0)	0.8 (0.7)	0.7 (0.5)	0.6 (0.5)
UCB	0.7 (0.5)	1.7 (1.9)	0.9 (0.7)	0.9 (0.5)	0.9 (0.6)

[(a)] Values in brackets refer to the standard deviation

The comparison of the predicted steady-state skin temperatures using the different models are shown along with the measured data in Figures 22 to 25. In general, the three models showed very reasonable predictability. The MS-Pierce and the Fiala models had higher predictability, for all test conditions, than the UCB model especially for the extremities. The MS-Pierce model had the lowest average absolute deviation (AAD) from the measured data for the 5 cases. Table 3 gives the AAD values and the standard deviation (SD) from the measured data for the predictions by the 3 models. The comparison can be considered comprehensive as it includes different levels of clothing, a wide range of uniform neutral, warm and cold conditions, as well as cases under asymmetrical thermal conditions. However, the comparison is limited to seated persons carrying out sedentary activities.

The dynamic performance of the MS-Pierce model along with the Fiala model was tested against the measured data given in Munir's et al. study (2009). Figure 26 shows the variation of the calculated and measured skin temperatures with time. The step changes are denoted on the figure with capital letters from A to E where A, C and E denote the neutral condition (29.4°C); B denotes the cold condition (19.5°C); and D denotes the warm condition (38.9°C). In general, the MS-Pierce showed relatively better predictions than the Fiala model when compared to the measured data. For most body parts, the dynamic performance of the two models is in good agreement (max. deviation ≈1K) with the measured data. For few body segments (e.g. Thigh), the maximum deviation between the measured data and the predicted temperatures by the two models was close to 2K. The maximum deviations were mainly during the step change from B to C at which the rate of change in the measured body temperatures was mostly steeper. The deviations at the first step (A) were partly from the models' start-up phase and starting values.

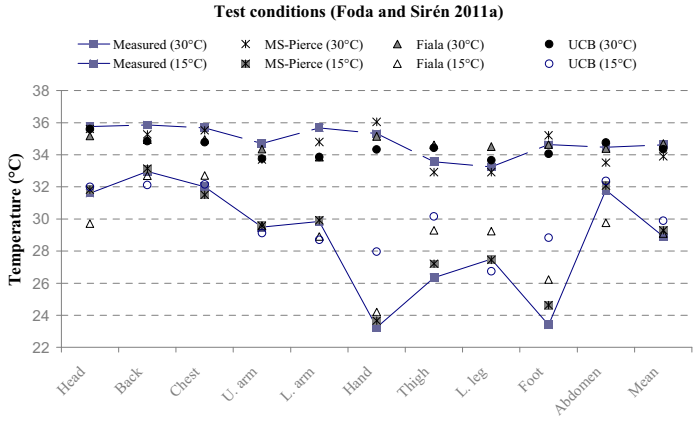

Figure 22 Comparison between the predicted skin temperatures by the physiological models and measured data under uniform warm and cold conditions

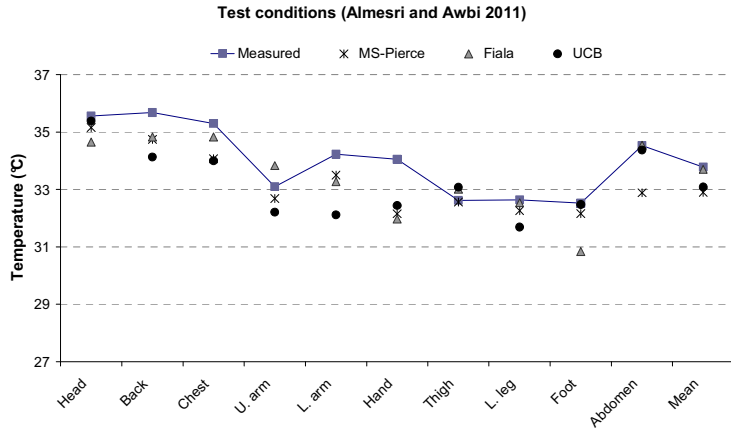

Figure 23 Comparison between the predicted skin temperature by the physiological models and measured data under uniform neutral condition

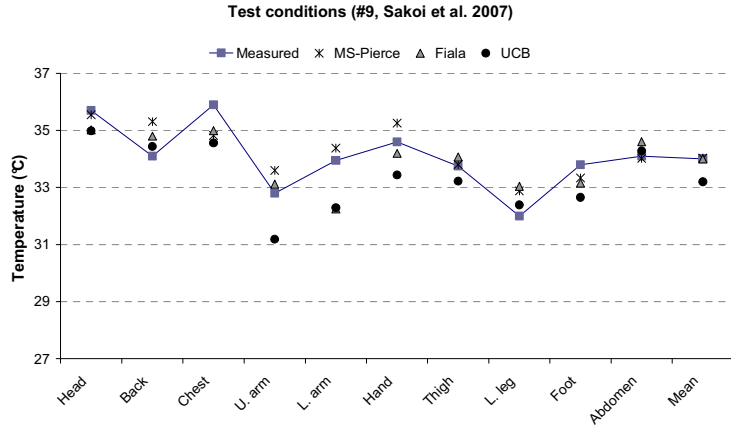

Figure 24 Comparison between the predicted skin temperature by the physiological models and measured data under front-back thermal asymmetrical conditions

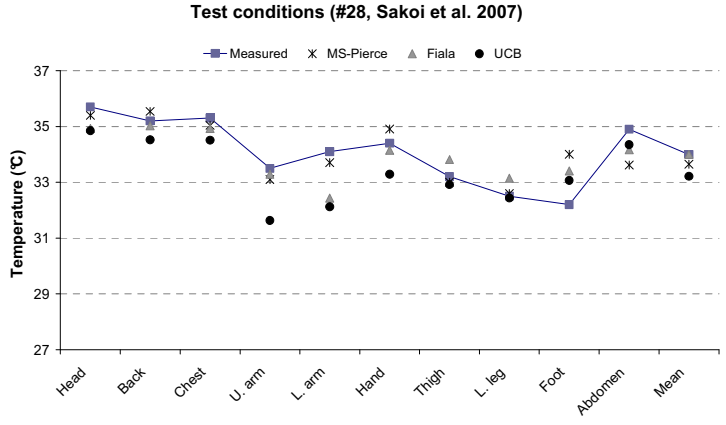

Figure 25 Comparison between the predicted skin temperature by the physiological models and measured data under up-down thermal asymmetrical conditions

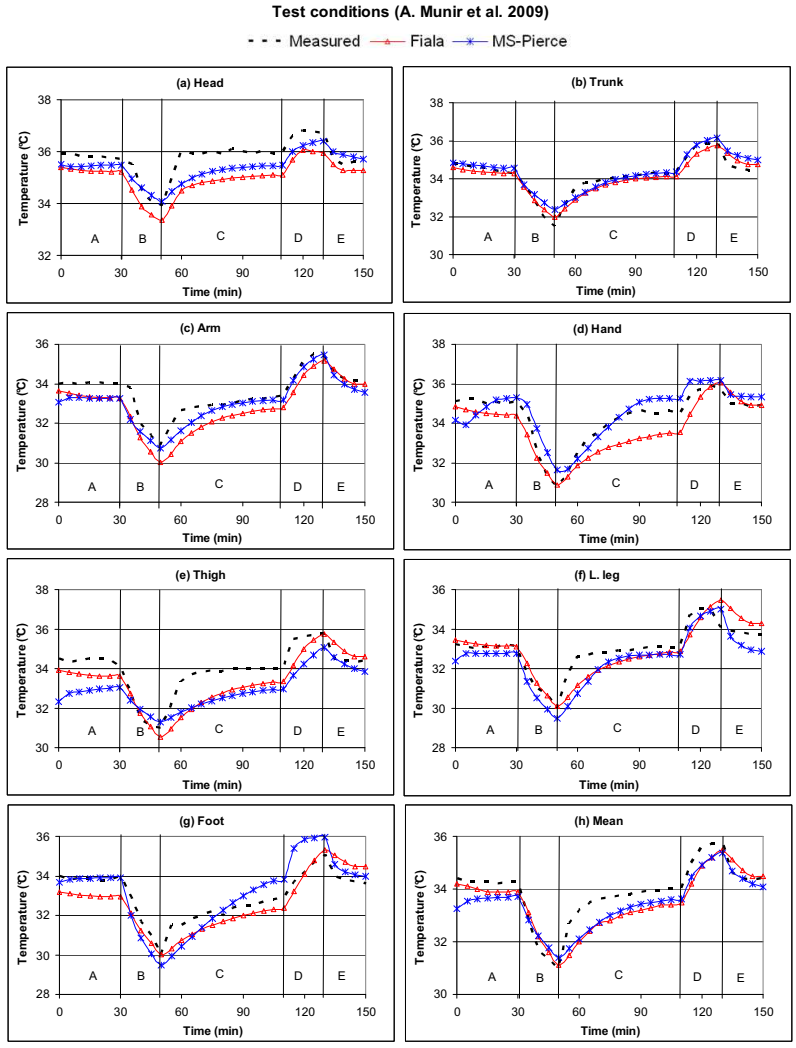

Figure 26 Comparisons between the dynamic performance of the Fiala and MS-Pierce models and measured data from the literature

3.11. Summary

A multi-segmental two-node Pierce model was developed from the original Pierce model based on the following approach: using neutral condition measurements to adjust skin set-points and to fit the model output with the measured data by manipulating the local core set-points; using a modified calculation procedure for the convective heat transfer coefficients; and adjusting the heat transfer term from core to skin using common blood temperature along with local core temperatures.

The model predictability, modified by our own measurements under a neutral condition, was verified using measured data under cold and warm conditions and had the average absolute deviation of 0.3K (SD 0.2). The average absolute deviation was 0.6K (SD 0.3) when modifying the model

using measured data, under neutral conditions, from the literature. The model verification, using independent experimental data, for different activity and clothing level showed lower predictability for the limbs segments in extremely cold conditions and in general an absolute average deviation of 0.6K (SD 0.4). The model predictability was further compared with two recognized physiological models (i.e. Fiala and UCB models). The three models were tested against recently measured data from the literature under steady-state and dynamic conditions. The multi-segmental Pierce model showed very good predictability (average absolute deviation ranged from 0.3-0.8K) in steady-state and showed a good performance in the comparisons of the dynamic condition.

4. A thermal manikin with human thermoregulatory control

4.1. Objectives

This chapter describes the work for upgrading the control system of the thermal manikin 'THERMINATOR' to simulate adequately the human thermal presence in space. This was by adopting the use of the MS-Pierce model in its control. This aimed at enhancing the realism of the thermal manikin's experiments and improving the accuracy for the estimation of the so called equivalent temperature.

4.2. The thermal manikin 'THERMINATOR'

The thermal manikin 'THERMINATOR' (shown in Figure 27) is a European male size 50 that can stand, sit, move his arms and breathe. It consists of 24 body segments that can be individually heated and set at a target value. The manikin was constructed in the beginning of the 1990's.

Figure 27 The thermal manikin 'THERMINATOR'

The body core was made from plastic foam. The heating wires were wounded spirally around the body core of each body segment. This was

then coated with sprayed aluminum to attain even distribution of the surface temperature. The surface layer of the body was made from plastic that was molded for each body segment. The manikin original control system worked with the constant surface temperature (*CST*) control mode. Nickel resistance temperature detectors (NRTD) were isolated from the heating wires and used in the feedback control of the *CST* mode. The manikin software was based on Turbo-Pascal for DOS by which the segmental set-points could be set and the measurements were monitored. The manikin power supply unit with the distribution control cards can provide total power from 60 to 300W with a maximum voltage of 48V.

4.3. THERMINATOR's system with LabVIEW

The upgraded manikin system uses LabVIEW platform. National Instruments (NI) LabVIEW is a graphical programming language that has its roots in automation control and data acquisition. The graphical representation, similar to a process flow diagram, was created to provide an intuitive programming environment for scientists and engineers (Hansen et al. 2007). The MS-Pierce model was constructed on LabVIEW using its graphical programming language. The MS-Pierce model as the new control mode, called here the *MSP* mode, along with the *CST* mode regulate the manikin skin temperature through on-off control (time step=50ms, deviation<0.05K). An additional control option was implemented in LabVIEW that comprises a combination of a virtual proportional–integral–derivative controller and pulse width modulation control (PID-PWM). This option was valid for only eight segments based on the used NI interface (NI USB-6225). The virtual PID controller is used with lower/upper limits from 0 to 1 to calculate the duty cycle for the PWM control. The purpose of the PWM control is to obtain an approximately continuous or smoother control signal. However, the difference with a normal on-off control that is based on a very short time step was not significant. The NI interface USB-6225 was selected for its mobility and plug-and-play installation which minimizes the configuration and setup time. This interface also features the new NI signal streaming technology, which gives bidirectional high-speed streaming of data across a USB cable.

Figure 28 shows a schematic of the manikin system. As illustrated, the desired control mode is preselected to provide the segmental set-points to the virtual controller. The measured segmental values and the controller output are handled through the data acquisition assistant (DAQ-Assist). DAQ-Assist is a LabVIEW function that handles the data acquisition as well as the control signals in connection with the NI interface. Measurements of the indoor condition such as air temperatures, air velocities and globe

temperatures were connected through LabVIEW and used with the *MSP* control.

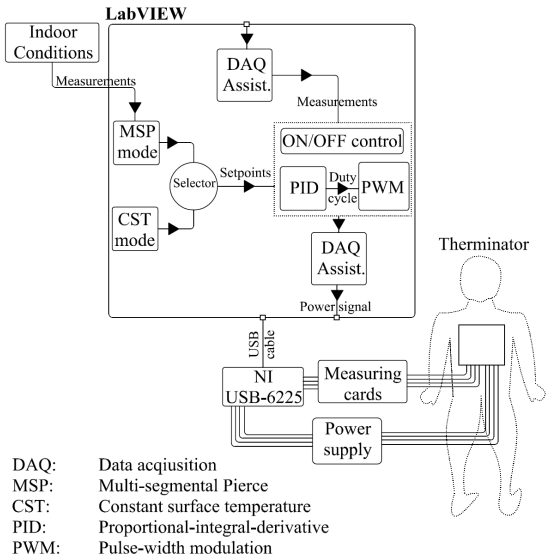

Figure 28 Schematic of the manikin system

THERMINATOR's original power supply unit and the power distribution control cards as well as measurement cards that correspond to the manikin's NRTD were kept in use with the new system. The manikin segmental NRTD were calibrated (in a passive mode) under 5 different levels of indoor uniform conditions (from 20 to 38°C). Furthermore, they were calibrated in an active mode with different skin temperatures under controlled environment against measurements using thermocouples attached on the skin surface (same probe mentioned in Chapter 2) and measurements by an infra-red camera.

The system front panel, on LabVIEW, shows the development of the segmental temperatures and heat losses during the measurements. The segmental skin temperatures and heat losses are recorded at 1 min time interval into a pre-named report.

4.4. Thermal manikin experiments

The upgraded manikin 'THERMINATOR', at this point, is ready for the use with the two control modes. This section describes the thermal manikin experiments that were conducted in order to validate the use of the new control mode (i.e. the *MSP* mode) in evaluating thermal comfort using the equivalent temperature (T_{eq}) approach. The validation of the *MSP* mode was based on a comparison with subjective assessments of the same indoor conditions and a comparison with the widely recognized *CST* mode.

The thermal manikin experiments were conducted in a test room at the HVAC laboratory at Aalto University (same room described in Chapter 2). The room's layout and setup are shown in Figure 29. The experiments were carried out using the *MSP* and *CST* (for whole-body at 34°C) control modes, in a 4-week period during April 2011, and were repeated twice for each procedure. This included the calibration of the manikin with the two control modes. The calibration, to estimate the segmental heat transfer coefficients, was carried out in uniform room temperature (at 18, 21, 24, 27 and 30°C) and still air (v<0.05m/s) conditions. Then, the thermal manikin was employed to estimate the T_{eq} under two different indoor conditions (Case 1 and Case 2).

In both cases a constant air volume/variable air temperature (CAVVAT) control scheme of the supply air was used to maintain the planned conditions at the test room. Case 1 and Case 2 were planned to simulate slightly cool and warm conditions that deviate 2-3K from the winter and summer set-points, respectively, (i.e. 21 and 24°C).

In Case 1, the operative temperature measured at the centre of the room (measured with a globe thermometer) was 19°C. The relative humidity (RH%) was kept at 40%. The mean air velocity in the room was 0.1 m/s (SD 0.01). An electrical floor heater was constructed and used in the occupied zone at a surface temperature of 28°C. The anterior-posterior and up-down radiant temperature asymmetry were 4 and 10K respectively.

In Case 2, the measured operative temperature was 27°C. The floor heater surface temperature was set at 37°C. The RH% was also kept around 40%. The air velocity and radiant temperature asymmetry (anterior-posterior and up-down) were similar to Case 1 conditions.

In all procedures, the manikin wore a clothing ensemble that consists of: under-shirt, shorts, denim trousers, long-sleeve shirt and calf-length cotton socks. A thick wooden board 0.5 x 0.2 x 0.1m (W x L x H) was placed under the manikin's feet during the tests. The clothing intrinsic thermal insulation value was measured (0.6clo, clo=0.155m²K/W) according to ISO9920 (ISO 2007) using the manikin in a sitting posture at the same test room. Online measurements of the indoor conditions were carried out during the whole experimental procedure. The air velocity was measured, at three different levels in the occupied zone, using transducers. The air and operative temperature, at same levels, were measured using thermistors and globe thermometers. This was used to calculate the radiant temperature at the same three levels according to ISO7726 (ISO1985).

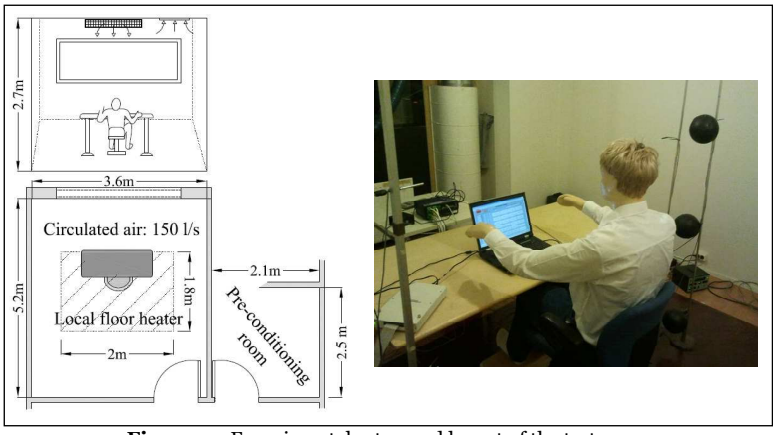

Figure 29 Experimental setup and layout of the test room

All room measurements were connected through a data acquisition unit and were recorded at 2-s time interval. The online measurements (at 1-min time interval) were used with the thermal manikin regulation as input parameters to the *MSP* control mode.

4.5. Calculation of the T_{eq}

The T_{eq} is defined as the temperature of an imaginary space with uniform and still air condition at which the body exchanges the same dry heat loss as in the actual environment. The segmental and overall T_{eq} are calculated, from thermal manikin experiments, using the following equation (Nilsson 2004):

$$T_{eq} = T_{sk} - \frac{Q_s}{h_{cal}}, (°C) \qquad (35)$$

where

T_{sk} ; is the manikin skin temperature (°C)

Q_s ; is the manikin sensible (dry) heat loss (W/m²)

h_{cal} ; is the calibrated heat transfer coefficient (W/m²K)

The calibrated heat transfer coefficient (h_{cal}) represents the rate of the dry heat loss (Qs) in the imaginary space as stated in the T_{eq} definition. It is calculated for each body segment as well as for the whole body from calibrations under uniform room temperature and still air conditions.

In this work, the segmental and overall h_{cal} were obtained (using the two modes) from the manikin calibrations under uniform and still air conditions at 5 different temperature levels from 18 to 30°C. The h_{cal} were then correlated with the correspondent Qs and the temperature difference ($\Delta T = T_{sk} - T_{eq}$) for the estimation of the T_{eq} under Case 1 and 2 conditions.

4.6. Comfort zone diagram

The estimated segmental and overall T_{eq} are then presented on the so called comfort zone diagram to link these estimated temperatures with a thermal comfort scale. Nilsson's new diagram that can be adjusted for different clothing values (Nilsson 2007) was used to present the estimated segmental and overall T_{eq} under Case 1 and 2 conditions. The diagram combines zones that imply different thermal sensations. Table 4 shows the suggested vote ranges for the different thermal sensations.

Table 4 Thermal sensation scale and suggested ranges [a]

Vote range	Thermal sensation
+1.5 : +3.0	Too hot
+0.5 : +1.5	Hot but comfortable or acceptable
-0.5 : +0.5	Comfort
-1.5 : -0.5	Cold but comfortable or acceptable
-3.0 : -1.5	Too cold

[a] Given by Nilsson (2004)

The comfort zones are constructed using the following correlation for each body segment and for whole-body (Nilsson 2007):

$$T_{eq} = T_{sk} - R_T * (a + b * MTV)\ , (°C) \qquad (36)$$

where

R_T; is the clothing total thermal resistance (m²K/W)

a and b are the linear regression coefficients (W/m²) from Nilsson (2004).

In this work, the comfort zones were obtained by substituting the segmental R_T, a, b and the MTV border values as well as the T_{sk} (equals 34°C) in Eq.36. The obtained zones were slightly different from Nilsson's (2004) for R_T =1.3clo.

4.7. Manikin calibrations

The manikin calibrations were carried out and repeated twice under 5 different indoor temperatures (from 18 to 30°C). Figure 30 shows the obtained h_{cal} at the different temperature levels for the clothed whole-body using the *MSP* and the *CST* modes. The figure also shows the coefficients of determination (R^2) for linear correlations with the room temperature. The obtained values for whole-body using the *MSP* mode were nearly constant at the different temperature levels. This trend is similar to obtained results by Melikov and Zhou (1999) using the *CE* mode. The average *%Diff* between the repeated measurements was 4% and 7% for the *MSP* and the *CST* modes respectively.

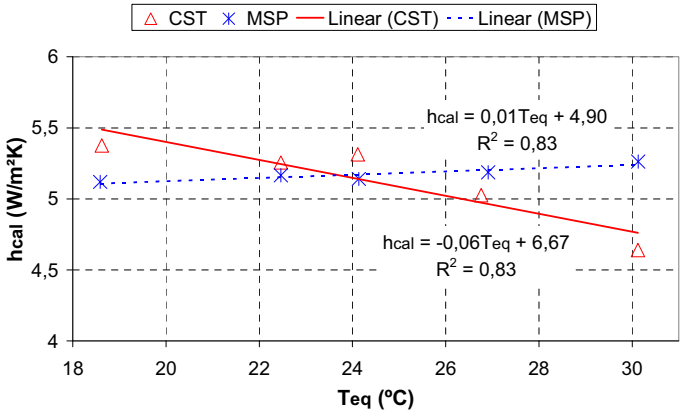

Figure 30 Heat transfer coefficients at the different temperature levels and linear correlations for the clothed whole body using the *MSP* and the *CST* modes

Table 5 Correlations' constants and their coefficient of determination for the two modes

	CST mode			*MSP mode*		
	$h_{cal} = x\Delta t + y$			$h_{cal} = x\Delta t + y$		
Segment	*x*	*y*	R^2	*x*	*y*	R^2
Head	0.03	7.59	0.75	0	7.94	0.05
U. Back R	-0.09	7.33	0.9	-0.13	8.37	0.92
U. Back L	-0.04	6.07	0.72	-0.1	7.38	0.95
Chest R	0.02	3.14	0.11	-0.01	3.47	0.29
U. Arm R	0.08	6.88	0.86	0.1	6.27	0.94
L. Arm R	0.16	4.54	0.95	0.14	4.94	0.98
Hand R	0.21	7.25	0.92	0.06	8.29	0.64
Chest L	-0.05	4	0.73	-0.07	4.28	0.94
U. Arm L	0.09	6.54	0.85	0.14	5.61	0.93
L. Arm L	0.12	5.13	0.93	0.09	5.58	0.99
Hand L	0.17	7.21	0.87	0.02	8.36	0.11
Thigh R	0.10	1.90	0.78	0.11	1.71	0.93
Leg R	0.05	5.62	0.86	0.04	5.15	0.95
Foot R	0.13	4.92	0.97	0.07	5.33	0.26
Thigh L	0.12	2.01	0.84	1.97	0.17	0.94
Leg L	-0.07	7.33	0.65	-0.12	7.11	0.72
Foot L	0.06	6.53	0.88	-0.19	7.63	0.78
L. Back R	0.04	3.16	0.56	-0.03	3.85	0.67
L. Back L	0.04	3.12	0.48	-0.03	3.79	0.95
Pelvis	0.07	1.91	0.64	0.09	1.77	0.98
Overall	0.06	4.52	0.83	-0.02	5.32	0.82

In order to fulfill the definition of the T_{eq} and satisfy Eq.35 the segmental h_{cal} need to be correlative to the heat losses (Q_s) and the temperature difference ($\Delta T = T_{sk} - T_{eq}$). Thus, the obtained h_{cal} from the calibrations were correlated with the correspondent Q_s and ΔT. Fig. 31, 32 and 33 show the obtained h_{cal} for 20 body segments against the ΔT using the two modes under the calibration conditions. Generally, the difference between the obtained values (at nearly similar ΔT) by the two modes was mostly within 0.5 W/m²K which is in same level as the differences related to the

measurements' repeatability. The obtained values using the *MSP* mode were under a narrower range of ΔT (especially for the feet and hands) since this mode sets the skin surface temperature based on the indoor condition.

Table 5 shows the linear h_{cal} correlations' constants and the R^2 for the two modes. For most body segments, the R^2 of the linear correlations was in a range from 0.6 to 0.9. The segments with weak linear correlation (e.g. head with the *MSP* mode) had nearly constant h_{cal} under the different calibration conditions. For these segments, the obtained h_{cal} values at 24°C were used directly in the T_{eq} estimations.

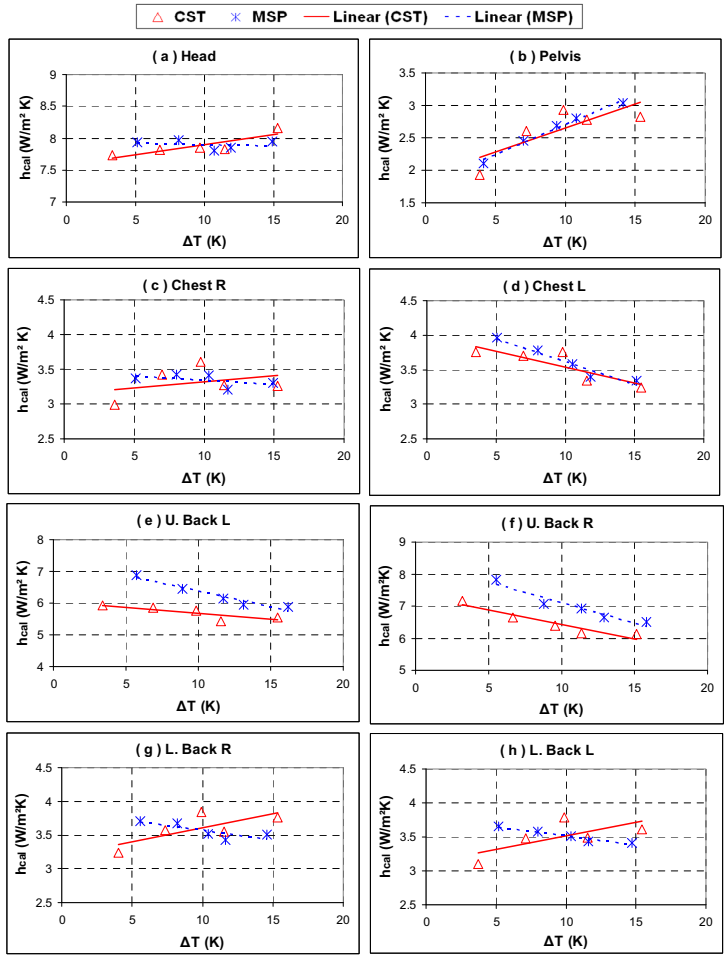

Figure 31 Heat transfer coefficients at the different temperature levels and linear correlations for head and trunk segments using the *MSP* and the *CST* modes

The obtained h_{cal} are specific to the manikin 'THERMINATOR' with the used clothing ensemble. The accuracy of the obtained h_{cal} may be influenced by uncertainties of measuring instruments, slight changes in the manikin posture and the clothing thermal insulation impact on the convective air flow under the different room temperatures. The differences between right and left body segments (e.g. feet, legs) may be additionally

related to a slight non-uniformity in clothing and room condition. The impact of the clothing insulation on the estimation of the heat transfer coefficient was emphasized in earlier studies. Nilsson (2004) stated that the less clothing insulation, the more sensitive will be the manikin segments to the thermal influences. The same was reported by Melikov and Zhou (1999) that the clothing insulation diminished the impact of air temperature on the heat transfer coefficient.

In these experiments, the same clothing ensemble was used throughout all procedures, including the calibrations, following Nilsson's recommendations (Nilsson 2004). The heat transfer coefficients of some body's segments (e.g. chest, upper back) were nearly constant and with slight instrumental errors their correlations may be misinterpreting the physical relationship with the ΔT. Therefore, the authors need to emphasize that the obtained h_{cal} are maybe comparable to data from the literature; however, they primarily correspond to the manikin segmental geometry, physical condition and the used clothing insulation as well as the used measurement devices under these experiments' conditions.

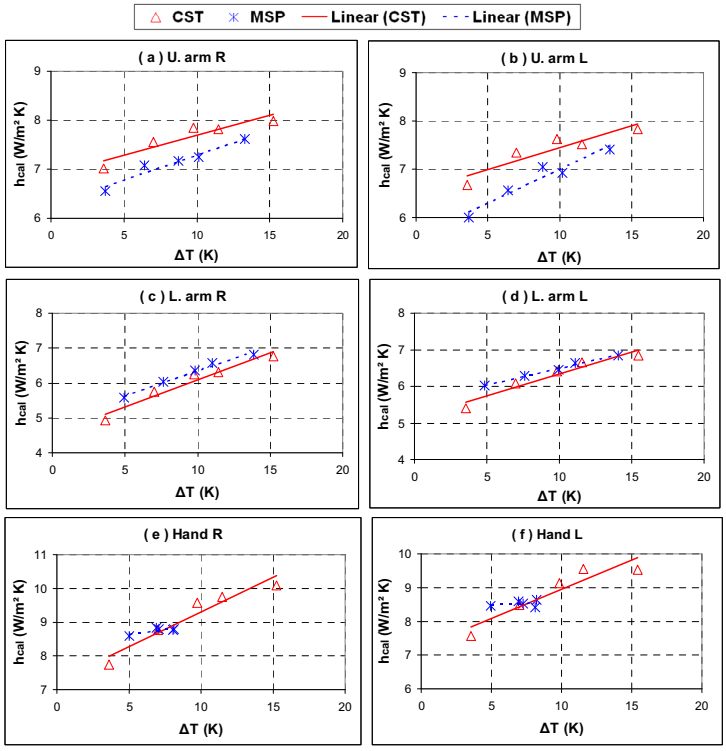

Figure 32 Heat transfer coefficients at the different temperature levels and linear correlations for upper limbs segments using the *MSP* and the *CST* modes

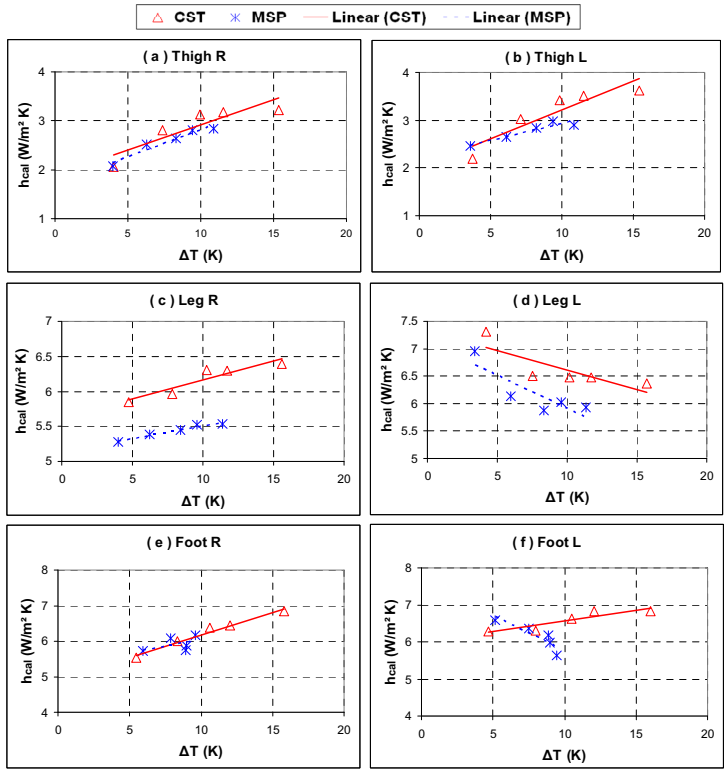

Figure 33 Heat transfer coefficients at the different temperature levels and linear correlations for lower limbs segments using the *MSP* and the *CST* modes

4.8. Subjective assessments

Seventeen male subjects voluntarily participated in the assessment of the two indoor conditions (i.e. Case 1 and Case 2). The mean age of the participants was 32 years old (SD 7), their mean body mass index (BMI=Weight/Height²) was 26 kg/m² (SD 4) and their mean body fat percentage, calculated using Hodgdon and Beckett 1984, was 23%. (SD 7). The subjects wore the same clothing ensemble from the manikin experiments and had exactly the same setup. The human subjects were asked to refrain from eating 2-3 h and to remain indoors at least for 1-h before the pre-conditioning period of the experiments.

The measurements of their body weight, height using a regular balance beam scale and oral temperatures using ear thermometer were carried out upon their arrival to the test place. The pre-conditioning period lasted for 20-30 min and was spent in an adjacent room. The pre-conditioning room (shown in Figure 29) was set at a slightly cooler temperature and was equipped with an infra-red heater. The subjects were allowed to control the heater power to attain comfort sensations for all body segments before moving to the main test room. The subjects had normal office work with

their own portable computers during the whole test period. The test duration was 1 h at which the subjects reported their segmental and overall thermal votes twice. The votes were on the given scale by Nilsson (2004) in the comfort zone diagram. The subjects first were asked to vote their thermal sensations according to the comfort zones (too hot, hot but comfortable or acceptable, comfort, cold but comfortable or acceptable, too cold) and then give the numeric votes according to the zone's suggested range (as shown in Table 4). The voting using the comfort zone diagram aimed at enhancing the relevance for the comparisons between the thermal manikin experiments and the subjective assessment.

The subjective votes were reported twice in the 1-h tests (every 30 min). In Case 1, the relative percent difference (*%Diff= |(Diff/Average)*100|*) between the two votes was significant, for example, the *%Diff* was 50% for the feet, 40% for the hands and 20% for the overall vote. In Case 2, the *%Diff* decreased by 30-50% (compared to Case 1) for most body segments. However, the average of the *%Diff* was still around 20%. Thus, the final votes that were reported at the end of the 1h duration for both cases were the considered ones. Figure 34 and 35 show the mean, min, and max thermal votes as well as the standard deviation (SD) for Case 1 and 2 respectively. The values shown on the figures are obtained from the subjects′ reported votes after 1h. In Case 1, the variability in the thermal votes was higher for the limbs segments (e.g. SD 0.8 for the feet). The variability increased for all body segments (SD 0.6-0.85) in Case 2. In general, the high variability is mainly related to the diverse sample of the human subjects who participated in the assessment. The difference in the variability between the limbs and other body segments in Case 1 may be related to the differences between the subjects in their thermoregulatory responses under cool conditions especially at the limbs. While in Case 2 the equable variability may be explained by the narrow range of body skin temperatures (i.e. ≈2.5K) that occur in warm conditions (Foda and Sirén 2011b).

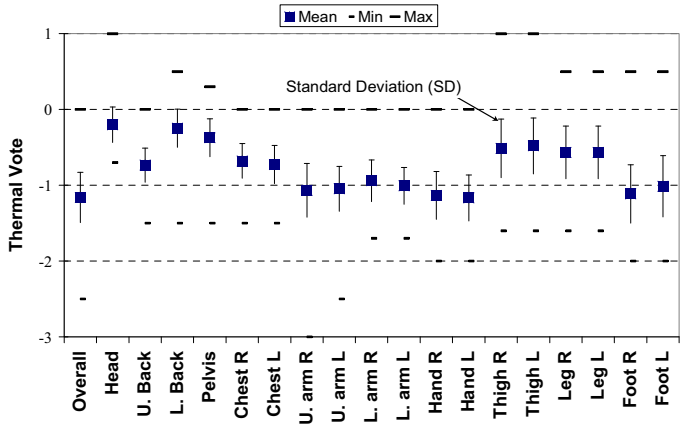

Figure 34 Subjective votes under Case 1 conditions (slightly cold)

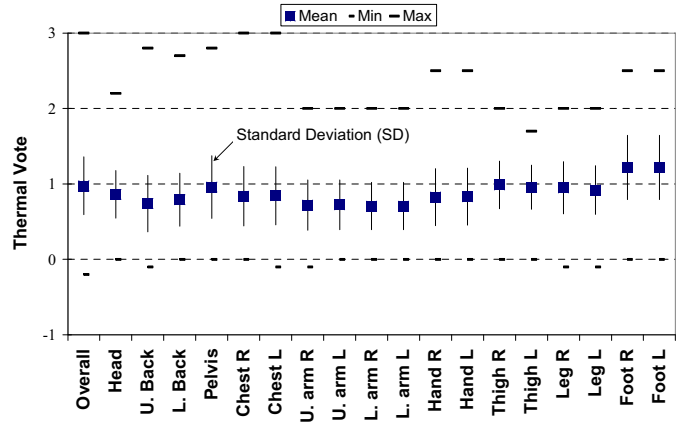

Figure 35 Subjective votes under Case 2 conditions (slightly warm)

4.9. Comparison's results

The thermal manikin experiments were conducted under two conditions (i.e. Case 1 and Case 2) using the *MSP* and the *CST* modes. The segmental and overall heat losses and the measured skin temperatures were recorded at 1 min time interval. These were substituted along with the obtained h_{cal} in Eq.35 to calculate the segmental and overall T_{eq}. The estimated segmental and overall T_{eq} by the *MSP* and the *CST* modes as well as the estimated values (using Eq. 36) from the subjective assessment are shown in Figures 36 and 37. The comfort zones' borders are also presented on the figures.

Table 6 Absolute differences between the estimated T_{eq} by the two modes and the subjective assessment

Used coefficients in Eq.(2)			Δteq (K)	Case 1			Case 2		
			→1 *MTV*	Δteq (K)	Δteq (K)	Δteq (K)	Δteq (K)	Δteq (K)	Δteq (K)
RT (m²K/W)	*a*[a]	*b*[a]		|*MSP-MTV*|	|*CST-MTV*|	|*MSP-CST*|	|*MSP-MTV*|	|*CST-MTV*|	|*MSP-CST*|
0.18	46.7	-20.3	2.58	3.27	3.73	0.46	1.72	1.60	0.12
0.18	46.7	-20.3	2.58	2.45	2.09	0.36	0.91	0.44	0.47
0.18	46.7	-20.3	3.67	3.99	4.26	0.27	0.76	0.41	0.36
0.18	46.7	-20.3	3.67	4.19	4.46	0.27	1.08	0.73	0.36
0.19	46.7	-20.3	3.94	0.39	1.20	0.82	0.29	0.67	0.96
0.19	46.7	-20.3	3.94	0.97	0.00	0.97	1.29	2.39	1.10
0.34	39.5	-19.5	6.53	3.34	2.99	0.35	1.34	3.23	1.89
0.20	65.5	-33.9	4.81	0.65	0.87	0.22	0.27	0.67	0.41
0.11	84.9	-57.2	6.23	0.08	0.83	0.75	3.67	3.51	0.16
0.11	84.9	-57.2	6.23	0.85	0.95	0.10	3.38	3.20	0.18
0.24	43.0	-21.1	5	0.94	0.63	0.31	0.16	0.34	0.18
0.24	43.0	-21.1	5	0.12	0.62	0.50	0.09	0.52	0.44
0.24	43.0	-21.1	5.15	0.39	0.27	0.12	0.45	0.18	0.63
0.24	43.0	-21.1	5.15	1.72	1.55	0.17	0.32	0.88	0.56
0.28	36.1	-20.5	5.68	2.35	3.56	1.21	2.31	1.61	0.70
0.25	36.1	-20.5	5.15	3.99	5.00	1.02	0.11	1.27	1.38
0.20	43.8	-13.3	2.55	2.57	4.55	1.98	0.55	0.62	1.17
			ADD (SD)	1.9 (1.4)	2.21 (1.7)	0.58 (0.5)	1.11 (1.1)	1.31 (1.1)	0.65 (0.5)

[a] These values are obtained from Nilsson (2007)

Table 6 shows the absolute deviations from the subjective assessment and between the two modes as well as the segmental ΔT_{eq} which implies 1 degree (*MTV*) on the sensation scale. The table also shows the segmental *RT*, *a* and *b* coefficients which were used to construct the comfort zone diagram.

As can be seen, the estimated T_{eq} (for most body segments) by the *MSP* mode were closer to the subjective assessment for the two cases. In Case 1, the average absolute deviation (AAD) was about 1.9K (SD 1.4) while the maximum absolute deviation was around 4K at the legs and back segments. In Case 2, the AAD decreased to 1.1K (SD 1.1) while the maximum deviation was 3.7K at the hands. The deviations on the thermal sensation scale can be calculated by dividing the absolute deviation values by the correspondent segmental ΔT_{eq} from Table 5. On the thermal sensation scale, the AAD from the subjective assessment was only 0.5 (SD 0.4) and 0.25 (SD 0.2) for the *MSP* mode in Cases 1 and 2 respectively while it was slightly higher for the *CST* mode.

Generally, the estimated T_{eq} values by the *MSP* mode were favorably comparable with the values by the *CST* mode. The AAD was 0.6 and 0.7K (SD 0.5) for Cases 1 and 2 respectively. The maximum absolute deviation between the two modes was <2K. The AAD between the obtained values by the two modes on the thermal sensation scale was less than 0.2.

The results show that the *MSP* mode is a valid control mode for the estimation of the T_{eq}. The realized improvements by the *MSP* mode for the simulation of the human thermal presence were not significant based on

these results for the estimation of the T_{eq}. However, the *MSP* mode introduces more realism to the thermal manikin experiments and represents adequately the body state subject to the clothing insulation and the indoor conditions. It is easy to implement onto the control system of thermal manikins and has a short response time.

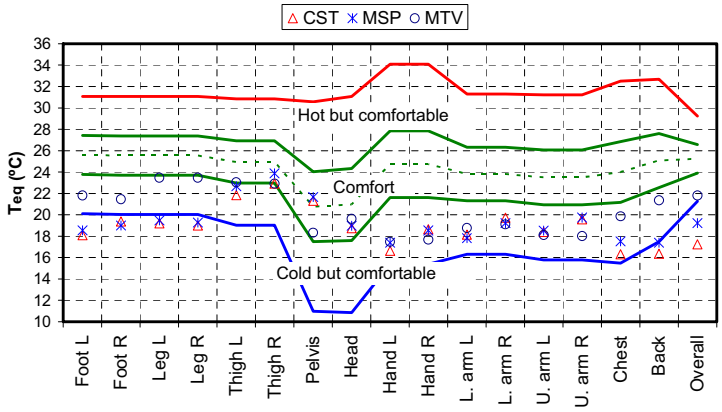

Figure 36 Estimated T_{eq} (on the comfort zone diagram) using the *CST* and *MSP* modes as well as the subjective votes '*MTV*' under Case 1 conditions

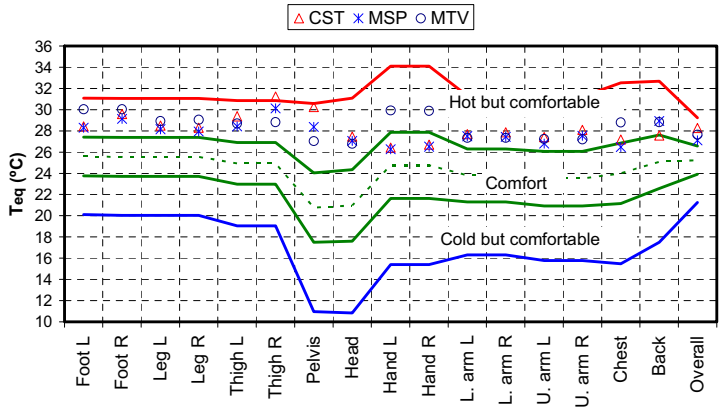

Figure 37 Estimated T_{eq} (on the comfort zone diagram) using the *CST* and *MSP* modes as well as the subjective votes '*MTV*' under Case 2 conditions

4.10. Summary

A new thermoregulatory control mode (i.e. the *MSP* mode) based on the MS-Pierce model was implemented onto the control system of the thermal manikin 'THERMINATOR'. This was carried out using LabVIEW platform which introduces intuitive programming environment. THERMINATOR was used in the estimation of the equivalent temperature under two different indoor conditions using the *MSP* mode along with the widely recognized constant surface temperature mode (*CST*). Additionally, subjective assessments of the same indoor conditions were carried out using 17 subjects. The obtained values by the *MSP* mode, compared to the *CST* mode, were closer to the subjective assessment for most body segments

under the two conditions. The average absolute deviation between the MSP mode and the subjective votes on the thermal sensation scale was 0.5 (SD 0.4) and 0.25 (SD 0.2) under the two conditions respectively. Moreover, the obtained values by the *MSP* mode were favorably comparable to the values by the *CST* mode. The average absolute deviation was around 0.7 K (SD 0.5) that is <0.2 on the thermal sensation scale under the two conditions. These results suggest that the *MSP* mode is a valid mode for the estimation of the equivalent temperature. This new mode offers more possibilities for enhancing the use of conventional thermal manikins and improving the simulation of the human thermal presence in space. It can easily be implemented and has a short response time.

5. Application of thermal manikins in the design of HVAC systems

5.1. Objectives

The work of this chapter aimed at employing the thermal manikin 'THERMINATOR' with the new control mode in the design process of localized HVAC systems towards energy efficiency in buildings. This work focused on localized floor-heating systems. However, the same methodology may also be applied for the investigation of other localized systems.

5.2. Optimization-based design strategy

Optimization-based design is a used technique to assist the engineering design process. This is by setting clearly the design problem; addressing the objectives and constraints; and providing optimum solutions. The optimum solution may be found by solving the optimization problem in many different ways. In this study, an experimental technique was used to find the optimum configuration(s) among a set of variants of a localized floor-heating system, focused on the surface area; geometry and surface temperature. The optimum surface temperature of each system variant is experimentally found subject to a thermal comfort criteria and a constraint for the allowed maximum temperature. The evaluation of the thermal comfort was carried out using a thermal manikin with human thermoregulatory control. The energy consumption was measured at each case to find the minimum consumption among the experimented variants.

The design problem may be formulated on the shape of an optimization problem to minimize the system power and hence, maximize the energy efficiency of the system:

$$\text{Min} \quad P(x, A, T_s, T_{amb}) \tag{37}$$

Subject to $T_s \leq 40$

$$-1.5 \leq \text{LTC} \leq 1.5$$

$$I_{cl} = 0.6$$

$$\text{OTC} = -1.5\,,$$

where

P is the system power (W)

x is the floor heater geometry

A is the floor heater surface area (m²)

T_s is the floor surface temperature (°C)

T_{amb} is the ambient temperature (°C)

I_{cl} is the clothing intrinsic thermal resistance (clo=0.155m²K/W)

LTC is the local thermal comfort index

OTC is the overall thermal comfort index.

The inequality constraint for the floor surface temperature sets a maximum surface temperature of 40°C. The selected value of the maximum surface temperature was chosen according to the system's maximum power under 17-18°C ambient temperature. The value does not follow the given limit of floor's temperature in ISO7730 (ISO 2005) which may not be applicable for a localized system in such large spaces; and it is going to be evaluated in this study using the local comfort concept. The inequality and equality constraints for the local and overall comfort criteria respectively, are adopted from the comfort zones introduced by Nilsson (2004). The equality is used only with the overall thermal comfort to set an easier approach for the comparison between the different variants. Furthermore, the lower limit of the comfort zone (i.e. -1.5) was used in the equality taking into account the light clothing ensemble (0.6 clo) used in these experiments.

5.3. Modifications to THERMINATOR's program

In this work, THERMINATOR's program on LabVIEW was modified to use the *MSP* control in a dynamic mode for real-time measurements and present correspondent estimation of the local and overall thermal comfort (using Eq.35 and 36) as well as the online measurements of the micro-climate environmental conditions on the system's front panel. The *MSP* model was used to calculate the steady-state skin temperatures during the manikin's warming up period to set the initial values for the dynamic mode with the real-time measurements. The segmental set-points were updated

at 1min time step based on the averaged environmental measurements over that interval.

5.4. Floor heater variants

Heated floor tiles (60x60cm) were used to form the different floor heater variants. These variants had different surface areas and/or geometries as shown in Figure 38. The black node shown on the figure represents the manikin position on the floor and the dotted rectangles gather the different geometries of variants that have the same surface area.

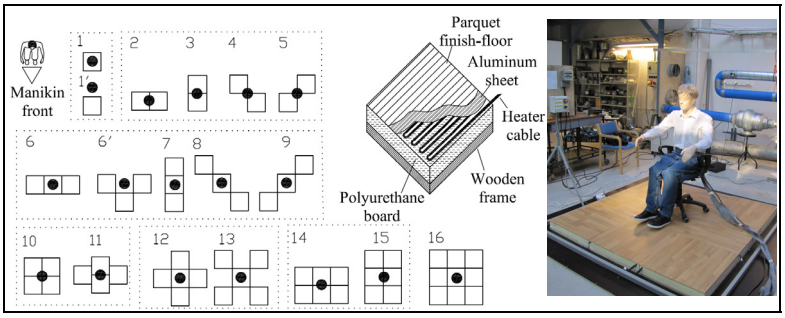

Figure 38 Different variants of the floor heater and a cutaway diagram of the floor tile

The figure also shows a cutaway diagram for the construction of the floor tile and a photo for the manikin at the task area. The tiles were heated using a floor heater cable (deviflex DTIP-18, Danfoss) that was wound over a 10cm thick polyurethane grooved-board. This was covered with a 2mm thick aluminum sheet and parquet finish-floor. All layers were tightened using screws from all sides on a 3cm thick wooden frame. The use of electrical heating, in this study, was to simplify the experimental setup and measurements; however, the heating of the floor tiles could preferably be based on a hydronic system.

5.5. Experimental setup and procedure

The experiments were conducted in a large hall space at the HVAC laboratory at Aalto University. The hall layout and experimental setup are shown in Figure 39. The different variants of the floor heater system were used at the task area under a lowered ambient temperature around 18°C. The thermal manikin 'THERMINATOR' was employed with the *MSP* control mode to verify the fulfillment of the thermal comfort criteria at each test. The energy consumption by each system variant was periodically measured over the whole experiment period using a domestic electricity meter (analog meter). This was used to estimate the variant's power under steady-state operation. The surface temperature of the floor tiles was controlled using a proportional–integral–derivative (PID) temperature

controller (TTM-04SP, Toho Elec. Inc.). An infra-red camera (ThermaCam-P60, Flir Systems Inc.) was used to calibrate the surface temperature of the floor tiles and obtain the average mean value for each system variant.

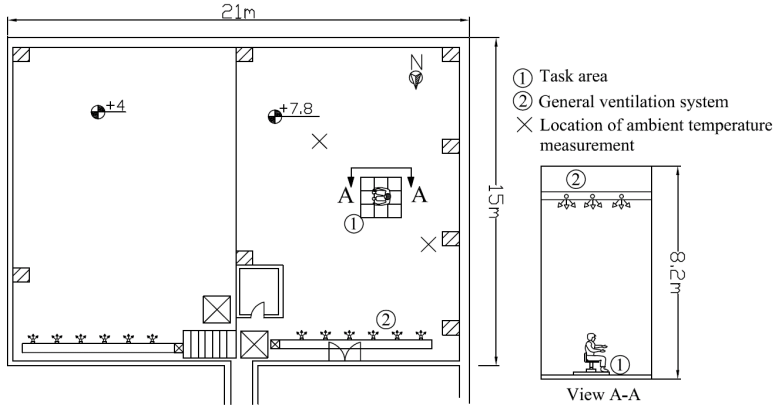

Figure 39 Hall layout and experimental setup

A constant air volume/variable air temperature (CAVVAT) control scheme of the supply air was used with the general ventilation system to maintain the planned ambient condition at the hall space. However, fluctuations of air temperature and velocity as well as temperature gradients can expectedly occur in such a large hall space. In pilot tests, these room physical parameters were evaluated. Generally, the mean air velocity in the hall (at 0.6m height) was around 0.15m/s with turbulence intensity of 20%. The mean ambient temperature in the hall (at 0.6m height) was around 18°C (SD=0.1) with a vertical temperature gradient of 1K between 0.1 and 1.1m height. The use of the *MSP* control mode with the manikin measurements in a dynamic mode aimed at accounting for these fluctuations and interacting accurately with the surrounding environment. In addition, the experiments were carried out in the peaceful evenings to have nearly fixed internal gains and enhance the relevance of the comparisons between the different system variants.

In all procedures, the manikin wore a clothing ensemble that consists of: under-shirt, shorts, denim trousers, long-sleeve shirt, calf-length cotton socks and shoes. The clothing intrinsic thermal insulation value was measured (0.6clo) according to ISO9920 (ISO 2007) regulations using the manikin in a sitting posture under uniform conditions in a controlled environment. Online measurements of the indoor conditions were carried out during the whole experimental procedures. The air velocity was measured, at 3 different heights in the task area, using transducers (8465/75, TSI Inc.). The air and operative temperatures, at same heights, were measured using thermocouples and globe thermometers (T type, accuracy ±0.5K). This was used to calculate the radiant temperature at the

same three heights according to ISO7726 (ISO 1985). The measurements at the task area were connected through the manikin's data acquisition interface (NI USB-6225, National instruments). These measurements averaged over 1 min interval were used with the manikin's *MSP* control. Furthermore, the ambient temperature was measured using thermistors (U type, Grant instruments) at same 3 heights from two locations in the hall (shown on Figure 39). Airflow indicator kit (CH00216, Dräger Tube) was randomly used during the experiments at the task area to visualize the air movements. Generally, horizontal air draughts were observed at the task area below 0.6 m height and toward the north direction (see Figure 39). The relative humidity (*RH%*) was around 30% during all experiments. This was measured using a humidity indicator (HM141, Vaisala). The ambient measurements were connected through a data acquisition unit (Squirrel SQ2040, Grant instruments) and were recorded at 10s time interval. The average outdoor temperature during the time of the experiments in January 2012 was -2°C (SD=2K). A test procedure normally started by: setting the floor variant at a certain surface temperature, meanwhile the thermal manikin was operated in active mode and then the data were collected for approximately 1h when the manikin/floor system reached steady-state and stabilized at the target temperature. The same procedure was then repeated with another surface temperature in case the selected surface temperature did not fulfill the comfort criteria. All measurements were connected on a personal computer and were monitored by the author during the whole experimental procedures.

5.6 Optimum configuration(s) of a floor-heater

The experiments were carried out to evaluate the performance and find the optimum configuration including geometry, surface area and temperature from the different floor-heater variants under the described conditions in the hall space. The local and overall comfort levels measured by the thermal manikin were the driver of the performance evaluation of these system variants. Figure 40 shows the local and overall comfort level under the conditions by the different system variants. The figure was subdivided into 6 subfigures to help improve the visibility of the data. Figure 40a shows the results of the largest and smallest variants while the subfigures from b to f gather variants with the same surface area. The MTV's for a reference condition with no local heating and the borders of the comfort criteria (adopted from Nilsson, 2004) are marked on all subfigures. As can be seen, less than half of the experimented variants could fulfill the comfort criteria. The comfort level was near to the lower bound of the comfort criteria (i.e. -1.5) at the upper back, chest and leg segments while it

was mostly around neutral at other segments such as lower back, thigh, foot and pelvis.

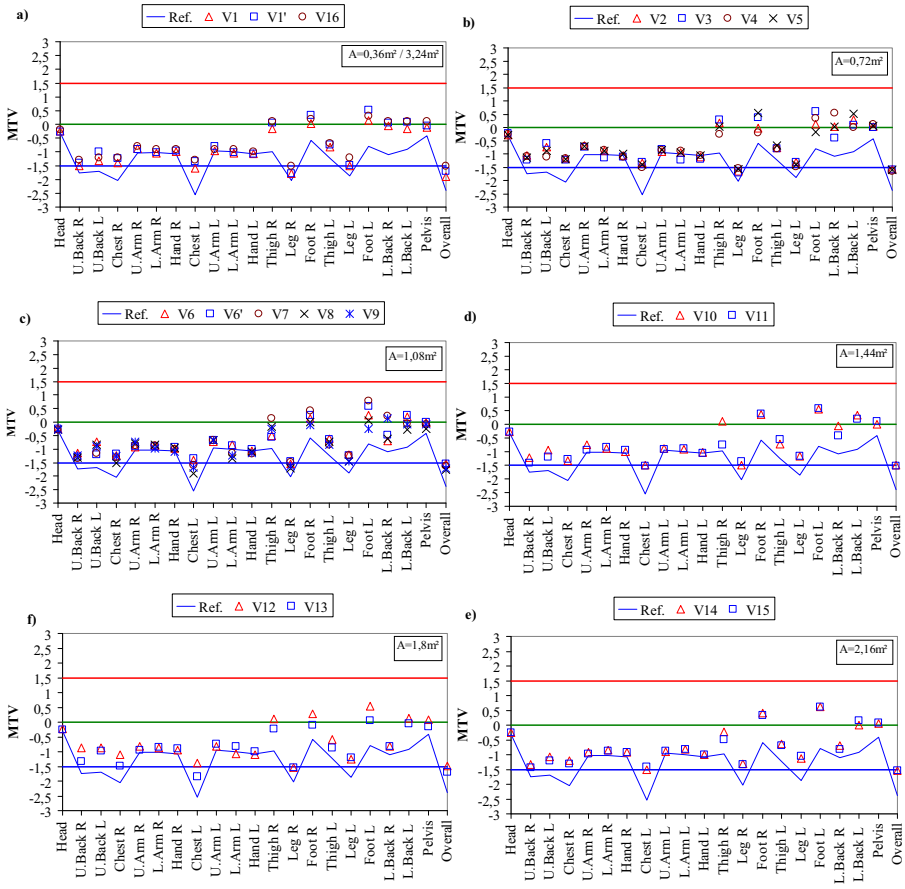

Figure 40 Segmental and overall mean thermal votes (MTV) measured by the thermal manikin for all tested variants

The optimum surface temperature for each variant was experimentally found subject to the thermal comfort criteria and limited by the allowed maximum floor temperature. The allowed maximum floor temperature (i.e. 40°C) was not sufficient to fulfill the comfort criteria for all variants with 1 or 2 tiles. Furthermore, it was neither sufficient for most of the 3 tiles variants nor for the "X" shape variant (V13). Generally, the optimum surface temperatures of the qualified variants were in a range from 31 to 40°C. Figure 41 shows the measured power of each system variant and the overall thermal comfort (OTC) realized by these variants. The figure shows the qualified variants with shaded markers and a dotted line for the lower bound of the OTC. Error bars were used on the figure with the measured powers to indicate uncertainty of 5% in this measurement with the analog electricity meter used. Table 7 gives the characteristics of the different system variants and the order of optimum configurations. Generally, the

surface area of the heated floor was proportionally correlated with the surface temperature. This was physically consistent with respect to radiant and convective heat transfer phenomena. The geometry of the variants had a clear impact on the results. For example, variants with the same surface area (e.g. V14, V15 and V10, V11) required different surface temperatures to fulfill the comfort criteria. Furthermore, variants with the same surface area (e.g. V6, V7 and V12, V13) fulfilled or did not fulfill the comfort criteria.

Additionally, variants with considerable difference in the surface area as V14 and V16 required surface temperatures of only 1K difference (i.e. 32 and 31°C respectively) to fulfill the comfort criteria. Based on these experimental results, it was found that careful geometrical planning of a heated floor area around a seated person can lead to energy-efficiency and be more effective pertaining to thermal comfort. The heated floor posterior to the manikin position was less beneficial since the body from that side was mostly insulated by the seat back-rest. This was clearly manifested from results of different variants (e.g. V14 and V15).

Furthermore, the heated floor diagonally placed against the manikin's position was also proven to be less beneficial when compared the results from V1 with V8 or V9 results. On the other hand, the heated floor on the sides and anterior to the manikin position was proven to be most effective. The experiments of variants V1 and V1' showed that the placement of a heated tile under the seated manikin was less effective than with the anterior position. With variant V1', the OTC was improved by 0.2 on the comfort scale compared to variant V1. Then based on this finding and when variant V6 was found to fulfill the comfort criteria, we formulated the variant V6' and expected further better energy performance. The variant V6', as expected, fulfilled the comfort criteria with the least system power.

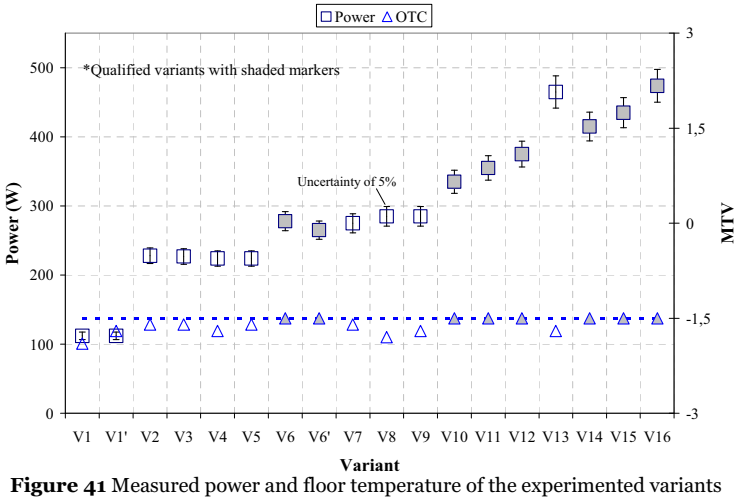

Figure 41 Measured power and floor temperature of the experimented variants

Based on the verifications carried out, these findings may be generalized to similar types of spaces. However, they are partly related to the experimental setup described and may have been partly influenced by the direction of the observed air draughts (see section 5.5) at the task area. In these experiments, the lower bound (i.e. -1.5) of the acceptable comfort range (Nilsson 2004) was used in the comfort criteria with that light summer clothing (0.6clo) of the manikin. Then with winter clothing used normally indoors, these system variants with the suggested surface temperatures may provide higher comfort level or can be optimized to operate with lower surface temperatures.

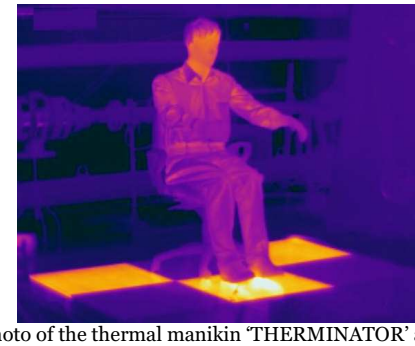

Figure 42 IR-photo of the thermal manikin 'THERMINATOR' and the floor heater variant V6'

Table 7 Characteristics of the experimented floor-heating system variants and optimum configurations

Variant	Surface area, A (m²)	No. of tiles	Floor temperature, T_s(°C)	Comfort Criteria	Power (W)	Order of optimum configurations
1& 1'	0,36	1	40		112	
2	0,72	2	40		228	
3	0,72	2	40		227	
4	0,72	2	40		224	
5	0,72	2	40		224	
6	1,08	3	40	×	277	2
6'	1,08	3	39	×	265	1
7	1,08	3	40		278	
8	1,08	3	40		285	
9	1,08	3	40		285	
10	1,44	4	37	×	335	3
11	1,44	4	38	×	355	4
12	1,80	5	36	×	375	5
13	1,80	5	40		465	
14	2,16	6	32	×	415	6
15	2,16	6	34	×	435	7
16	3,24	9	31	×	474	8

The scope of this study was mainly to find the optimum configuration related to geometry, surface area and temperature that minimize the energy use. The measured power figures may further be minimized by optimizing the construction and heating method of the floor heater. However, the monthly energy saving due to this localized system (based on current construction) along with the reduction in the temperature set-point was

estimated to be in a range from 10-65% while the annual saving was around 17% for the shopping mall's application. This was estimated using IDA-ICE 4.0 building energy simulator based on the capacity of the general ventilation system of our hall and assumption that 10% of the hall area is considered as the resting spots. The illustrated methodology may be also be implemented in the design of other types of localized HVAC systems towards energy-efficiency and thermal comfort in buildings.

5.7. Summary

An experimental setup was constructed to simulate a task area in a large hall space under a lowered ambient temperature (i.e. ≈18°C). Eighteen variants of localized floor-heating system with different surface areas and/or geometry (formulated using heated tiles 60x60cm) were tested at the task area subject to comfort criteria. The fulfilment of the comfort criteria was evaluated using a thermal manikin with human thermoregulatory control that dynamically interacts with the surrounding environment. The objective was to obtain the optimum geometry, surface area and temperature that minimize the energy use. The experiments showed that the geometry of the heated floor had a clear impact on the effectiveness pertaining to thermal comfort; and hence, the energy-efficiency. The heated floor posterior, under the seat and diagonally placed subject to the manikin position was proven to be less effective compared to heated floor on the sides and anterior to the manikin position. These findings may be partly related to our experimental setup including the ambient condition and the used clothing ensemble. Only 8 system variants (among 18) could fulfil the comfort criteria. The system variant that could fulfil the comfort criteria with the least measured power consisted of 3 tiles that surrounded the manikin from the two sides and in anterior position. The total surface area of that variant was nearly 1m² while the required surface temperature was around 39°C. The annual energy saving due to this localized system along with the reduction in the temperature set-point was estimated to be around 17% for the shopping mall's application. The used methodology may be implemented similarly in the design of other types of localized HVAC systems towards energy-efficiency and thermal comfort in buildings.

6. Predictive methods of thermal comfort

6.1. Objectives

The work in this chapter aimed at investigating and comparing the available methods for the prediction of the local and overall thermal comfort using subjective tests from the literature. The methods in the scope of this chapter are those which are based on psycho-physical and physiological quantities in their construction. Then, this chapter introduces a psychological comfort model that was adapted for the use with the multi-segmental Pierce model.

6.2. Comparison of local thermal comfort models

Two known methods for the prediction of local thermal comfort, on body segmental basis, of individuals that are the T_{eq} approach (Wyon 1989) and the UCB comfort models (Zhang 2003).

The T_{eq} approach is represented in this comparison by the suggested comfort zone diagram (clothing independent diagram) in Nilsson's thesis (2004). Nilsson (2004) carried out experiments in 30 different climatic conditions using two thermal manikins to measure the segmental and overall sensible heat losses. The measured heat losses were used to calculate the segmental and overall T_{eq}. Then, the obtained T_{eq} under these conditions were correlated with subjective votes from human subjects' tests under the same test conditions. The subjects (20 subjects at each condition) reported their local and overall thermal sensations on a scale similar to the Bedford scale. The individual's votes were averaged for each test condition and reported as a mean thermal vote (*MTV*). A model for each body segment (Eq.36, Chapter 4) was formulated using linear regression to construct the comfort zone diagram.

Nilsson's model is correlating the indoor conditions (represented by the T_{eq}) with the local or overall *MTV*. In this comparison, the model was used to predict the local sensations, as the local *MTV*, under well defined indoor conditions by substituting the segmental thermal insulation values and the T_{eq} estimated from the indoor conditions using an empirical equation given by Madsen et al. (1986).

The UCB comfort models (Zhang 2003) were based on large-scale experiments that were carried out under uniform, non-uniform and transient conditions (109 human subjects' tests). The models comprises four different models for the prediction of: local thermal sensation for 19

body segments, local thermal comfort for 19 body segments, overall thermal sensation and overall thermal comfort. However, these four quantities are predicted in consequent steps where the overall sensation is based on weighting the local sensations and the comfort is based on a linear correlation with the sensation. The models consist of static and dynamic terms to account for both steady state and transient conditions. In these models, the model of the local thermal sensation represents the motor of that combination. The model proposes that the local sensation is a logistic function of the local skin temperature, represented by the deviation between the local skin temperature and its set-point (i.e. skin temperature at neutral sensations). The model also includes the impact of the whole body state, represented by the deviation between the body mean skin temperature and its set-point, on local sensations.

The UCB thermal sensation model is represented by the following formula (Zhang 2003):

$$\mathrm{LTS} = 4 * \left(\frac{2}{1 + EXP\begin{pmatrix} -C_1 * (T_{skin,local} - T_{skin,local,set}) - K_1 * ((T_{skin,local} - T_{skin,local,set}) \\ -(T_{skin,mean} - T_{skin,mean,set})) \end{pmatrix}} - 1 \right) + C2_i \frac{dT_{skin,local}}{dt} + C3_i \frac{dT_{co}}{dt}, \quad (38)$$

where LTS; is the local thermal sensation, C_1; is a regression coefficient that varies for different body segments, $T_{skin,local}$; is the local skin temperature (°C), and $T_{skin,local,set}$; is its set-point (°C), K_1; is a regression coefficient for the whole body's state impact on the local sensations, $T_{skin,mean}$; is the mean skin temperature (°C), and $T_{skin,mean,set}$; is its set-point (°C), $C2_i$ and $C3_i$; are the thermal capacities at the skin and core nodes respectively, and T_{co}; is the body core temperature.

The UCB model is not a stand-alone model and needs coupling with a physiological model or to be fed with a measured data. In this comparison, the UCB model was coupled with the multi-segmental Pierce model.

The above two predictive models were tested against subjective tests from a recent study by Cheong et al. (2007). In that study, Cheong investigated the thermal sensation and comfort in an environment served by displacement ventilation. Sixty human subjects (30 males and 30 females) participated in a total of 15 tests, carried out sedentary activities and wore clothing ensembles with an intrinsic thermal insulation value that varied from 0.63 to 1.15clo for the different tests. The local thermal insulation

values were estimated, in this comparison, based on the described garments using the ISO9920 (2007).

The estimation of the LTS was carried out using the coupled MS-Pierce-UCB model (P-UCB) and Nilsson's model (Eq.36) for the 15 different cases given in Cheong's study and was compared with the subjective local *MTV* values given on the ASHRAE and Bedford scales. Figure 43 shows the estimated LTS along with the local *MTV* values. As can be seen, the predictions by both models were nearly in agreement for most body segments (i.e. back, chest, arm, thigh and leg). The discrepancies between the predictions by both models and the local *MTV* values varied for the different body segments. The predicted values were more close to the local *MTV* values for the lower body's segments (e.g. thigh, leg). The discrepancies with the local *MTV* values may, to a small extent, be related to the estimation of the local clothing values for the upper body segments, the assumed metabolic rate (i.e. 65W/m²) and to the models' predictability for tropically-acclimatized subjects.

The comparison between the estimated LTS by the P-UCB model and Nilsson's model was mainly to indicate the differences between the only two known methods for such a prediction (i.e. the equivalent temperature approach and the UCB comfort model). Generally the two methods can provide a nearly similar assessment of the local thermal sensation for some body segments. The UCB comfort model has a variable profile (relies on the skin temperature) at each room condition and involves the whole body effect on the local sensations. The output from the UCB comfort model depends on the skin temperatures predicted by a physiological model. Therefore, the accuracy of its predictions is partly influenced by the predictability of the used physiological model. However, the MS-Pierce model was selected for this coupling as it showed a very good predictability of skin temperature as discussed in Chapter 3.

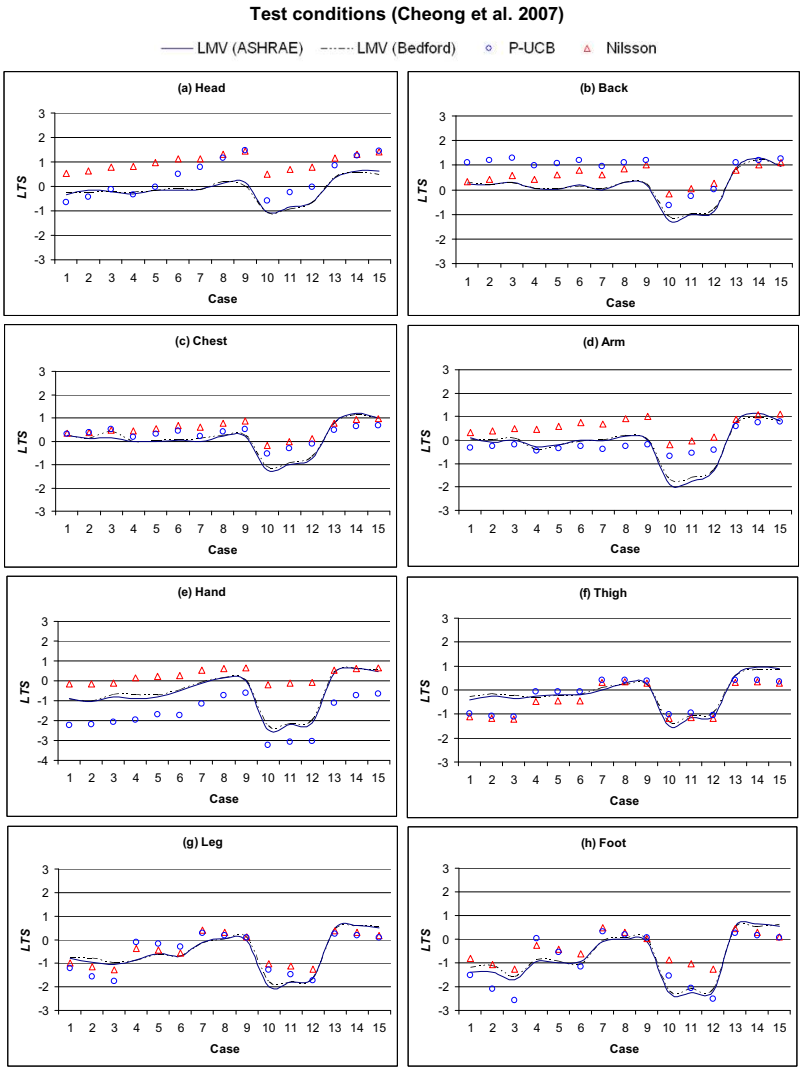

Figure 43 Comparison between the estimated local sensations and subjective votes

Nilsson's model suggests an equally distributed profile for the sensation at different T_{eq} for each segment. While it includes the clothing effect, it does not include physiological or physical effects of the human body on the thermal sensations. The model is limited for a seated person carrying out sedentary activities based on the sample of the measured data. Furthermore, the prediction of the LTS was carried out using the P-UCB model for 16 test conditions given in Nilsson's thesis (Nilsson 2004). These tests were used in the construction of Nilsson's model (Nilsson 2007). The given experimental data includes the segmental T_{eq} along with the local *MTV* values for the different conditions.

The tests involved various asymmetrical thermal conditions. Asymmetries were produced by vertical air temperature gradients and solar radiation.

The twenty male subjects who participated in the experiments wore summer clothing ensembles (R_T =1.3clo). The test duration was 1h in which the subjects voted twice on a scale similar to the Bedford scale once every 30mins. The comparison between the predictions by the P-UCB model and the local *MTV* from Nilsson's thesis may seem irrelevant since the UCB model is based on an extended 9-points ASHRAE scale. However, the favorable performance of the two models (i.e. P-UCB, Nilsson) for the conditions in Cheong's study (Cheong et al. 2007) and the very minor differences between the subjective voting on both scales in that study were encouraging to apply this comparison. The comparison at least should be acceptable for the scale range ±1 which refers to comfortable sensation on both scales. Figure 44 shows the estimated LTS for the body segments by the P-UCB model compared with the subjective local *MTV* values. The estimated LTS by the P-UCB model were nearly in agreement (especially at the higher T_{eq} levels) with the local *MTV* values for most body segments (i.e. back, chest, arm, thigh and leg). For these body segments, the discrepancies between the estimated LTS and the local *MTV* values increased at the lower levels of T_{eq}. The discrepancies at these levels may be related partly to the different sensation scales in that range. The estimation of the LTS by the P-UCB model showed large discrepancies with the local *MTV* values for the head, hand and foot segments. The main discrepancies were at the cold side at which the P-UCB model predicted considerably lower values of LTS.

6.3. Comparison of overall thermal comfort models

While the *PMV* model (Fanger 1970) still holds its position in the standards and guidelines as the most recognized method for the prediction of the overall thermal comfort, several recent models were introduced to overcome the *PMV* limitations in non-uniform and dynamic conditions. The models in this comparison follow the same (engineering) approach that is used with the *PMV* model and are based on psycho-physical and physiological quantities in their construction. These models are the UCB model (Zhang 2003), the dynamic thermal sensation (DTS) model (Fiala 1998), and Nilsson's model (Eq.36 for whole-body).

Fanger (1970) introduced a comfort equation based on the heat balance over the surface of the clothed human body. The comfort equation was then solved for different clothing values and human activities to present the comfort diagrams by which the comfort temperature may be determined for different room conditions. Thereafter, Fanger introduced the *PMV* (predicted mean vote) model in order to quantify the deviation from the comfort condition. The *PMV* index represents the predicted mean vote, on a

thermal sensation scale, of a large population of people (1396 subjects clothed in a standard uniform with a clo-value 0.6) under controlled environmental conditions (in a climate chamber) for three hours. The *PMV* value lies between -3 and +3 based on a symmetric seven point thermal sensation scale in which the zero is the neutrality for thermal comfort and the other six points from -3 to +3 excluding the zero are defined as: cold, cool, slightly cool, slightly warm, warm, and hot, respectively.

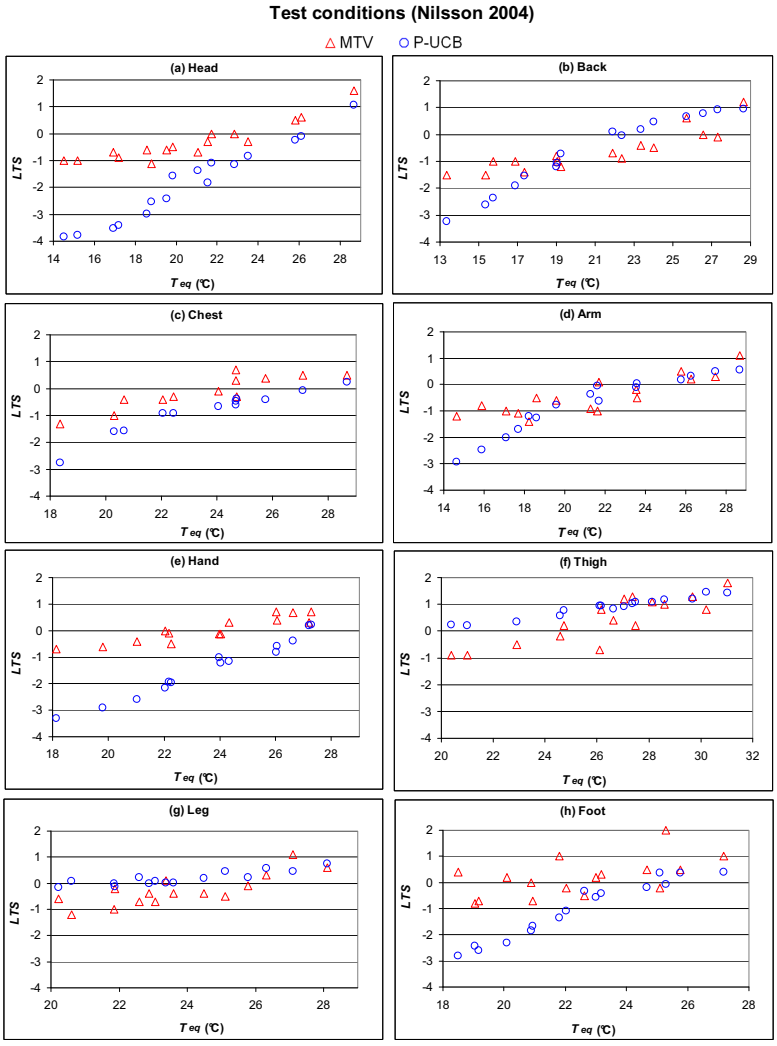

Figure 44 Comparison between the estimated local sensations and subjective votes

In Fanger's derivation of the *PMV* model, the mean vote was thought to be a function of the comfort equation's residue (i.e. the thermal load from combining the left and right hand sides in the comfort equation) and the internal heat production. Then, the partial derivative of that function is estimated by exposing the large population of people to different conditions

to fit a curve.Eventually, the integrated partial derivative is itself introduced as the *PMV* index and is calculated as (Fanger 1970):

$$PMV = \left(0.352 * EXP\left(-0.42\frac{M}{A_D}\right) + 0.032\right) * \left\{\frac{M}{A_D}(1-\eta) - 0.35 * \left[43 - 0.061\frac{M}{A_D}(1-\eta) - p_a\right] - 0.42\left[\frac{M}{A_D}(1-\eta) - 50\right] - 0.0023\frac{M}{A_D}(44 - p_a) - 0.0014\frac{M}{A_D}(34 - T_a) - 3.4 * 10^{-8} f_{cl} * \left[(T_{cl} + 273)^4 - (T_{mrt} + 273)^4\right] - f_{cl} h_c (T_{cl} - T_a)\right\}, \quad (39)$$

where A_D is Dubois body surface area (m²), η is the external mechanical efficiency, p_a is the water vapor pressure (Pa), M is the metabolic rate (kcal/h), T_a is the air temperature (°C), T_{cl} is the clothed body surface temperature (°C), T_{mrt} is the mean radiant temperature in relation to a person at a given location (°C).

The UCB model (Zhang 2003) estimates the overall sensation by weighting the LTS (predicted using the LTS model described in section 6.2) of different body segments. The model may be expressed by the formula:

$$\mathrm{OTS} = \frac{\sum weight_i . \mathrm{LTS}_i}{\sum weight_i}, \quad (40)$$

where OTS is the overall thermal sensation, *i* denotes different body segments, and $weight_i$ is calculated from:

$$weight_i = a * (\mathrm{LTS}_i - \overline{\mathrm{LTS}_i}), \quad (41)$$

where *a* is the slope of the linear model given in Zhang (2003), $\overline{\mathrm{LTS}_i}$ is averaged local sensation (arithmetic mean of LTS_i).

The model proposes a constant slope (from regression) but a variable weight, for each body segment, for each single case.

The above model was replaced recently by Zhang et al. (2010b). As stated in that study, the new model was introduced to improve the predictability of the above model (Zhang 2003). The new UCB model uses a different approach that involves different calculation procedures for different cases and introduces the so called no-opposite and opposite sensation models. However, the model's several calculation procedures seem complex to apply in practice.

Fiala's DTS model (Fiala 1998) calculates the dynamic thermal sensation and accounts for the changes of the core and skin temperatures in steady-state and dynamic situations. The model was constructed using subjective

data under different indoor conditions from the literature and that was correlated with the predicted skin temperatures by Fiala's physiological model (Fiala et al. 1999, 2001). The model is expressed by the following formula:

$$DTS = 3 * \tanh(f_{sk} + \Phi + \Psi), \quad (42)$$

where f_{sk} is a function that accounts for the effect of the deviation between the skin temperature and its set-point, Φ accounts for the effect of core temperature, and Ψ accounts for the dynamic changes in core and skin temperatures on the thermal sensation.

Nilsson's model (Nilsson 2007) is represented by (Eq.36) using the obtained regression coefficients for whole body.

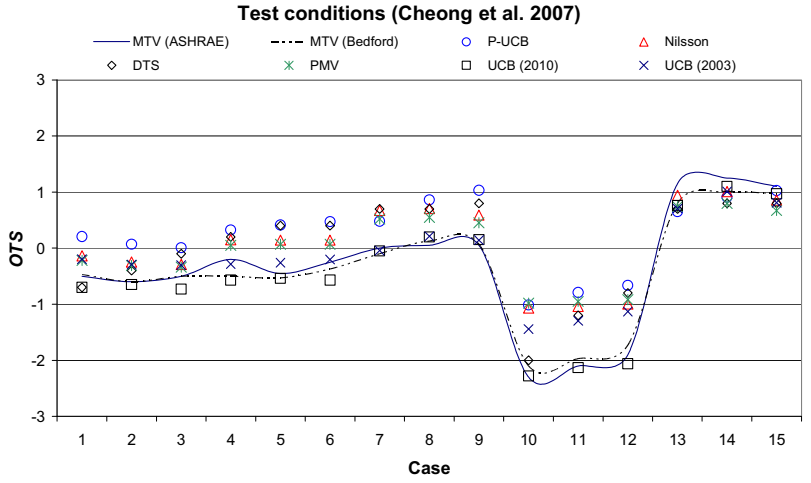

Figure 45 Comparison between the estimated overall sensations from different models and subjective votes

The above methods were tested also against the cases given in Cheong's study (Cheong et al. 2007). The LTS values were substituted in the UCB model (Zhang 2003) from the predicted values by the P-UCB model and using the subjective local *MTV* values. Figure 45 shows the estimated OTS values by the models mentioned above plus the predicted values by Zhang et al. (2010b) using the subjective local *MTV* values for the same cases in validating their new OTS model (Zhang et al. 2010b). The predictions by these different models were nearly in agreement for most cases with discrepancies less than 1 on the scale. The discrepancies with the subjective votes varied for these models and increased for the Cases 10-12. For these cases, the predicted OTS by the UCB model, using the subjective local *MTV* values, shows discrepancies from 0.8-0.9 on the scale. This may explain the poor predictions by the P-UCB model for those cases which is partly due to the comfort model structure. The prediction of the OTS by the P-UCB model is based on the predicted LTS votes by weighting their effects on

whole body state while the other models (i.e. *PMV*, DTS and Nilsson) predict the OTS based on mean physiological variables or based on a separate formula. Although the first approach seems more logical, in this comparison it mostly showed the highest discrepancy with the actual votes. Generally, the lower prediction of the OTS by all these models may be partly related to the assumed metabolic rate and the models' predictability for tropically-acclimatized subjects.

Table 8 Predicted OTS votes by the different models

Cases	MV (ASHRAE)	MV (Bedford)	P-UCB	DTS	Nilsson	PMV	UCB [2][(a)]	UCB [21][(b)]	Max	Min	Average
1	-0.50	-0.47	0.21	-0.70	-0.14	-0.22	-0.20	-0.70	0.21	-0.70	-0.21
2	-0.60	-0.60	0.07	-0.40	-0.25	-0.31	-0.29	-0.65	0.07	-0.40	-0.24
3	-0.50	-0.50	0.01	-0.10	-0.29	-0.34	-0.30	-0.73	0.01	-0.34	-0.20
4	-0.20	-0.50	0.32	0.20	0.15	0.05	-0.28	-0.57	0.32	-0.28	0.09
5	-0.45	-0.53	0.41	0.40	0.14	0.07	-0.26	-0.54	0.41	-0.26	0.15
6	-0.25	-0.37	0.47	0.40	0.14	0.07	-0.20	-0.57	0.47	-0.20	0.18
7	0.00	-0.10	0.48	0.70	0.67	0.52	-0.04	-0.05	0.70	-0.04	0.47
8	0.05	0.13	0.86	0.70	0.71	0.55	0.21	0.20	0.86	0.21	0.61
9	0.05	0.07	1.03	0.80	0.59	0.45	0.14	0.15	1.03	0.14	0.60
10	-2.30	-2.10	-1.01	-2.00	-1.07	-0.98	-1.44	-2.28	-0.98	-2.00	-1.30
11	-2.10	-1.97	-0.79	-1.20	-1.04	-0.95	-1.30	-2.13	-0.79	-1.30	-1.05
12	-1.90	-1.73	-0.66	-0.80	-1.00	-0.92	-1.13	-2.06	-0.66	-1.13	-0.90
13	1.15	0.80	0.65	0.70	0.94	0.74	0.71	0.76	0.94	0.65	0.75
14	1.25	1.00	0.91	0.80	1.01	0.80	1.01	1.10	1.01	0.80	0.91
15	1.10	0.97	1.03	0.80	0.85	0.67	0.81	0.97	1.03	0.67	0.83
AAD			0.73	0.55	0.50	0.53	0.24	0.16			
SD			0.36	0.27	0.31	0.34	0.17	0.12			

[(a)] Calculated using the actual *LMV* values.
[(b)] Obtained directly from [21] and it was calculated there using the actual *LMV* values.

Table 8 shows the predicted votes by these 5 methods plus values from Zhang's study (Zhang et al. 2010b). The table also shows the min, max and mean as well as the standard deviation (SD) values of the results of 5 methods for the different cases. The average absolute deviation (AAD) and the SD for each method are also shown in the table.

6.4. Thermal sensations or comfort

The difference between sensations and comfort can be simply explained that people may indicate warm or cool sensations for whole body or over body segments but meanwhile they may report of perceiving these sensations as comfortable or even preferable conditions. The split between sensations and comfort may be necessary under conditions with extreme thermal asymmetries as in the vehicle environment. Under these conditions, the deviation between the thermal sensations and comfort may increase. Therefore, researchers developed models for the prediction of thermal sensation and for thermal comfort separately (e.g. UCB models, Zhang 2003). However, HVAC practitioners would express less interest in these arguments about thermal sensations and comfort. Indeed, an easier

approach is needed to directly link the thermal sensations to the thermal comfort. The link may be implemented in the used thermal sensation scale. The thermal sensation is usually evaluated using the ASHRAE 7-point scale in which the range from -1 (slightly cool) to +1 (slightly warm) is widely considered as comfort limits. This range may deviate with extreme thermal asymmetries but should be sufficient for evaluations in buildings.

A scale such as Bedford 7-point scale was used in earlier studies as a scale for both thermal sensations and comfort. However, the Bedford scale is not widely used as the ASHRAE scale. Both scales are illustrated in Figure 46.

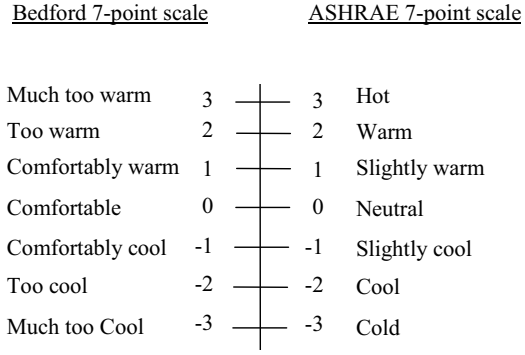

Figure 46 Bedford and ASHRAE 7-point scales

As can be seen, the Bedford scale addresses well the comfort sensations especially in the range from -1 to +1. Then, using a predictive method that is based on such a scale may allow the evaluation of both thermal sensations and comfort and solve this dispute.

6.5. Adaptation of a thermal comfort model

6.5.1. Model construction

The used approach in the construction of this model was focused on adapting a simple rational model for the use with the MS-Pierce model. The local comfort is predicted using a model that is based on the UCB local sensation model's structure (Zhang 2003). However, the UCB model's proposed term for the impact of the overall sensation on body segments was excluded for further simplification at the current research stage. Then, the adapted model accounts only for the local skin temperature's deviation from its set-point. In addition, a standard 7-point scale (Bedford scale) was used instead of the extended 9-points ASHRAE scale (including very cold '-4' and very hot '+4') that is used with the UCB model. Then, when the local skin temperature deviates much from its set-point, the local comfort approaches its extreme values (i.e. -3 and +3 according to Bedford scale). As discussed previously (in section 6.4), the Bedford scale was used in

earlier studies to asses both thermal sensation and comfort. Therefore, it may be seen in that sense as an inclusive good option.

The proposed local thermal comfort model has the following form (Zhang 2003):

$$\mathrm{LTC} = 3 * \left(\frac{2}{1 + EXP(-C * (T_{skin,local} - T_{skin,local,set}))} - 1 \right), \qquad (43)$$

where LTC is the local thermal comfort (based on Bedford 7-point scale); C is a coefficient with a value from 0 to 1 that varies for different body segments; $T_{skin,local}$ is the local skin temperature (°C); and $T_{skin,local,set}$ is its set-point (°C).

In this work, the regression coefficient (*C*) was obtained using subjective votes (on Bedford scale) from two studies (Nilsson 2004 and Cheong et al. 2007) along with the predicted skin temperature's deviation by the MS-Pierce model under the test conditions from these studies. The experimental work in these two studies is described in section 6.2. The approach of this modeling is also similar to Fiala's approach in constructing the DTS model (Fiala 1998).

Table 9 Model's coefficients and correlation with actual votes

Segment	Regression coefficient, *C*		Coefficient of determination for correlation with actual vote (R^2)
	$\Delta T<0$	$\Delta T>0$	
Head	0,14	0,85	0,46
U. Back	0,47	0,55	0,75
Chest	0,4	1	0,79
U. Arm	0,58	0,59	0,75
L. Arm	0,72	0,55	0,69
Hand	0,1	0,4	0,56
Thigh	0,1	0,49	0,88
L. Leg	0,1	0,83	0,75
Foot	0,29	0,85	0,8
L. Back	0,65	0,61	0,86
Abdomen	1	1	0,86
Overall	NA	NA	0,75

The environmental parameters (i.e. air temperature, air velocity and radiant temperature) and the segmental clothing insulation values from the above mentioned studies were entered to the MS-Pierce model to predict the local skin temperatures. The predicted local skin temperatures were correlated with the actual local comfort votes to obtain the coefficient *C* for the different body segments. The coefficient *C* for each body segment was obtained for two cases: when the skin temperature deviation

$\Delta T (= T_{skin,local} - T_{skin,local,set}) < 0$ and when $\Delta T > 0$. Table 9 shows the obtained regression coefficients, and their coefficient of determination (R^2).

The overall thermal comfort (OTC) is estimated, following the local comfort concept, using a weighted average of the local thermal comfort perceived by the different body segments. In this model, the OTC is estimated from the local thermal comfort using the seven point weighted average (Hardy and DuBois 1938) as follows:

$$OTC = 0.07 * LTC_{head} + 0.35 * LTC_{trunk} + 0.14 * LTC_{l.arm} + 0.05 * LTC_{hand} + 0.19 * LTC_{thigh} + 0.13 * LTC_{leg} + 0.07 * LTC_{foot} \quad (44)$$

where the trunk's LTC represents the average of the LTC of the chest, back and abdomen and the extremities' LTC represent the average of the right and left segments. This was featured to account for thermal asymmetries in the space.

The basis for this modeling work was outlined in cooperation with the TSBE centre in Reading University.

6.5.2. Model predictability

The adapted model is specific to the MS-Pierce model and applicable for the predictions of thermal comfort in physiological steady state conditions under uniform or non-uniform environments. The model predictability was initially verified, before integration with CFD simulations described in next chapter, against the subjective data under the described conditions in Chapter 4. This was under two thermally asymmetric conditions that represent slightly cold and warm conditions. Figure 47 and 48 show the predicted and actual votes under the conditions of the two cases. As can be seen, the model predictability, in general, was very good for most body segments and for whole-body based on the 7-point weighting. The AAD was 0.3 (SD 0.2) on the thermal comfort scale for both cases. The model predictability was slightly lower for the feet in Case 1 (slightly cold condition) and for the hands in Case 2 (slightly warm condition). The maximum deviation was 0.9 at the left foot for Case 1 conditions while it was 0.7 at the hands for Case 2 conditions. The 7-point weighting approach predicted well the overall thermal comfort with a deviation that is less than 0.5 on the scale for both cases.

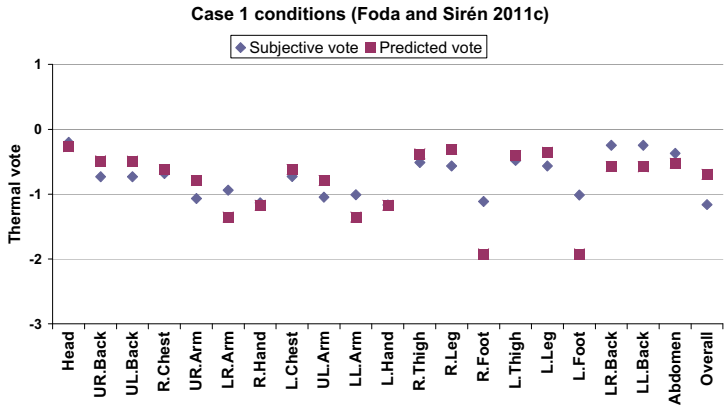

Figure 47 Comparison between predicted votes and actual votes under Case 1 conditions

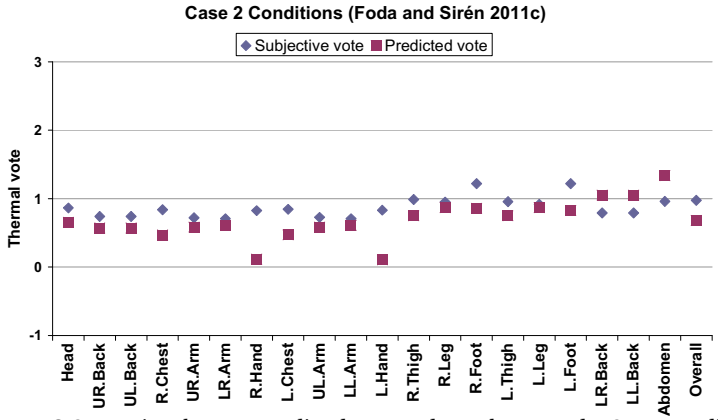

Figure 48 Comparison between predicted votes and actual votes under Case 2 conditions

6.6. Summary

In this chapter, a variety of predictive methods of thermal comfort was investigated. This was focused on methods that are based on psycho-physical and physiological quantities in their construction for the prediction of the local and overall thermal comfort. A recent thermal comfort study that included subjective assessments of the indoor conditions was used to compare the performance of these methods. The MS-Pierce model was coupled with the UCB comfort model to predict the local thermal sensation for the15 different indoor conditions from that study. The predictions by the coupled model (P-UCB) along with Nilsson's model (based on the T_{eq} approach) were compared with the subjective votes from these 15 conditions. The predictions by the two models were nearly in agreement for most body segments. The discrepancies with the subjective votes varied under the different indoor conditions and were generally within reasonable limits. The P-UCB model was further used to predict the local thermal sensation for 16 indoor conditions from the literature. The predictions were nearly in agreement with the subjective votes for most body segments

especially at higher T_{eq} values. The discrepancies between the predictions and the subjective votes increased for the head, hand and foot segments especially under cold conditions.

The prediction of the overall thermal sensation was carried out using four different models (i.e. *PMV* model; UCB comfort model; DTS model, Nilsson's model) for those 15 indoor conditions. The results showed variations in the predicted votes by these models (<1 on the scale). The discrepancies between these models and the subjective votes varied for the different conditions and were in average within 1 on the scale.

A thermal comfort model that is based on the structure of the UCB model was then adapted for the use with the MS-Pierce model. The model construction was based on a large scale subjective assessment from two studies and the predicted skin temperature by the MS- Pierce model for the test conditions from these studies. The overall thermal comfort is estimated, following the local comfort concept, using a weighted average of the local thermal comfort perceived by the different body segments. The model predictability was initially verified with subjective data from two cases and showed a very good performance.

7. Thermal comfort evaluation using a virtual manikin with human thermoregulatory control

7.1. Objectives

The work described in this chapter aimed at developing a simulation-based tool for the evaluation of local and overall thermal comfort. The MS-Pierce model (Chapter 3) and the adapted comfort model (Chapter 6) were used with a virtual manikin on VORTEX 4.0 CFD code. This was validated using two cases from laboratory-based measurements. The work is also part of Almesri's PhD thesis in which a new air distribution index is introduced to assess both thermal comfort and indoor air quality subject to different ventilation systems.

7.2. Physiological-psychological model

The physiological-psychological model represented by the coupled MS-Pierce thermoregulation and comfort model was used in these simulations. The physiological quantity is mainly represented by the skin temperature while the psychological term refers to the subjective perception of the indoor condition. These models′ details are described in Chapter 3 and 6. The MS-Pierce model's predictability of skin temperature was verified for

steady state and dynamic conditions using measured data at uniform neutral, cold and warm as well as several different asymmetric thermal conditions and had the average absolute deviation in a range of 0.3-0.8K. The adapted comfort model was constructed based on the UCB model's structure by correlating the local subjective votes from 45 different indoor conditions (1050 human subjects' test), given in two recent studies (i.e. Nilsson 2004 and Cheong et al. 2007) with predicted skin temperatures by the MS-Pierce model for these tests' conditions. The prediction of the overall thermal comfort in this model is based on a weighted average of the local comfort predictions. The coupled model only needs to be fed with the room physical parameters and the human subject's characteristics to estimate the distribution of the body skin temperature and hence the local and overall thermal comfort vote. In this work, the coupled MS-Pierce thermoregulation and comfort model was used in the thermoregulation of the virtual manikin as a boundary condition in the CFD simulations, and for the prediction of the thermal comfort. The simulations' results are compared with the measured data to validate the use of this evaluation tool.

7.3. CFD Simulations

CFD technique has progressed during the last years and has been proven powerful and efficient tool for simulating air flow and contaminant dispersion in indoor environments (Awbi 2003). The numerical calculations were carried out using CFD code VORTEX 4.0 (Awbi 2005) to predict the airflow properties in the chamber. This program has been developed for the simulation of airflow, heat transfer, concentration and mean age of air distribution in indoor environments.

In the simulations, the measured mean surface temperatures of all six chamber's walls, the measured inlet velocity, temperature and turbulence intensity, the measured laptop heat flux, the measured light surface temperature, the measured inlet CO_2 concentration and the predicted occupant's heat flux using MS-Pierce model have been used as boundary conditions. The rate of human's CO_2 production used in CFD simulations was estimated using the following equation (Awbi 2003):

$$G = 4 * 10^{-5} * M * A_D, \qquad (45)$$

Where G is the CO_2 production per person (l/s), M is the metabolic rate (W/m²) and A_D is the body surface area (m²). The body surface area is calculated using Eq.6 (DuBois 1916).

The estimated CO_2 production per person used in the CFD simulations was 0.00464 l/s based on assumed metabolic rate for the sedentary activity (i.e. 1.1met=64 W/m²).

The virtual manikin used in the CFD simulations (Figure 49) has a total surface area of ≈ 2.03 m² which represents the clothed whole body. The segmental area ratios correspond to the thermal manikin 'THERMINATOR'. The generated mesh was 3-D structured grid with 80*80*80 points (in x, y and z direction) giving a total of 512,000 cells for both ventilation systems (mixing and displacement ventilation). The equations for the momentum, energy, concentration, kinetic energy and turbulent dissipation rate are discretized with HYBRID scheme (Runchal 1972). The pressure-velocity coupling algorithm SIMPLE (Patankar and Spalding 1972) was used to solve the continuity equation and the RNG $k-\varepsilon$ (Yakhot et al. 1992) was used to predict the airflow's turbulent behavior within the chamber. The near wall nodes were located 5 mm from the wall surfaces as this is the optimum distance to use as recommended by Awbi (1998).

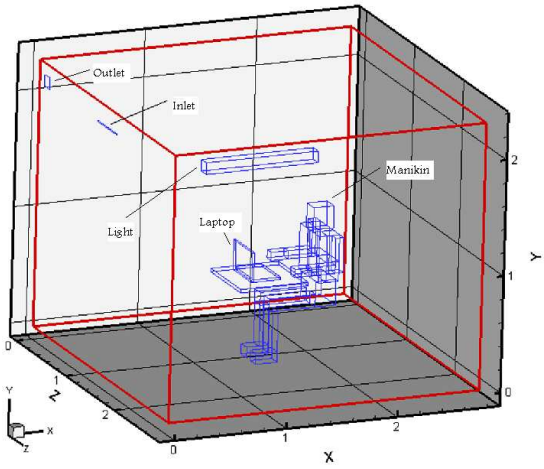

Figure 49 The virtual 'THERMINATOR' used in the CFD simulations

7.4. Human subjects' tests

The experiments (Almesri and Awbi 2011) were conducted in the University of Reading's environmental test chamber (2.78m x 2.78m x 2.3m). Two ventilation systems were tested; mixing ventilation (MV) and displacement ventilation (DV). The test conditions were the same for both ventilation systems with an air flow rate of 15 l/s, air entering the working compartment at 18°C, RH≈40% and total room load of 21.2 W/m². The physical indoor environmental parameters as well as the CO_2 concentrations were measured during the experiments. The air temperatures were measured using Platinum resistance temperature detectors (PRTD), air velocities were measured using velocity data-logger with omni-directional anemometers and CO_2 concentrations were measured using a 12-channel gas analyzer. Air temperatures and velocities

were measured at the inlet and outlet and at a height of 0.1, 1.1 and 1.8 m for several locations in the occupied zone and at a height of 0.1, 0.6, 1.1 and 1.6 in the vicinity of the occupant. The CO_2 concentrations were measured at the inlet and outlet and at a height of 1.1 and 1.8 m for many locations in the occupied zone. The local mean age of air was measured at the breathing zone at a point located 20 cm from occupant's nose using a standard tracer gas decay technique with SF_6 (sulphur hexafluoride) used as a tracer gas. Eight college-aged and healthy subjects (4 male and 4 female) participated in the experiments. The subjects sat at a desk facing the inlet diffuser and performed sedentary activities such as reading or using a laptop and were not allowed to move inside the chamber. They were exposed to the thermal environment for 2 hours and have been asked to fill in a questionnaire every 15 minutes to rate their local and overall thermal sensation levels based on the 7-point ASHRAE scale. All participants wore an ensemble of typical office clothing with estimated overall clo-value of 0.72 for and 0.64 for females.

7.5. Comparison's results

7.5.1 Room physical parameters

The predicted air velocity, temperature and CO_2 concentration profiles are presented in Figure 50, 51 and 52 respectively. Figure 50 shows the air velocity profile at a plane located in the middle of the chamber where the manikin is seated. There was no sign of draft observed around the manikin or in the occupied zone for both ventilation systems. Only draft is noticed near the ceiling for the case of mixing ventilation. These regions of high air velocity were generated by the air jet from the throw of MV inlet diffuser which is then decreased as the flow progressed towards the opposite wall. Figure 51 shows the temperature contour at the heights of 0.1, 0.6 and 1.1 m. It is obvious from Figure 51 that the air temperatures at these levels for DV system were in general cooler than those for the MV system. The predicted air temperatures at these levels (0.1, 0.6 and 1.1 m) and 10 cm away from the corresponding body segments (i.e. ankle, abdomen and head) were 22.4, 27.2 and 26.8°C respectively for the DV system and 25.1, 28.6 and 27°C respectively for the MV system. Thermal plumes from heat sources (i.e. manikin and laptop) are shown in Figure 52. As can be seen, lower air temperatures were near the inlet diffusers and were then increased gradually until it reached maximum values around the heat sources. Figure 53 shows the CO_2 concentration at a plane located in the middle of the chamber. The CO_2 concentration in the occupied zone was stratified and showed lower values for the DV system case compared with the MV system as shown in the figure. Obviously, the DV system provided

better air quality in the occupied zone. The maximum CO_2 concentration for both systems was located at the breathing zone which is normally the source of the CO_2 production.

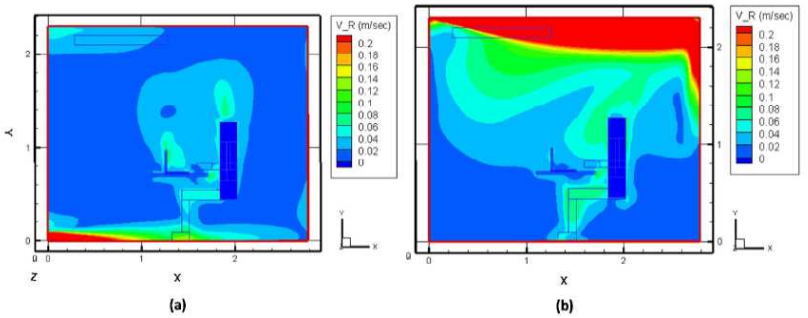

Figure 50 Velocity contour plots at a plane located at the middle of the chamber (a) DV system (b) MV system

Comparisons between the predicted and measured air temperatures, velocities and CO_2 concentration at the different locations in the occupied zone are shown in Figure 54. As can be seen from Figure 17, the predicted and measured air velocities for DV system were generally in good agreement with some minor discrepancy especially at the measuring points nos. 1, 2, 4 and 11. In contrast, the discrepancy between the predicted and measured air velocities is noticeable for the MV system at some measuring points. However, for the locations where the measured air velocity is lower than 0.1 m/s, the discrepancy could be due to the velocity sensors' large uncertainty for velocities below 0.1 m/s. Whilst for the locations where the measured air velocity is greater than 0.1 m/s (e.g. measuring points nos. 1, 4 and 13 for the MV system, which are located a distance of 0.1 m from the floor surface), the discrepancy could be attributed to disturbance of the air flow at these locations of the test chamber resulting from the dense sensors' wiring near to floor level.

The predicted and measured air temperatures were in a good agreement. The difference between the predicted and measured temperatures was in a range from -0.08 to 0.97K for DV system and from -0.03 to 0.8K for the MV system. While most of the predicted CO_2 concentrations were over-estimated, the percentage difference for CO_2 concentration was in small range from -0.13% to -11.09% for the DV system; and from -0.78% to -10.4% for the MV system. In general, the minor discrepancies between the predicted and measured quantities may be related to the simplifications in the modeling of the real enclosure or to errors in the measurements.

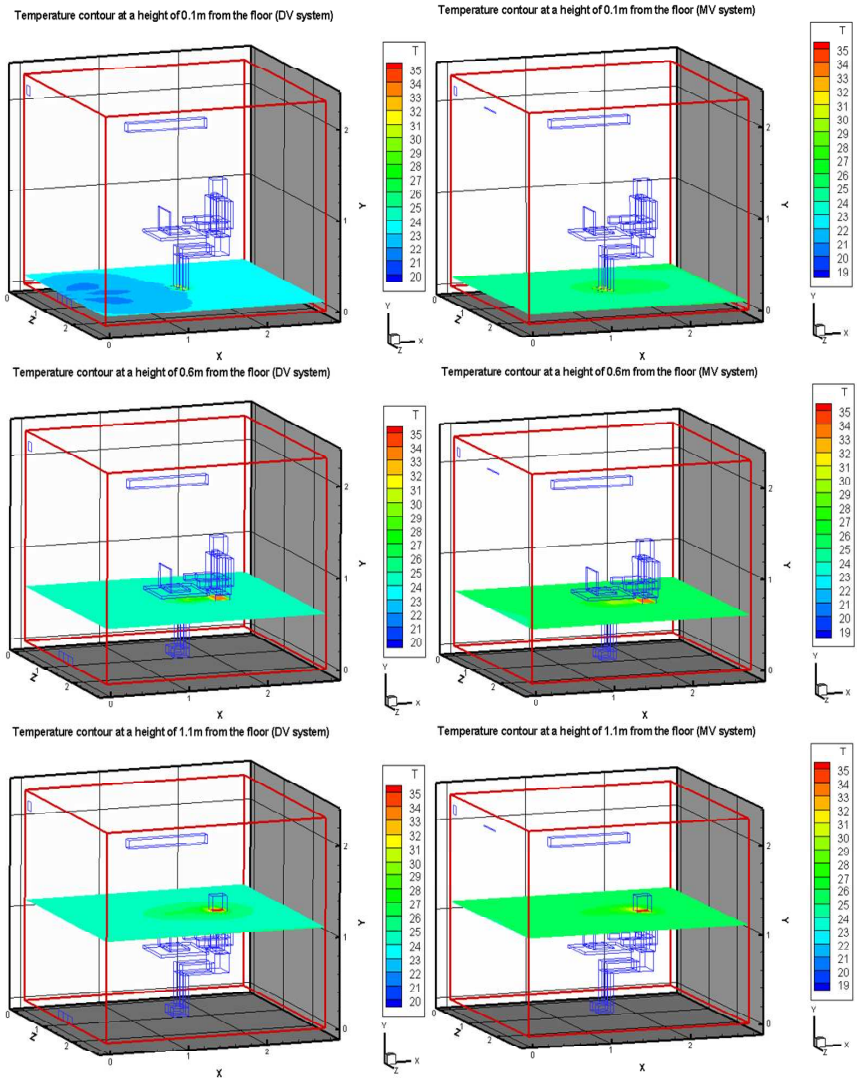

Figure 51 Temperature contour at different heights (0.1, 0.6 and 1.1 m) for both DV and MV systems.

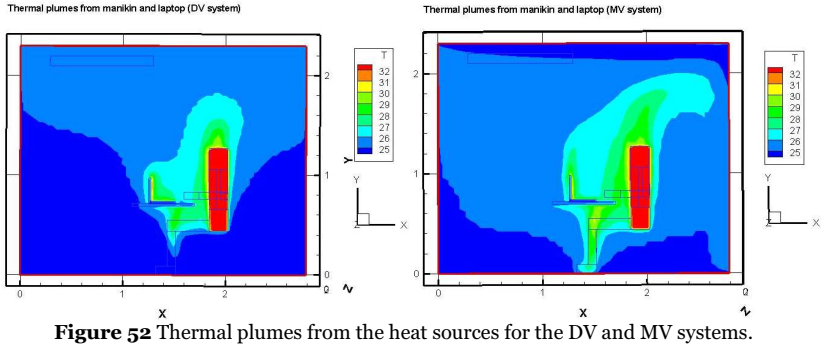

Figure 52 Thermal plumes from the heat sources for the DV and MV systems.

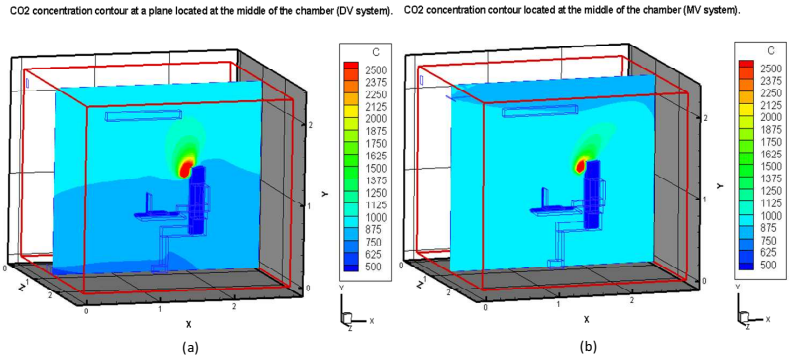

Figure 53 CO_2 concentration contour at a plane located at the middle of the chamber (a) DV system, (b) MV system.

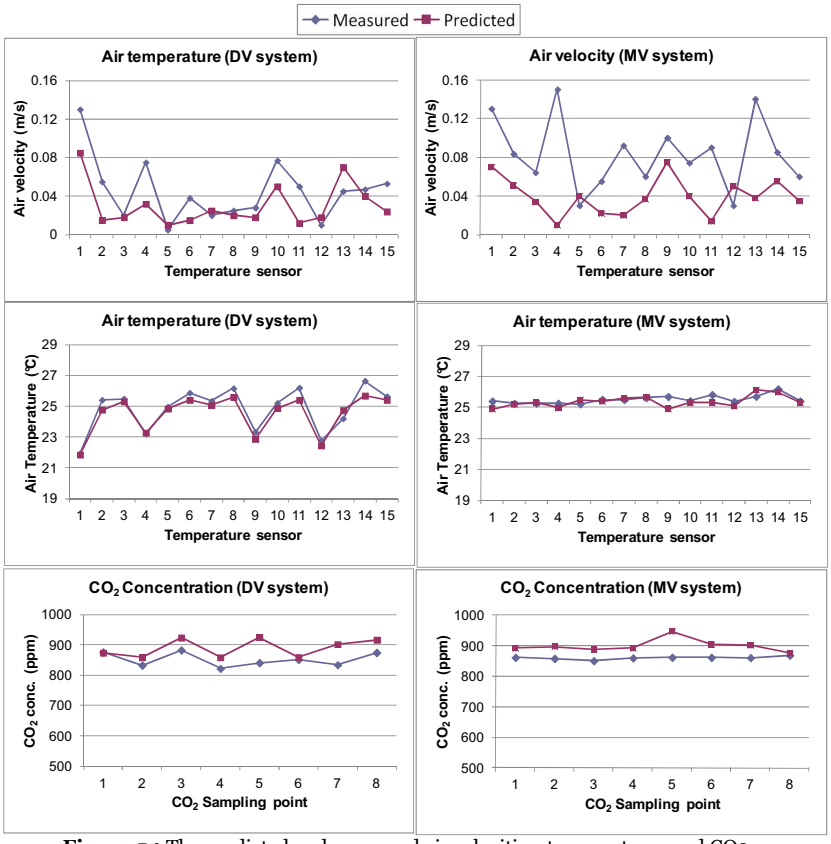

Figure 54 The predicted and measured air velocities, temperatures and CO2 concentration

7.5.2. Thermal comfort

The predicted local and overall comfort votes from the simulations along with the actual subjective votes are shown in Figure 55 and 56 for the two cases with the DV and MV systems respectively. The figures show the predicted and actual votes for the head, chest, back, pelvis and the right-side body limbs as well as for the whole body. The predicted votes were in good agreement with the actual votes for most body parts under the two

exposures with the DV and MV systems. The AAD was 0.5(SD 0.3) and 0.4(SD 0.3) on the comfort scale for the DV and MV cases respectively. The maximum deviation was <1 on the comfort scale at the pelvis segment for the exposure with the DV system and at the foot segment for the exposure with the MV system. The overall thermal comfort prediction based on the 7-site averaging was in a good agreement with the subjective votes. The deviation was 0.5 and 0.2 on the comfort scale for the DV and MV cases respectively. The 7-site averaging approach seems to be working well based on this comparison. The subjective votes in these tests were based on the ASHRAE 7-point scale while the comfort model is based on the Bedford 7-point scale. However, the difference between the two scales is believed to be very minor in the range around the neutral sensations (i.e. from -1 to 1) perceived under these two exposures.

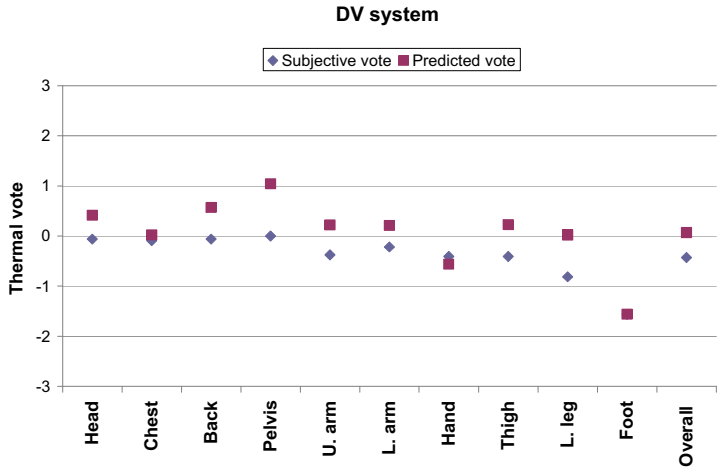

Figure 55 Predicted and actual votes for the exposure with the DV system

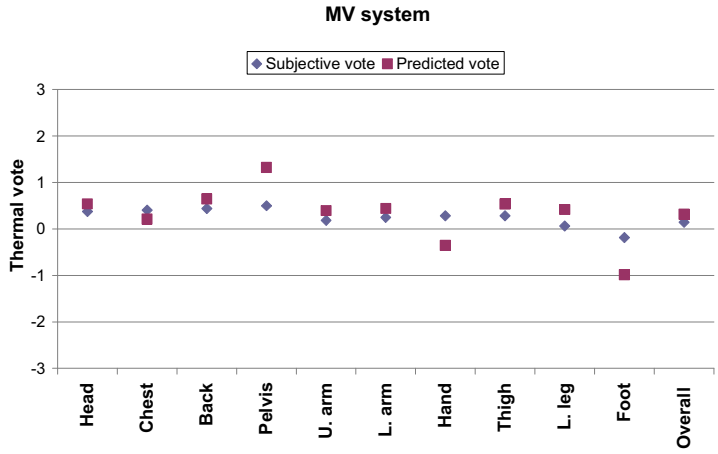

Figure 56 Predicted and actual votes for the exposure with the MV system

7.6. Summary

In this chapter, the multi-segmental Pierce model and the adapted comfort model were integrated on VORTEX 4.0 CFD code. A virtual manikin was constructed and thermally regulated using the MS-Pierce model. The prediction of this combination was then compared with measured data from human subjects' experiments. In these experiments, the indoor conditions were created by two different ventilation systems, mixing (MV) and displacement ventilation (DV) systems. The predicted physical parameters were in a good agreement with the measured ones. The local thermal comfort predictions were in good agreement with the subjective data. The AAD was from 0.4 to 0.5 for the two exposures and the maximum deviation was <1 on the comfort scale. The prediction of the overall comfort was also in a good agreement with the subjective data. The deviation was 0.5 and 0.2 on the comfort scale for the exposure with the DV and MV systems respectively.

8. Discussion

The work of this thesis introduced further developments to the evaluation methods of thermal comfort that can be used for existing buildings, buildings in the design phase and the design process of HVAC systems. The evaluation of thermal comfort, in this work, was carried out using the following two approaches:

- A thermal manikin that is thermally regulated by a physiological (thermoregulation) model for the estimation of the segmental and overall equivalent temperature and hence the local and overall thermal comfort.
- A physiological-psychological comfort model that is fed with the room measured physical parameters or integrated with a virtual manikin on CFD simulations.

The physiological MS-Pierce model was developed based on the Pierce two-node model and was used in both approaches.

In the first approach the local and overall comfort are predicted based on the estimated equivalent temperatures by the manikin and presented on Nilsson's comfort zone diagram (Nilsson 2007) to indicate the predicted votes.

In the second approach the local comfort is predicted using a model with a slightly modified structure from that used in the UCB local sensation model (Zhang 2003). The model was adapted for the use with the MS-Pierce model and was based on subjective assessments under 45 different

indoor conditions from two studies. The prediction of the overall comfort was based on a weighted average of the local comfort at body segments.

These two approaches, based on the results shown in this thesis, seem to produce a very reasonable predictability of the local and overall thermal comfort. However, they do still need further validations and perhaps further developments. Although the prediction of the human physiological variables such as the skin temperature could be accurate enough by the physiological models especially when individualizing (adjusted for a certain group of people) its parameters, the predictability of thermal comfort perception was expectedly not on the same level but maybe sufficient for such a psychological quantity. The individualization of the comfort models to represent a certain group of people can be also used when necessary.

The comfort models are usually based on large-scale subjective tests and accordingly predict the mean thermal vote. Therefore, there is still a need for a quantity such as the predicted percentage of dissatisfied (*PPD*) introduced by Fanger (1970) or an acceptable range as introduced by Wyon (1989) and Nilsson (2004) for the general application. After all, validation studies will still show biases for these comfort models when applying them intimately for every single case. Thus, when a higher predictability is desired, the individualization and development of models for different specific cases in building applications may be a necessary procedure.

In the evaluation of thermal comfort in buildings, the introduced two approaches are still necessary. While the use of physical thermal manikins is more feasible for evaluations in existing buildings and design process of HVAC systems (as introduced in Chapter 5), the use of the physiological-psychological approach is feasible in the building's design phase. The experimental work, in total, that was used in the construction of both approaches was focused on sedentary activities; therefore, it may be stated that these methods work best for predictions of sedentary people.

In the buildings sector, the HVAC practitioners seem to be reluctant in using methods else than the *PMV* model (Fanger 1970) that is in many cases applied out of its specified limits. This may be related to the complexity and lack of confidence in other introduced methods. Nevertheless, the limitations of the model and the necessity of evaluating the local comfort in non-uniform environments should be considered (see discussion in Chapter 1).

In this work, the developed methods combine useful features such as the simplicity along with the good accuracy in estimating local skin temperatures and hence the thermal comfort perception. The MS-Pierce model can be easily constructed and implemented in the thermo-regulation of thermal manikins to predict the thermal sensations either by the estimation of the equivalent temperature or by its adapted comfort model. Then, this toolkit can be used in real-life measurements or in simulations.

9. Conclusions

In this work, methods for the evaluation of thermal comfort were further investigated and developed. The work included human subjects' experiments for the measurement of skin temperature under different indoor conditions. The experiments revealed valuable data over the local responses and the skin temperature distribution, in physiological steady state, of the body segments. A new approach to formulate a multi-segmental (MS) physiological model based on the Pierce two-node model was developed. The developed model was validated under several indoor conditions and showed a very good predictability of the skin temperature. The model is accurate, simple and easy to implement. The model was then used in the control system of the thermal manikin 'THERMINATOR'. This represented a new control mode (*MSP*) in the thermoregulation of thermal manikins. The manikin was used with that control mode, along with the constant surface temperature (*CST*) mode, to estimate the equivalent temperature under two conditions and the results were compared with subjective assessments of the same conditions. The new mode showed slight improvements to the simulation of the human thermal presence in space with the clothed thermal manikin based on that comparison. The improvements could be more sensible with a naked manikin; however, the experimental work was focused on the use of normal office clothes. Furthermore, the thermal manikin was employed with the *MSP* mode in the design of a localized floor-heating system. This was carried out using the *MSP* control in dynamic mode with real-time measurements to find the optimum configuration related to geometry, surface area and temperature. The results showed that with certain geometries a nearly 1m² of heated floor could fulfill thermal comfort criteria and represented the optimum configuration.

In the work of this thesis, the equivalent temperature was not the only approach for the prediction of the local and overall thermal comfort. The MS-Pierce physiological model was coupled with the UCB psychological

comfort model to investigate the predictability of the physiological-psychological approach. This was compared along with Nilsson's model against subjective assessments under 15 different cases from a recent study. The two methods showed nearly similar predictions of the local thermal comfort for most body segments under the different conditions. A comparison of overall comfort predictions was carried out including 3 more additional models. The different models could not predict well the overall thermal sensations under the cold conditions given in that study.

After that investigation of methods, a comfort model based on a simplified structure of the UCB model was adapted for the use with the MS-Pierce model. The model is based on the Bedford scale which is used in evaluating both thermal sensations and comfort. The model was constructed using two studies from the literature that included 1050 subjective tests. The overall comfort in that model is predicted based on a weighted average of the local comfort. The model predictions were compared with subjective assessments under two thermally asymmetrical (slightly cold and warm) conditions. The predictions of the local and overall comfort were in a good agreement for these two cases. Furthermore, the MS-Pierce combined with the psychological comfort model was integrated on a CFD code. A virtual thermal manikin was constructed and regulated by the MS-Pierce model in the CFD simulations. This combination on CFD was used to predict the thermal comfort under two conditions from laboratory measurements. The predicted thermal votes were in good agreement with the subjective votes from these measurements.

The work in this thesis introduced an enhanced toolkit for the evaluation of thermal comfort based on the local comfort concept that can be used in real-life measurements or simulations. The toolkit has a balance between the simplicity and the accuracy that may be of interest for the HVAC practitioners.

References

Almesri I, Awbi HB (2011) Evaluation of air distribution systems using new air distribution index. Proceedings of Indoor air 2011- the 12th international conference on indoor air quality and climate, Austin, Texas.

Almesri I, Awbi H, Foda E, Sirén K (2011) A new air distribution index for evaluating non-uniform thermal environments, Building and Environment Journal, accepted paper (19 May 2012).

Amai H. et al. (2007) Thermal sensation and comfort with different task conditioning systems, Building and Environment 42: 3955-3964.

Arens E et al. (2006) Partial- and whole-body thermal sensation and comfort- Part I: Uniform environmental conditions, Thermal Biology, 31: 53-59.

Arens E et al. (2006) Partial- and whole-body thermal sensation and comfort- Part II: Non-uniform environmental conditions, Thermal Biology, 31: 60-66.

ASHRAE (1993) Handbook—Fundamentals, Physiological principles and thermal comfort, Chapter 8, 8.6-8.17, ASHRAE, Atlanta.

ASHRAE Standard 55 (2004), Thermal environmental conditions for human occupancy, ASHRAE, Atlanta.

Atmaca I, Kaynakli O, Yigit A (2007) Effects of radiant temperature on thermal comfort. Building and environment 42:3210-3220.

Awbi HB (1998) Calculations of convective heat transfer coefficients of room surfaces for natural convection, Energy and Building 28:219-27.

Awbi HB (2003) Ventilation of Buildings, London, Spon Press, Taylor & Francis Group.

Awbi HB (2005) VORTEX: A computer code for airflow, heat transfer and concentration in enclosure, Version 3C and 4D-RNG. Reading, UK.

Azer NZ, Nevins RG (1974) Physiological effects of locally cooling the head in a 95F and 75%RH environment, ASHRAE transactions, 2297: 93-100.

Bauman F et al. (1995) Testing and optimizing the performance of a floor-based task conditioning system, Energy and Buildings, 22: 173-186.

Cheong KW et al. (2006) Assessment of thermal environment using a thermal manikin in a field environment chamber served by displacement ventilation system, Building and Environment 41:1661-1670.

Cheong KW et al. (2007) Local thermal sensation and comfort study in a field environment chamber served by displacement ventilation system in the tropics, Building and Environment 42: 525-533.

CEN Standard CR 1752 (1998) Ventilation for buildings: design criteria for the indoor environment, CEN, Brussels.

CEN Standard EN15251 (2007) Indoor environmental input parameters for design and assessment of energy performance of buildings addressing indoor air quality, thermal environment, lighting and acoustics. CEN, Brussels.

de Dear RJ et al. (1997) Convective and radiative heat transfer coefficients for individual human body segments. International Journal of Biometeorology 40:141-156.

de Dear RJ, Brager GS (2002) Thermal comfort in naturally ventilated buildings: revisions to ASHRAE Standard 55, Energy and Buildings 34: 549-561.

DuBois D, DuBois EF (1916) A formula to estimate the approximate surface area if height and weight be known, Arch Intern Medicine 17:863-71.

Dufton AF (1936) The equivalent temperature of a warmed room, Journal of IHVE 4: 227-229.

EU Directive 2010/31/EU of the European Parliament and of the Council of 19 May 2010 on the energy performance of buildings, Official Journal of the European Union, 53.

Fanger PO (1970) Thermal comfort: Analysis and applications in environmental engineering. Danish Technical Press, Copenhagen.

Fanger PO, Toftum J (2002) Extension of the *PMV* model to non-air-conditioned buildings in warm climates, Energy and Buildings 34: 533-536.

Fiala D, Lomas K, Stohrer M (1999) A computer model of human thermoregulation for a wide range of environmental conditions: the passive system. Journal of applied physiology 87(5):1957-1972.

Fiala D, Lomas K, Stohrer M (2001) Computer prediction of human thermoregulatory and temperature responses to a wide range of environmental conditions. International Journal of Biometeorology 45:143-159.

Fiala D. (1998) Dynamic Simulation of Human Heat Transfer and Thermal Comfort, Ph.D. thesis, De Montfort University.p.293.

Foda E, Sirén K (2011a) A new approach using Pierce two-node model for different body parts. International Journal of Biometeorology, 55(4):519-532.

Foda E et al. (2011) Models of human thermoregulation and the prediction of local and overall thermal sensations, Building and Environment Journal 46: 2023-2032.

Foda E, Sirén K (2011b) Dynamics of human skin temperatures in interaction with different indoor conditions, Proceedings of Roomvent 2011- 12th international conference on air distribution in rooms, Trondheim, Norway.

Foda E, Sirén K (2011c) A thermal manikin with a human thermoregulatory control: Implementation and validation, International Journal of Biometeorology, DOI: 10.1007/s00484-011-0506-6.

Gagge AP, Fobelets AP, Berglund LG (1986) A statndard predictive index of human response to the thermal environment. ASHRAE Transactions.92 (2B):709-731.

Gagge AP, Stolwijk JAJ, Nishi Y (1971) An effective temperature scale based on a simple model of human physiological regulatory response. ASHRAE Transactions 77(1):247-262.

Hansen R et al. (2007) National Instruments LabVIEW: A Programming Environment for Laboratory Automation and Measurement, Journal of the Association for Laboratory Automation 12(1): 17-24.

Hardy JD, DuBois EF (1938) The technic of measuring radiation and convection. Journal of nutrition 15(5):461-475.

Havenith G (1997) Individual heat stress response. PhD thesis, Radboud repository, TNO human factors institute, 200pp.

Hodgdon J, Beckett M (1984) Prediction of percent body fat for U.S. navy men and women from body circumferences and height. Reports No. 84-11 and 84-29, Naval Health Research Center, San Diego, California.

Holmér I (2004) Thermal manikin history and applications, European Journal of Applied Physiology.92: 614-618.

Holmér I et al. (1999) Equivalent temperature in vehicles-conclusions and recommendations for standard, CABCLI seminar dissemination of results from EQUIV-project: 89-94.

Huizenga C, Zhang H, Arens E (2001) A model of human physiology and comfort for assessing complex thermal environments. Building and Environment 36:691-699.

Humphreys MA, Nicol JF (2002) The validity of ISO-PMV for predicting comfort votes in every-day thermal environments, Energy and Buildings 34: 667-684.

ISO (1985) Thermal environments–Instruments and methods for measuring physical quantities. Standard ISO 7726-1985 (E), International Organization of Standardization, Geneva, Switzerland.

ISO (2004) Ergonomics of the thermal environment–Determination of metabolic rate. Standard ISO 8996:2004(E), International Organization of Standardization, Geneva, Switzerland.

ISO (2005) Ergonomics of the thermal environment–Analytical determination and interpretation of thermal comfort using calculation of the PMV and PPD indices and local thermal comfort criteria, Standard ISO 7730:2005, International Organization of Standardization, Geneva, Switzerland.

ISO (2007) Ergonomics of the thermal environment–estimation of the thermal insulation and water vapor resistance of a clothing ensemble. Standard ISO 9920:2007(E), International Organization of Standardization, Geneva, Switzerland.

Kaynakli O, Pulat E, Kilic M (2005) Thermal comfort during heating and cooling in an automobile. Heat and mass transfer 41:449-458.

Kohri I, Mochida T (2002) Evaluation method of thermal comfort in a vehicle with a dispersed two-node model, Journal of the Human Environmental System 6(1):19-22.

Kraning KK (1995) Validation of mathematical models for predicting physiological events during work and heat stress, Biophysics and biomedical modeling division U.S. army research institute of environmental medicine, Natick, MA 01760-5007.

Madsen T et al. (1984) Comparison between operative and equivalent temperature under typical indoor conditions, ASHRAE Transactions 90(1): 1077-1090.

Madsen T et al. (1986) New methods for evaluation of the thermal environment in automotive vehicles, ASHRAE Transactions 92(1B):38–54.

McIntyre DA (1982) Indoor Climate, Applied Science Publishers, Barking, London.

McCullough E (2005) The use of thermal manikins to evaluate clothing and environmental factors, Elsevier Ergonomics Book Series, volume 3:403-407

Mc Gregor GR (2012) Special issue: Universal Thermal Comfort Index (UTCI), International Journal of Biometeorology, 56 (3), DOI: 10.1007/s00484-012-0546-6.

Melikov A, Zhou H (1999) Comparison of methods for determining T_{eq} under well-defined conditions, CABCLI seminar dissemination of results from EQUIV-project: 41-52.

Munir A, Takada S, Matsushita T (2009) Re-evaluation of Stolwijk's 25-node human thermal model under thermal-transient conditions: Predictions of skin temperature in low-activity conditions. Building and Environment 44:1777-1787.

Nicol JF, Humphreys MA (2010) Derivation of the adaptive equations for thermal comfort in free-running buildings in European standard EN15251, Building and Environment 45(1):11-17

Nilsson H (2004) Comfort Climate Evaluation with Thermal Manikin Methods and Computer Simulation Models, PhD thesis ISBN 91-7045-703-4.

Nilsson H et al. (1999) Definition and theoretical background of the equivalent temperature, CABCLI seminar dissemination of results from EQUIV-project: 31-40

Nilsson H (2007) Thermal comfort evaluation with virtual thermal manikin methods, Building and Environment 42:4000-4005.

Olesen BW, Fanger PO (1973) The skin temperature distribution for resting man in comfort. Arch. Sci. Physiology 27:385-393.

Oliveira AVM, Gaspar AR, Qunitela DA (2008) Measurements of clothing insulation with a thermal manikin operating under the thermal comfort

regulation mode: comparative analysis of the calculation methods, Eur J Appl Physiol 104: 679–688.

Patankar SV, Spalding DB (1972), A Calculation Procedure for Heat, Mass And Momentum Transfer In Three-Dimensional Parabolic Flows; Int. J Heat Mass Transfer 15: 1787-1806.

Quintela DA, Gaspar AR, Borges C (2004) Analysis of sensible heat exchanges from a thermal manikin, Eur J of Appl Physiol 92: 663-668.

Raven PR, Horvath SM (1970) Variability of physiological parameters of unacclimatized males during a two-hour cold stress of 5°C. International journal of biometeorology 14(3):309-320.

Runchal AK (1972), Convergence and Accuracy of Three Finite-Difference Schemes for a Two-Dimensional Conduction and Convection Problem, Int'l J. Num. Methods in Engineering 4:540-550.

Sakoi T et al. (2007) Thermal comfort, skin temperature distribution, and sensible heat loss distribution in the sitting posture in various asymmetric radiant fields, Building and Environment 42:3984-3999.

Stolwijk JAJ, Hardy JD (1966) Temperature Regulation in Man - A Theoretical Study. Pflügers Archiv 291:129-162.

Sørlie R. et al., Maintaining acceptable thermal comfort with a low air temperature, by means of local heating, Indoor air congress, Helsinki - Finland (1993).

Tanabe S et al (1994) Evaluating thermal environments by using thermal manikin with controlled skin surface, ASHRAE Transactions 100(1):39-48.

Tanabe S et al. (2002) Evaluation of thermal comfort using combined multi-node thermoregulation (65MN) and radiation models and computational fluid dynamics (CFD). Energy and Buildings 34:637-646.

Tikuisis P, Bell DG, Jacobs I (1991) Shivering onset, metabolic rate, and convective heat transfer during cold air exposure. Journal of applied physiology 70(5):1996-2002

van Ooijen AMJ et al. (2004) Seasonal changes in metabolic and temperature responses to cold air in humans. Physiology& Behavior 82:545-553.

Watanabe S et al. (2009) Thermal evaluation of a chair with fans as an individually controlled system, Building and Environment 44: 1392-1398.

Werner J, Reents T (1980) A contribution to the topography of temperature regulation in man. European journal of applied physiology 45:87-94

Wyon DP, Larsson S, Forsgren B, Lundgren I (1989) Standard procedures for assessing vehicle climate with a thermal manikin; SAE Paper 890049.

Wyon DP, Sandberg M (1990) Thermal manikin prediction of discomfort due to displacement ventilation. ASHRAE Transactions 96(1):67-75.

Yakhot V et al. (1992), Development of turbulence models for shear flows by a double expansion technique, Physics of Fluids 4(7):1510-1520.

Yao R, Li B, Liu J (2009) A theoretical adaptive model of thermal comfort – Adaptive Predicted Mean Vote (aPMV), Building and Environment 44(10):2089-2096.

Zhang H, Arens E, Arens C (2002) Using a driving game to increase the realism of laboratory studies of automobile passenger thermal comfort. SAE paper 2003-01-2710.

Zhang H (2003) Human thermal sensation and comfort in transient and non-uniform thermal environments, PhD thesis, CEDR, University of California, Berkeley, 415pp

Zhang H et al. (2010a) Comfort, perceived air quality, and work performance in a low-power task-ambient conditioning system. Building and Environment, 45(1):29-39

Zhang H et al. (2010b) Thermal sensation and comfort models for non-uniform and transient environments: Part III: Whole-body sensation and comfort, Building and Environment 45:399-410.

Aalto-DD 129/2012

ISBN 978-952-60-4814-7
ISBN 978-952-60-4815-4 (pdf)
ISSN-L 1799-4934
ISSN 1799-4934
ISSN 1799-4942 (pdf)

Aalto University
School of Engineering
Department of Energy Technology
www.aalto.fi

BUSINESS + ECONOMY

ART + DESIGN + ARCHITECTURE

SCIENCE + TECHNOLOGY

CROSSOVER

DOCTORAL DISSERTATIONS